The cellular functions of TREM2 in microglia in relation to Alzheimer's disease

Wenfei Liu

University College London

Thesis submitted for the degree of Doctor of Philosophy

September 2017

Declaration

I declare that the work presented herein is my own, except where indicated below.
Genotyping of all mice was performed by Rivka Steinberg and Shabinah Ali. Transgene copy number confirmation of the TauD35 mice was performed by Stuart Martin. The transcription factor binding site analysis was performed by Evan Santo and Dervis Salih. Flow cytometry was performed by Pablo Garcia-Reitboeck, who also helped me with subsequent data analysis.

Acknowledgements

Firstly, I would like to express my sincere gratitude to my supervisor Dr Frances Edwards for providing me this great opportunity to work in her lab. I am extremely thankful to her for such a nice support and guidance, and for encouraging and helping me to grow as a research scientist.

My special appreciation and thanks must go to Dr Dervis Salih, without whom I really couldn't have been able to complete this project. His guidance helped me in all the time of experiments and writing of this thesis.

I am also extremely grateful to Dr Damian Cummings for his brilliant scientific advice and knowledge and many insightful discussions and suggestions.

A huge amount of thanks go to all my fellow lab mates during the last few years. It has been a great pleasure to work in such a lovely lab with so many lovely people.

Finally, thank you to Dr Jennifer Pocock and Dr Pablo Garcia-Reitboeck for providing really helpful advice and teaching me a lot of microglial skills.

Abstract

Alzheimer's disease (AD) is the most common cause of dementia. Neuroinflammation is one of the key pathological features of AD, suggesting microglia, the major immune cell type in the brain, may play an important role in AD development. Furthermore, GWAS studies have found rare variants in immune-related gene *TREM2* that increase AD risk by ~2-3 fold. TREM2 therefore seems critically implicated in the microglial functions in AD progression, and targeting its role may yield protective agents for AD. Although several recent studies have begun to shed light on the importance of microglia in dementia and the cellular function of TREM2, at time this thesis was started there was very little known about TREM2.

To investigate microglia and TREM2 implications in AD, first I characterized the microglial response in relation to different stages of pathology development of AD via molecular biology and immunohistochemistry in brain samples of mice modeling either abnormal amyloid beta accumulation (APPSwe/PS1M146V transgenic mice) or tauopathy (TAUP301L transgenic mice). Both mouse models showed robust microglial activation, as manifested by expansion of microglial population along with pathology progression in the brain and up-regulation of microglial genes. I subsequently established an *in vitro* primary microglial model with acute *Trem2* knock-down to study the role of TREM2 loss-of-function in microglia. Endogenous *Trem2* expression in primary microglia was largely inhibited with pro-inflammatory stimulation such as LPS but up-regulated with anti-inflammatory stimuli such as Interleukin-4. *Trem2* knock-down resulted in significant gene expression changes in the microglia, and also impaired anti-inflammatory responses and phagocytosis. The results suggest decreased expression and/or function of TREM2, due to accumulated inflammatory stimuli in the brain or loss-of-function variants of TREM2, may shift the transcriptional and functional balance of microglia away from anti-inflammatory and phagocytic properties towards pro-inflammatory properties, which might contribute to AD progression.

Table of contents

List of figures

Chapter 1

Chapter 3

Chapter 4

Chapter 5

Chapter 6

List of Tables

Chapter 1

Chapter 2

Chapter 3

Chapter 1

Introduction

Alzheimer’s disease

Dementia refers to a category of diseases resulting in memory loss and cognitive decline, which mainly affects the elderly. Increasing life expectancy has led to a dramatic increase in the incidence of dementia. Alzheimer's disease (AD) is the most common cause of dementia, accounting for proximately 60-70% of cases (World Health Organization, 2017). It has gained a huge amount of scientific interest and also public concern, considering that the exact pathogenesis mechanism is still not clear and there is neither effective methods for early diagnosis nor a cure for this complex multifactorial syndrome. As the number of the AD cases is expected to continue increasing, both the huge economic burden on society and the enormous emotional pain of the patients and their families require more intensive research for further understanding of the disease mechanisms and effective preventative / curative methods.

Apart from progressive degeneration of multiple neuronal populations in the brain, AD is characterized by two major pathological hallmarks: amyloid plaques and neurofibrillary tangles. Amyloid plaques are mainly formed by extracellular deposition of aggregated amyloid beta (Aβ) peptides (products of intramembranous proteolysis of amyloid precursor protein (APP)). Neurofibrillary tangles are generated by intracellular aggregation of abnormally hyperphosphorylated microtubule-associated protein tau. In addition, neuroinflammation is another important characteristic in the AD brain, in terms of reactive microglia, astrocytes and various inflammatory components associated with AD pathology.

What do we know about the mechanisms underlying AD?

Since its first description in the early 20th century, AD has been studied intensely for its underlying mechanisms by neuroscientists and neurologists. Although the final conclusion has not been reached, accumulated research has led to a few hypotheses trying to reveal how the disease occurs, of which the predominant one is the amyloid cascade hypothesis, referring to an initial and central role of Aβ dysregulated metabolism in AD pathogenesis. It was first established over 25 years ago (Hardy and Allsop, 1991; Hardy and Higgins, 1992; Selkoe, 1991), which was prompted by the revelation and genetic location of Aβ peptide from senile plaques and the findings of familial-AD–causative mutations in genes involved in Aβ production. More and more evidence since then has accumulated to support and further develop the amyloid hypothesis, and formed the basis for our current understanding of AD pathogenesis.

Research into APP and presenilins (the active core of γ-secretase) has provided key mechanistic discoveries on Aβ production. In brief, APP is a constitutive transmembrane protein that can routinely undergo differential pathways of progressive proteolysis to produce various products. Aβ peptides of different length are generated via an initial cleavage at the APP extracelluar domain by β-secretase that is followed by multiple sequential γ-secretase cleavages at the intramembrane domain. Released Aβ peptides aggregate and deposit in the extracellular space, which constitute the major component of Aβ plaques. The longer the Aβ peptide, the more hydrophobic and more aggregating it is. In the case of familial AD, mutations in *APP* or presenilin genes affect APP processing, resulting in either elevated total Aβ generation or shifted Aβ production towards longer and more toxic species (Benilova et al., 2012; Chavez-Gutierrez et al., 2012; Goate et al., 1991; Kretner et al., 2016; Levy-Lahad et al., 1995; Mullan et al., 1992; Rogaev et al., 1995; Sherrington et al., 1995; Zhou et al., 2011). In these cases Aβ dysregulated production is the causative factor of the disease. Although the familial subtype only constitutes a very small percentage of the total AD population (<5%), it

still suggests that Aβ abnormality can initiate the full spectrum of AD pathology, including tau tangles and neuronal death.

In the case of the more common sporadic form of AD, despite its exact cause not being defined, abnormal Aβ metabolism, e.g. disability in efficient clearance of Aβ, is considered to be an early causative event in AD development. In particular, genetics has identified several gene variants associated with sporadic AD risk, which delineates extra biological processes contributing to AD progression. Further research into these molecules has revealed an important role in the Aβ homeostatic mechanisms. The strongest common AD risk factor is the *APOEε4* allele (Corder et al., 1993). It was suggested in AD mouse models that *ApoE-ε4* expression induced attenuated soluble Aβ clearance and more severe Aβ deposition in the brain compared to ε3 and ε2 isoforms (Castellano et al., 2011; Holtzman et al., 2000). Other AD-associated risk factors such as *SORL1* (Caglayan et al., 2012; Lambert et al., 2013; Pottier et al., 2012; Rogaeva et al., 2007) and *ABCA7* (Chan et al., 2008; Cuyvers et al., 2015; Kim et al., 2013; Meurs et al., 2012; Steinberg et al., 2015) were also found to regulate the APP amyloidogenic processing pathway or Aβ clearance from the brain. Moreover, given that microgliosis associated with Aβ deposition is an important pathological characteristics in AD, immune-related genes have more recently found to be AD risk associated, such as *CD33* (Hollingworth et al., 2011; Naj et al., 2011), *TREM2* (Guerreiro et al., 2013b; Jonsson et al., 2013) *PLCG2* and *ABI3* (Sims et al., 2017), indicating that the innate immune response, especially microglial dysregulation (discussed below) may contribute to AD pathogenesis via over- or less sufficient reaction in response to Aβ build-up.

Despite the strongly addressed central initial role of Aβ in AD pathogenesis and also the observed neuro-/synapto- toxicity of Aβ in laboratory studies (Jin et al., 2011; Shrestha et al., 2006; Snyder et al., 2005; Townsend et al., 2006; Walsh et al., 2002), it is still worth noting that Aβ deposition does not seem to directly associate with eventual neurodegeneration of AD. A lot of researchers have reported that the cognitive decline or the neurodegeneration in AD patients did not correlate well with the increase of Aβ deposition in the brain,

while the disease severity did strongly correlate with the neurofibrillary tangle load and the neuronal/synaptic loss (Arriagada et al., 1992; Giannakopoulos et al., 2003; Gomez-Isla et al., 1997; Gomez-Isla et al., 1996; Terry et al., 1991). Furthermore, there is more than one report showing non-demented elderly cases with comparable plaque burden in the brain to AD patients (Aizenstein et al., 2008; Katzman et al., 1988). Also, transgenic mouse models overexpressing familial-AD-causative mutations in *APP* with or without *PSEN1* show lack of neurofibrillary tangle formation and neuronal loss even at very late stages with enormous Aβ plaque deposition (Gotz et al., 2004). Collectively, the precise contribution of Aβ to the full development of AD, e.g. how it associates with subsequent disease processes, particularly tau tangles and neuroinflammatory processes, and whether it drives and/or cooperates with other biological processes to eventually lead to neurodegeneration, still need to be further clarified. Moreover, since Aβ toxicity studies suggest that the small soluble oligomers are the major neurotoxic species rather than the plaques (Selkoe, 2008; Townsend et al., 2006; Walsh et al., 2002; Walsh and Selkoe, 2007), it has brought about the idea that packing of Aβ oligomers into plaques could represent a type of protective mechanism to remove the more toxic species, and more importantly, any other biological processes, such as reactivated microglia and astrocytes, contributing to this mechanism or altering the plaque kinetics could potentially be involved in AD pathogenesis. Of various candidates, the innate immune system, especially the microglia are one of the earliest and most important components reacting to changed brain homeostasis, suggesting there are critical in the process of initial Aβ build up, Aβ-triggered subsequent events, and/or the association between neuronal loss and Aβ/tau pathology.

Microglia

Microglia, constituting ~10% of the total glial population in healthy adult brain, are the key immune cell type in the brain parenchyma. Microglia, together with meningeal, choroid plexus and perivascular macrophages, compromise the

brain myeloid cell population that plays an important role in the CNS immune response and homeostasis maintenance.

Physiology of microglia

Since first description by Pío del Río Hortega in the early 20th century, the origin of microglia had been controversial for many years until recently fate-mapping studies have revealed that microglia are derived from prenatal precursor cells in the yolk sac, which invade the CNS during embryogenesis (Ginhoux et al., 2010; Schulz et al., 2012). Further research added more to our understanding of microglia development. The source of microglia is found to be a population of $CD45^{-}$ $c\text{-}kit^{+}$ erythromyeloid precursor cells in the yolk sac; these cells undergo PU.1- and IRF8- dependent development characterized by down-regulation of c-kit and up-regulation of F4/80 and CX3CR1, and become the only progenitors of microglia that migrate, differentiate, proliferate, and distribute across the developing CNS (Kierdorf et al., 2013).

Microglia in the developing brain bear distinct morphological and transcriptional characteristics from those in the mature healthy brain (Kierdorf et al., 2013; Matcovitch-Natan et al., 2016), which is not surprising as they not only undergo terminal differentiation in the CNS environment but also exhibit functional phenotypes adapted to neural maturation. One of the most important functions of microglia in the developmental brain is the synaptic pruning process. It has been found microglia actively engulf synapses and promote maturation of brain circuitry in the developing brain, mainly through the classical complement cascade of which the major components are highly expressed by microglia during postnatal periods (Paolicelli et al., 2011; Schafer et al., 2012; Stevens et al., 2007).

In the mature, healthy brain, microglia are found in a ‘resting’ state with a typical ramified morphology (a small soma and fine branching processes) and

relatively low expression of macrophage-function-related molecules. However, increasing evidence suggests that resting microglia exhibit a surveillance state in the healthy mature brain rather than just resting (Hanisch and Kettenmann, 2007). Studies using time-lapse in vivo two-photon microscopy have revealed that the 'resting' microglia keep scanning their territories by transient and frequent process extension and retraction, and make rapid contacts with nearby neurons, glia, and blood vessels (Davalos et al., 2005; Li et al., 2012; Nimmerjahn et al., 2005; Wake et al., 2009). Through this kind of dynamics microglia may rapidly detect and remove even tiny micro-damage without full microglial activation; besides, 'resting' microglia may also play a role in constitutively monitoring neuronal synaptic activity. It is supported by the finding of frequent purinoreceptor-signaling-dependent physical interactions between 'resting' microglial processes and neuronal synaptic elements, which preferentially occurs on neurons of higher activities (Davalos et al., 2005; Eyo et al., 2015; Li et al., 2012; Tremblay et al., 2010; Wake et al., 2009). Recently, induction of long-term potentiation in mouse hippocampus was shown to be accompanied by an increase of surrounding microglial process contacts with dendritic spines, suggesting a potential role of normal microglia in activity-induced synaptic plasticity (Pfeiffer et al., 2016). Moreover, *in vivo* microglia depletion in adult mice exhibited impaired learning-induced synaptic formation and altered electrophysiological property in cortical neurons and also significant learning deficits (rotarod, fear conditioning, and novel object recognition) without any signs of inflammation (Parkhurst et al., 2013), which suggests a role of 'resting' microglia in synaptic activity, although another study employing CSF1R inhibitor to deplete microglia in adult mice did not observe significant cognitive or behavioral changes (elevated plus maze, open field, Barnes maze, rotarod, and fear conditioning) after up to 2-month microglial depletion (Elmore et al., 2014). Collectively, the surveillance status of microglia seems to be not only a scrutinizer of potential threats in the brain but also an important candidate for an active sensor and modulator involved in activity-dependent synaptic alterations and neuronal circuit remodeling. Further study and more evidence are still necessary for validating the exact contribution of microglia to normal neuronal synaptic dynamics.

Microglia expressing various receptors (*e.g.* scavenger receptors, Fc receptors, toll-like receptors (TLRs), *etc.*) to receive various signals from their domain are the first in the CNS to respond to a variety of stimuli such as infections or neuronal damage, so as to resolve the threats and restore the CNS homeostasis. The stimuli triggering microglial activation are considered to be the presence of an 'on' signal (e.g. microbial structure, abnormal protein aggregates, abnormal release of intracellular constitutes, and opsonizing complements), or loss of an 'off' signal (e.g. fractalkine and CD200 signals from neurons) (Hanisch and Kettenmann, 2007; Kettenmann et al., 2011). Once activation is stimulated, microglia undergo a range of changes within seconds to hours, including morphological changes, chemotactic reorientation, cytokine release, and other non-transcriptional and transcriptional adjustments to support disease defense and tissue repair. Notably, microglia are able to acquire distinct activation phenotypes depending on different stimulating cues or different stages of disease dynamic progression. An M1 or M2 terminology has been widely used to describe microglial activation in various studies. This definition first came from *in vitro* macrophages stimulated by T_H1 or T_H2 cells cytokines, which express distinct arrays of cytokines (Boche et al., 2013). The M1 classical activation is defined as LPS and/or IFNγ induced macrophage phenotype expressing high levels of pro-inflammatory cytokines, which is mainly involved in host defense. The M2 alternative activation is defined as IL4 and/or IL13 induced macrophage state with high expression levels of anti-inflammatory and tissue repairing markers. Both types of activation in microglia have also been extensively studied *in vitro*. But this terminology is recently considered to be over-simplified (Ransohoff, 2016). The major issue is that, different from microglia polarized to M1/M2 states with purified stimuli from various *in vitro* studies, microglia *in vivo* never receive only one single stimulus to govern their activation states. They are modulated by mixed cues including various regulatory/stimulating signals from nearby brain cells, emerged pathogens and various cytokines, leading to a mixed, dynamic and context-dependent microglial phenotype *in vivo*. Indeed, transcriptomic profile analysis of isolated microglia from either healthy or diseased brains did not show the typical M1 or M2 states that were revealed by *in vitro* studies (Holtman et al., 2015; Kim et al., 2016; Morganti et

al., 2016); instead *ex vivo* isolated microglia tended to show a mixed phenotype with co-expression of both M1 and M2 marker genes. It is becoming obviously inappropriate to simply apply the *in vitro* M1/M2 category to *in vivo* microglial phenotype. However, the signaling pathways underling the activation of M1 or M2 states may still be part of the intrinsic network regulating microglia. Various pathways including those involved in M1/M2 activation might work coherently to regulate microglial phenotypes. Also, the balance between M1 and M2 states may still play an important role in microglial dealing with environmental stimuli and interacting with neurons. Therefore, fine regulation of microglial functions in response to different CNS micro-environmental requests seems of extreme importance, and failure to do so maybe a critical part of neurological diseases including AD. Practically, M1/M2 polarization strategy still provides useful information about how microglia behavior under different conditions, especially for dissecting the potentially affected pathways when we start to study a certain molecule of interest in regulating microglial activation.

Microglia and AD

Accumulation and activation of microglia associated with amyloid plaques is one of the major AD pathological characteristics, as described in both post-mortem AD brains and in animal models (Prokop et al., 2013). Development of *in vivo* imaging techniques using the TSPO (18kDa translocator protein) radiotracers and PET also provide evidence for microglial activation in AD brains (Owen and Matthews, 2011). A recent study employing both prodromal and severe AD patients has shown that microglial activation, as measured by ^{18}F-DPA-714 (a new generation of TSPO radiotracer), positively correlates with PiB (a marker for fibrillar amyloid deposition) and occurs at prodromal and even possibly preclinical stages of AD (Hamelin et al.). In recent years, immune/microglia-related gene variants as AD risk factors revealed by GWAS analysis, such as *TREM2*, *CD33*, *ABI3*, and *PLCG2* (Griciuc et al., 2013; Guerreiro et al., 2013b; Hollingworth et al., 2011; Jonsson et al., 2013; Malik

et al., 2013; Naj et al., 2011; Sims et al., 2017) particularly emphasized an important role of microglia in AD pathogenesis. However, the question as to how microglial activation contributes to AD development is still not completely resolved.

Scientists have investigated the potential microglial reactions in response to Aβ exposure. It was reported that both soluble and fibrillar Aβ caused apparent microglial chemotactic migration and localization *in vitro* (Cho et al., 2013), and microglia in culture could be activated by soluble Aβ via the scavenger receptor A activity even at very low nanomolar concentrations that are below the levels showing obvious direct neurotoxicity (Maezawa et al., 2011). Furthermore, an *in vitro* study revealed an assembled complex composed of CD36, α5β1-integrin and CD47 as a receptor on microglia membrane that binds fibrillar Aβ, mediating microglial activation and pro-inflammatory mediator secretion (Bamberger et al., 2003). Another study showed that CD14, TLR2 and TLR4 were also required for Aβ fibril-induced microglial activation and phagocytosis (Reed-Geaghan et al., 2009). Conclusively, accumulated evidence from *in vitro* studies suggests that microglia can be effectively activated by various Aβ species. However, what should be paid attention to is that microglia *in vivo* are finely regulated by the CNS environment, especially neuronal signals such as CD200 and CX3CL1, and retain a unique phenotype with low levels of typical macrophage markers, which is easily lost in culturing conditions (Butovsky et al., 2014). Thus *in vitro* microglial responses to Aβ application might be actually oversimplified and amplified. It is of critical importance to investigate the exact microglial reactions to Aβ pathology either *in vivo* or in a mixed culture system better mimicking the CNS environment.

Transgenic mouse models overexpressing familial AD mutations have provided a useful tool for people to investigate microglial changes in response to Aβ pathology. Generally, AD microglial activation has already been widely replicated in transgenic animal models with Aβ pathology, with an apparent expanded microglial population and accumulated microglia surrounding Aβ plaques exhibiting enlarged morphology and intensive phagocytic markers

(Birch et al., 2014; Liebmann et al., 2016). The accumulation of microglia covering plaques has recently seemed of particular neuronal protective aspects. For example, it was reported that microglia clustering around plaques promoted the plaques to become denser and compact, which restricted formation of protofibrillar Aβ 'hot-spots' and consequently reduced neuritic dystrophy (Condello et al., 2015). Furthermore, studies with TREM2 deficient mice showing less microglial clustering around plaques supported the effects of microglia on compacting plaques and restricting adjacent neuritic damage (Wang et al., 2016; Yuan et al., 2016). It thus emphasized that the microglial reaction to Aβ does provide protective functions via actively affecting Aβ dynamics, rather than just being a secondary event of little contribution to the AD progression.

In recent years, transcriptional network analysis of mouse models has revealed microglial gene expression signatures associated with neurodegenerative diseases, and particularly AD. In a paper our lab previously published, we investigated the gene expression changes in an array of mouse models exhibiting different stages of AD-related pathology, investing amyloid and tau mouse models separately, and identified a large group of microglial genes showing highly connected increased expression associating tightly with the Aβ deposition process, which suggested complex transcriptional changes in microglia in response to Aβ pathology (Matarin et al., 2015). Notably, several hub genes including *Trem2* exhibiting particularly high connectivity with other genes were highlighted in network analysis, perhaps suggesting their coordinating roles in expression of Aβ-induced microglial phenotypes. However, because the analyzed brain tissue was tested without isolation of specific cell types, the observed changes might be partially due to the expansion of the microglial population and also some genes' signals might be too diluted in the mixture of all brain cell types. Furthermore, Holtman and colleagues purified microglial population from various mouse models for ageing or neurodegenerative diseases and identified the gene expression profile related to aged or disease-associated microglia (Holtman et al., 2015), which indicated a high overlap in the up-regulated gene modules. Further GO and KEGG-pathway analysis showed

that the up-regulated microglial genes in AD mice mainly represented involvement in pathways of *e.g.* immune response, phagocytosis and antigen-presenting processes, and on the other hand, this phenotype accompanied down-regulated steady state microglial genes largely overlapping with microglial signature genes found in another study (Butovsky et al., 2014). In a very recent paper (Keren-Shaul et al., 2017), a 'disease-associated microglia' subgroup was found to associate with Aβ plaques in the 5XFAD mouse model, and the major signature markers were of a substantial overlap with the hub genes obtained from previous published network analyses. Especially, they found the expression of this phenotype was partially dependent on expression of one of the hub genes, *Trem2*. Together with the fact that GWAS-identified loss-of-function variants of TREM2 increased AD risks, it therefore seems that it might play causal regulatory roles in guiding a complex microglial phenotype induction in response to Aβ changes; such phenotype induction could be protective against further development of pathology, and failure to do so (*e.g.* due to loss-of-function mutations or abnormal downregulation of these genes) might result in insufficient or faulty activation of microglia leading to less efficient resolution of threats and perhaps detrimental effects.

However, the activated microglia in response to Aβ pathology may also suggest a loss of normal surveillance status of microglia and probably an acquirement of detrimental functions. Stevens' group found in AD models that there was an oligomeric-Aβ-induced reactivation of developmental synaptic pruning pathway by microglia, which underlined the synaptic loss and plasticity impairment caused by Aβ oligomers (Hong et al., 2016) and was mediated by C1q that was found to be one of the 'hub' genes in co-expressed networks in AD mouse models (Matarin et al., 2015). Considering the normal strict microglial phenotype switch from developmental stage to adulthood (Matcovitch-Natan et al., 2016), it might be possible that the microglial activation phenotype, which is supposed to resolve the Aβ elevation, to some extent re-shifts the microglial phenotype away from the mature surveillance status and re-gains some of the functions contributing to developmental brain modeling but which is then detrimental to the adult brain. The potential

neurotoxic roles of microglia in AD were also strongly suggested in a study employing microglial depletion via a recently developed CSF1R inhibiting strategy (Elmore et al., 2014), showing that elimination of microglia in 5XFAD mice resulted in rescued synaptic and neuronal loss without obviously affecting Aβ metabolism (Spangenberg et al., 2016). Therefore, detrimental functions of activated microglia in response to Aβ dys-homeostasis may also exhibit an important role in the Aβ-to-neurodegeneration pathway.

Despite the intensive study of microglia relating to the Aβ pathway, whether microglia contribute to tau pathology development still needs more investigation. Recently, research has suggested a role of microglia in tau propagation. The distribution and spreading of tau aggregates shows a strong correlation with AD dementia severity and allows staging of the disease (Braak and Braak, 1991; Braak et al., 2011). It was reported that the non-trans-synaptic propagation of tau depended on microglial uptake of tau followed by secretion of tau-containing exosomes (Asai et al., 2015). Furthermore, a study provided direct evidence showing clear internalization of various tau species by microglia in the brain of mice and AD patients (Bolos et al., 2016). It could thus be hypothesized that microglia take up both soluble and insoluble tau species from either neuronal release or damaged neurites, which on one hand represents debris clearance and tau degradation but on the other hand promotes tau propagation; the key point here could be in AD whether Aβ- (or other AD-related events)-induced microglia priming would affect tau processing of microglia, which could drive microglia towards the direction of the detrimental pro-tau-propagation role. Similar to what is suggested in Aβ studies, it seems that fine regulation of microglial phenotype might be one of the critical factors contributing to the pathology progression. GWAS-revealed AD risk factors have provided a few exciting potential candidates to such a regulating role in microglia, of which TREM2 is the most interesting candidate with which to start.

TREM2

TREM2 (triggering receptor expressed on myeloid cells 2) is a transmembrane protein containing a single immunoglobulin-superfamily (Ig-SF) domain. It is part of the *TREM* gene cluster on human chromosome 6p21.1, and the mouse orthologue is encoded on mouse chromosome 17d (Allcock *et al.*, 2003; Bouchon et al., 2000; Bouchon et al., 2001; Daws et al., 2001). The *TREM* gene cluster encodes a group of innate immune receptors (such as TREM1, TREM2, NKp44, and various TREM-like transcripts) sharing a high degree of similarity, albeit mainly limited to the immunoglobulin-like domain that serves as the ligand-binding region.

TREM2 expression is first observed in macrophages and dendritic cells, but not granulocytes or monocyte cells (Bouchon et al., 2000; Bouchon et al., 2001; Daws et al., 2001). It is widely found in various cell types derived from the myeloid lineage, such as bone osteoclasts (Humphrey et al., 2006; Paloneva et al., 2003), lung (Wu et al., 2015) and peritoneal (Turnbull et al., 2006) macrophages. In the brain, TREM2 is predominantly expressed by microglia (Paloneva et al., 2002; Schmid et al., 2002; Takahashi et al., 2005). In 2015, however, Jay et al. questioned the TREM2 expression by microglia in the brain, by reporting that TREM2-expressing cells in the 5XFAD mouse brain were all expressing high levels of CD45 cells, suggesting a peripheral monocyte origin (Jay et al., 2015; Savage et al., 2015). But the expression level of CD45 may not be an ideal criterion to classify parenchyma microglia versus infiltrating monocytes, because the microglial transcriptional signature could be changed upon stimulation. Later on, another study confirmed that TREM2-positive cells in the AD mouse brain were actually resident microglia rather than infiltrating monocytes using parabiosis experiments (Wang et al., 2016).

TREM2 structure and signaling pathway

The structure of TREM2 is composed of an extracellular region with a single V-type immunoglobulin-like domain, a transmembrane domain with a positively charged residue, and a short cytoplasmic domain (Bouchon et al., 2000). The immunoglobulin-like fold in TREM2 protein depends on an intra-chain disulfide bridge formed by two cysteine residues. As the cytoplasmic region is short and does not bear docking motifs for signaling mediators, TREM2 has to couple with the adapter protein DAP12 (DNAX-activating protein of 12 kDa) to transduce the intracellular signals (Bouchon et al., 2000; Bouchon et al., 2001). Additionally, cell surface TREM2 undergoes ectodomain shedding by ADAM10 resulting in a soluble TREM2 release, and then intramembrane proteolysis by γ-secretase to remove the C-terminal fragment (Kleinberger et al., 2014; Wunderlich et al., 2013).

DAP12, belonging to the type 1 transmembrane adapter protein family, is expressed as a homodimer at the cell surface and associated with its various partner receptors, including KIR receptors, NKp44, TREM1, TREM2, TREM3, *etc*., through an electrostatic association within the transmembrane domain. The downstream signaling transduction depends on the ITAM (immunoreceptor tyrosine-based activation motifs) present in the DAP12 cytoplasmic tail.

Upon TREM2 ligation, the tyrosine residues of the ITAM are phosphorylated by the Src family kinases, and then recruit and activate the tyrosine kinase Syk and/or ZAP70, which in turn initiates a cascade of downstream phosphorylation of other proteins (Paradowska-Gorycka and Jurkowska, 2013). One of the major involved downstream pathways is the PI3K/Akt pathway, that is Syk-activated PI3K catalyzes phosphatidylinositol-4,5-bisphosphate (PIP2) to phosphatidylinositol-3,4,5-triphosphate (PIP3), recruiting phospholipase C-γ (PLCγ), TEC-family kinases and Vav, which then results in recruitment and activation of Akt. Another target of Syk/ZAP70 is the LAT/LAB adapter that recruits various signaling mediators upon phosphorylation, which consequently converts PIP3 to inositol triphosphate

(IP3) and DAG and activates intracellular calcium mobilization, PKCθ and the RAS-ERK pathway. Integrated signals then contribute to cellular transcriptional regulations.

TREM2 ligands

The exact ligand of TREM2 has not been clearly understood. Studies have suggested that TREM2 exhibits a pattern recognition feature. It binds to a broad range of exogenous (Gram-positive and Gram-negative bacteria) and endogenous (astrocytoma cells, various membrane phospholipids, non-phosphate lipids, and nuclear components) materials, which might be partially dependent on recognition of anionic residues (Cannon et al., 2012; Daws et al., 2003; Kawabori et al., 2015; Wang et al., 2015). Recently, ApoE especially lipidated ApoE has been found as a high-affinity TREM2 ligand in *in vitro* studies (Atagi et al., 2015; Bailey et al., 2015; Yeh et al., 2016), which brings a lot of interest because both *TREM2* and *APOE* variants are associated with increased AD risk. In addition, other apolipolipids, such as ApoA1, ApoB and CLU, and HDL and LDL are also found as potential TREM2 ligands (Atagi et al., 2015; Song et al., 2017; Yeh et al., 2016).

Rare genetic variants of TREM2 and CNS diseases

The importance of TREM2 function is strongly suggested due to the genetic findings of the association between variants of *TREM2* or its adapter *DAP12* and human diseases. Homozygous loss-of-function mutations of *TREM2*/*DAP12* were first identified as the cause of polycystic lipomembranous osteodysplasia with sclerosing leukoencephalopathy (PLOSL; also known as Nasu-Hakola disease, NHD) (Dardiotis et al., 2017; Kondo et al., 2002; Paloneva et al., 2000; Paloneva et al., 2002), which described a rare autosomal recessive disease characterized by multiple bone cysts and presenile frontal lobe dementia. As TREM2 is predominantly expressed by osteoclasts and microglia in the bone and the brain

respectively, these studies have pointed to a critical role of TREM2 in regulating the function of these tissue myeloid cells to maintain tissue homeostasis.

In 2013, two independent GWAS studies (Guerreiro et al., 2013b; Jonsson et al., 2013) highlighted a rare variant rs75932628-T in *TREM2* gene exon 2, causing an Arginine-to-Histidine substitution at amino acid position 47 (R47H), to be highly significantly associated with increased AD risk, with a comparable effect size to the *APOEε4* allele (around 3-fold increased AD risk). The association between the R47H and both early-onset and late-onset AD was then verified in a number of studies employing various case populations, and besides, such association was confirmed to be independent of the *APOEε4* risk variant (Benitez et al., 2013; Jin et al., 2014; Pottier et al., 2013; Ruiz et al., 2014; Sims et al., 2017). Furthermore, the R47H variant was investigated in other neurodegenerative diseases; it was also found to be associated with frontotemporal dementia (Rayaprolu et al., 2013), Parkinson's disease (Rayaprolu et al., 2013), and amyotrophic lateral sclerosis (Cady et al., 2014), suggesting a more widespread role for TREM2-related microglial functions in maintaining neuronal function/survival throughout the brain.

In addition to the R47H, more *TREM2* variants were revealed to be risk factors of AD or other CNS diseases. Another *TREM2* exon 2 variant, R62H, was recently revealed to significantly associate with AD risk (Jin et al., 2014; Sims et al., 2017). The H157Y in TREM2 exon 3 was associated to AD in a Han Chinese population (Jiang et al., 2016a), albeit the R47H association was not replicated in this population due to an extremely low minor allele frequency (Yu et al., 2014). Three homozygous variants Q33X, T66M and Y38C, and a compound heterozygous variant [Y38C and D86V] were found to cause an FTD-like disorder in four Turkish patients respectively (Guerreiro et al., 2013a; Guerreiro et al., 2013c). Notably, Guerreiro and colleagues reported significantly more common presence of the heterozygous form of Q33X, T66M and Y38C variants in AD patients compared with the healthy controls (Guerreiro et al., 2013b; Jonsson et al., 2013). A brief summary of the

TREM2 protein structure along with the domain-localization of disease-associated variants was illustrated in Figure 1.2.

In conclusion, all the *TREM2* genetic linkage with neurodegenerative diseases suggests an important contribution of TREM2 to regulating microglial functions with respect to neuronal function/survival in the process of disease progression. In the context of AD, exploring the function and mechanism of action of TREM2 in microglia would be extremely worthwhile for our understanding of AD mechanisms and particularly the role the immune system plays in the disease progression, likely opening novel opportunities for therapeutic development.

Figure 1.1

Protein structure of full-length human TREM2

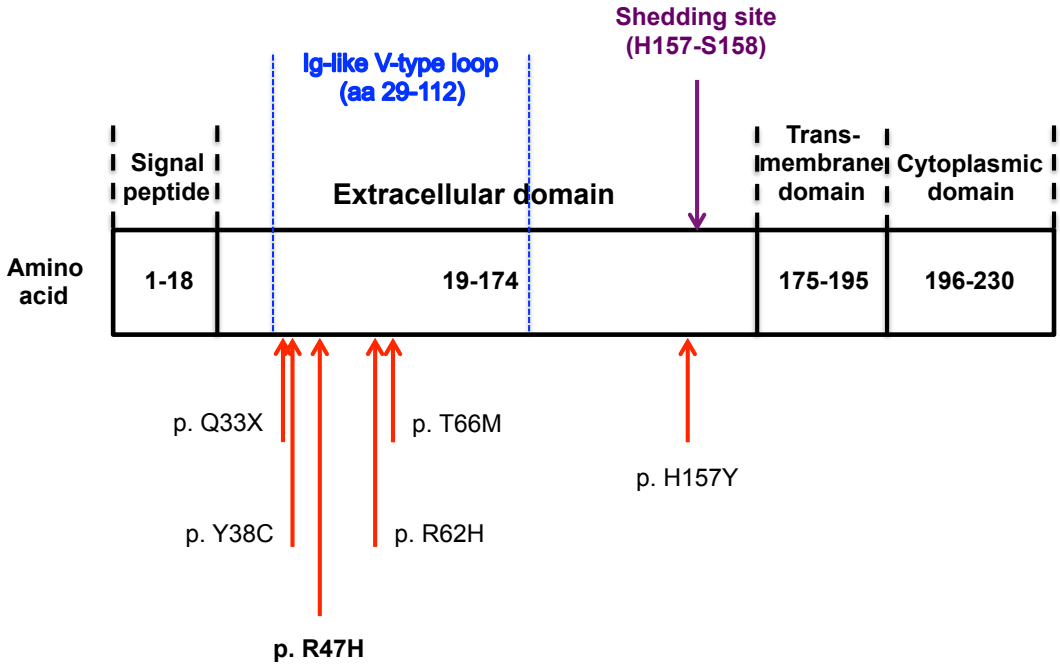

Figure 1.1. Protein structure of human TREM2 with major disease-associated rare variants highlighted. The panel shows the structure of human TREM2 (UP_061838.1, based on NM_018965; sequence information obtained from http://www.uniprot.org). The major rare coding variants associated with AD and other neurodegenerative diseases are indicated. Most variants including the R47H are located in the immunoglobulin-like fold of the extracellular domain, except that the H157Y that is within the region between the Ig-like loop and the transmembrane domain. Particularly, very recent studies suggested that the TREM2 shedding site was at the H157-S158 bond (indicated with a purple arrow) and an effect of H157Y ion TREM2 cleavage (Schlepckow et al., 2017; Thornton et al., 2017).

TREM2 and microglial function

TREM2 has been suggested to play an important role in phagocytosis and inflammation regulations in myeloid cells. TREM2's impact on microglial functions was first investigated by Takahashi et al., who manipulated *Trem2* expression in primary microglia *in vitro* by transduction of flag-tagged TREM2 or *Trem2* knockdown using lentiviral strategy and suggested TREM2 signaling supported microglial chemotaxis and phagocytosis, and inhibited inflammation induced by application of apoptotic neurones (Takahashi et al., 2005). TREM2 was also found to inhibit LPS-induced pro-inflammatory markers upregulated in primary alveolar macrophages *in vitro* (Gao *et al*., 2013) and the BV2 microglial cell line (Zhong *et al.*, 2015). With respect to AD, evidence has accumulated to support the involvement of TREM2 in microglia/macrophage phagocytosis of Aβ. For example, research employing primary microglia with either *Trem2* knockdown or over-expression via lentiviral strategies showed TREM2 facilitated Aβ1-42 uptake accompanied by down-regulation of the microglial pro-inflammatory cytokine response (Jiang et al., 2014). *Trem2* RNAi amplified the pro-inflammatory gene expression upregulation in the BV2 microglial cell line (Zhong et al., 2015). Primary microglial from *Trem2* knockout mice and transfected HEK293 or BV2 cells with TREM2 loss-of-function NHD/AD-associated variants all exhibited significant reduction in phagocytosis of bacteria, fluorescent beads, and Aβ1–42 aggregates, which for the first time highlighted the functional changes in microglia due to the disease-associated TREM2 variants (Kleinberger et al., 2014). Moreover, TREM2 deficient microglia/macrophages were also found to show decreased efficacy of antibody-stimulated Aβ uptake both *in vitro* and *ex vivo*, probably indicating a reduction in the total phagocytic capacity in TREM2 deficient myeloid cells (Xiang et al., 2016). As apolipoproteins have been found as TREM2 ligands, it was also shown that microglia/macrophages bearing the AD-associated TREM2 R47H variant exhibited lower binding affinity to ApoE, CLU, and LDL, which resulted in reduced microglial clearance of ApoE-bound apoptotic neurons (Atagi et al., 2015), and CLU/LDL-associated Aβ1–42 aggregates (Yeh et al., 2016). In contrast, primary microglia isolated from adult *Trem2* knockout mice and cultured in the presence of transforming

growth factor β (TGF-β) exhibited no impairment in phagocytosis of either apoptotic cells or Aβ compared to WT mice (Butovsky et al., 2014; Wang et al., 2015), suggesting different microenvironment factors might modulate the potential involvement of TREM2 in microglial phagocytosis. Overall, TREM2 is implicated in regulating microglial/macrophage phagocytic activities and restricting pro-inflammatory inductions.

Exploring TREM2 in AD mouse models

To further clarify the relevance of TREM2 in AD progression *in vivo*, recent studies have manipulated *Trem2* expression in AD mouse models and investigated the consequent effects on the AD-related pathology development.

Brain *Trem2* expression is up-regulated along with Aβ deposition in various transgenic AD mouse models (Frank et al., 2008; Guerreiro et al., 2013b; Jay et al., 2015; Melchior et al., 2010). We have also previously reported in an APP/PS1 mouse model that *Trem2* is up-regulated in both the cortex and the hippocampus, and in particular, microarray analyses combined with network analyses highlights *Trem2* as one of the 'hub genes' showing high connectivity to other genes in terms of the transcriptional changes, particularly in response to Aβ pathology (Matarin et al., 2015). It is therefore not surprising that theses mouse models could potentially be useful tools to investigate the functional role of TREM2, and in general, of microglia, in AD-related pathology progression, although the transgenic mice may not be the ideal models to completely mimic AD in humans given their overexpression.

Before addressing TREM2 deficiency in AD mice, it is important to note that *Trem2* knockout in wildtype control mice does not bring about obvious changes in the major brain histology, inflammatory status, neuronal health or behavioral performances (Poliani et al., 2015; Zhu et al., 2015), except an impairment in microglia increase and morphology change associated with

ageing. This microglial impairment observed only in aged or mice modeling dementia might suggest a role of TREM2 in modulating microglial functions in response to stress in the brain, rather than modulating microglia in healthy brains.

As TREM2 is suggested to be critical for microglial phagocytosis, it could be particularly relevant in AD as a mechanism for Aβ clearance. So far studies employing *Trem2* knockout or overexpression have all examined the impact on Aβ deposition in various AD mouse models. Indeed, they consistently found that TREM2 deficiency led to decreased microgliosis associated with Aβ plaques and attenuated microglial transcriptional changes. However, the results regarding the change in Aβ load in the brain showed a lot of discrepancies (Jay et al., 2017; Jay et al., 2015; Jiang et al., 2014; Jiang et al., 2016b; Ulrich et al., 2014; Wang et al., 2015; Wang et al., 2016), which has been summarized in Table 1.2. One of the possible causes seems to be the different stages of the Aβ pathology progression analyzed. Studies investigating mice at early to middle stages of pathology showed that *Trem2* deficiency reduced or did not obviously affect Aβ burden (Jay et al., 2017; Jay et al., 2015; Ulrich et al., 2014; Wang et al., 2016), while at late stages an increase in the brain Aβ deposition was observed (Jay et al., 2017; Wang et al., 2015). The differential interaction between TREM2 and Aβ pathology at different stages was also found in *Trem2* overexpression studies by Jiang and colleagues, in which they showed *in vivo Trem2* overexpression significantly enhanced microglial uptake of Aβ and ameliorated Aβ deposition only in the APPPS1 model at an early-middle stage, but not in aged mice (Jiang et al., 2014; Jiang et al., 2016b). Collectively, it appears that apart from TREM2-dependent microgliosis in response to Aβ pathology, TREM2-related microglial Aβ phagocytosis may be just one of the factors affecting Aβ deposition in the brain, which could also be affected by other factor like Aβ kinetics changes, differential microglial activation phenotypes, and possibly the functional reserve/capacity of microglial with ageing/stress. This also suggests that any therapies developed against TREM2 or microglia for use in AD need to be tailored for use at the correct stage of disease.

Interestingly, there are two reports both showing that TREM2 deficiency and consequent reduced microglia covering Aβ deposits resulted in a significant structural change of the Aβ plaques in the 5XFAD mouse model, which exhibited a smaller condensed plaque cores with wider fiber-like outwards diffusing structures, resulting in increased dystrophic neurites around Aβ plaques (Wang et al., 2016; Yuan et al., 2016). This finding possibly suggests a barrier function for microglia in insulating Aβ plaques, which could not only slow down the plaque growth but also restrict the interface diffusion of soluble Aβ from plaques so to limit the soluble-Aβ-induced neuronal toxicity. Therefore, TREM2-dependent microgliosis around Aβ deposits could be a critical mechanism of the brain to both remove Aβ and inhibit neurodegeneration.

Table 1.1

Mouse model	Age starting amyloid deposition	*Trem2* manipulation	Age of analysis	Aβ plaque load	Insoluble Aβ42 levels	Soluble Aβ42 levels	Ref.
APP/PS1-21	2m	*Trem2* hemizygosity	3m	=	=	NA	Ulrich et al., 2014
APP/PS1-21	2m	*Trem2*$^{-/-}$	4m	↓	↓	↓ (Trend)	Jay et al., 2015
APP/PS1-21	2m	*Trem2*$^{-/-}$	2m	↓	NA	NA	Jay et al., 2017
APP/PS1-21	2m	*Trem2*$^{-/-}$	8m	↑	NA	NA	Jay et al., 2017
5XFAD	2m	*Trem2*$^{-/-}$	8.5m	↑	NA	=	Wang et al., 2015
5XFAD	2m	*Trem2*$^{-/-}$	4m	=	NA	NA	Wang et al., 2016
APP/PS1dE9	4m	*Trem2* over-expression	7m	↓	↓	↓	Jiang et al., 2014
APP/PS1dE9	4m	*Trem2* over-expression	18m	=	=	=	Jiang et al., 2016b

Table 1.1. Effects of *Trem2* deficiency/overexpression on Aβ pathology in various transgenic AD models. Adapted from Jay et al. (Jay et al., 2017). Arrows indicate either increased or decreased pathology, and '=' indicates no significant changes observed.

TREM2 influence on microglial survival

Microglial survival requires continuous CSF1/IL34-CSF1R activation in the mature brain, and withdrawal of CSF1R signaling drives rapid microglial death (Elmore et al., 2014). Actually TREM2 was found to be involved in cell survival (monocyte-derived dendritic cells *in vitro*) soon after TREM2 was initially identified (Bouchon et al., 2001). Recently, it has been found TREM2/DAP12 also plays a role in microglial survival, which appears to work synergically with the CSF1R pathway. Otero and colleagues found in 2009 that DAP12 deficiency reduced viability of bone-marrow-derived macrophages *in vitro* by both inhibiting CSF1R-dependent proliferation and promoting macrophage apoptosis; mechanistically, it involves attenuated CSF1-CSF1R-signaling-induced β-catenin activation (tyrosine phosphorylation and nuclear translocation) resulted from DAP12 deficiency (Otero et al., 2009). They further showed that aged $DAP12^{-/-}$ mice exhibited decreased microglia number and increased signs of microglial degeneration compared to WT mice, which also supported the contribution of DAP12 signaling to the survival of microglia. As TREM2 is one of the major myeloid cell receptors transducing downstream signals via DAP12, it is likely that the role of DAP12 in supporting cell viability represents a contribution of TREM2. The important role of TREM2 in myeloid cell survival was then confirmed in bone-marrow-derived macrophages (Wu et al., 2015), osteoclast precursor cells (Otero et al., 2012), and lung macrophages (Wu et al., 2015). In the context of microglia, *Trem2* deficiency was found to accelerate reduction of microglial viability *in vitro* induced by CSF1R-signaling-deprivation, and *in vivo Trem2* knockout did lead to more microglial apoptosis in the 5XFAD mouse model (Wang et al., 2015). Recently it was shown in primary culture and mouse models that microglia required TREM2 activation to efficiently phosphorylate the Akt/GSK3β pathway to finely control the degradation of β-catenin that in turn maintained microglial survival and proliferation (Zheng et al., 2017). Collectively, TREM2/DAP12 may play an important role in the CSF1R-dependent microglial survival by regulating the β-catenin signaling pathway, although TREM2 does not seem to replace the function of the CSF1R-signaling in maintaining microglial survival as TREM2 normal expression does not prevent

microglial depletion due to CSF1R blockade (Elmore et al., 2014; Wang et al., 2015), suggesting two parallel pathways that cross-talk.
Since soluble TREM2 (sTREM2) was identified, studies have found sTREM might contribute to myeloid cell survival as well, which is discussed in the next session.

Soluble TREM2

Recently a soluble form of TREM2 has captured attention. Soluble TREM2 (sTREM2) was first described in research by Piccio and colleagues (Piccio et al., 2008), which was encouraged by the presence of soluble TREM1 and an alternative *TREM2* transcript only bearing the extracellular domain (although the expression levels of the alternative TREM2 isoform is much lower than full-length TREM2) (Allcock et al., 2003; Schmid et al., 2002). They detected sTREM2 in both human cerebrospinal fluid (CSF) and plasma, and showed that the CSF sTREM2 levels were higher in patients with multiple sclerosis or other inflammatory neurological diseases. The presence of CSF and plasma sTREM2 was then confirmed by other studies later.

Moreover, research has shed light on the processing of TREM2 protein, which by far seems to be the major origin of sTREM2 production. *In vitro* studies utilizing various cell lines transfected with tagged TREM2 suggested that TREM2 underwent maturation and localization to cell surface, and then ectodomain shedding by ADAM10 resulting in sTREM2 release, and then intramembrane proteolysis by γ-secretase to remove the C-terminal fragment (Kleinberger et al., 2014; Wunderlich et al., 2013). Remarkably, transfection of FTD- or FTD-like-associated TREM2 variants (T66M and Y38C) was found to heavily impair TREM2 maturation and transport to cell membrane and thus cleavage of TREM2, which led to largely reduced production of sTREM2; the AD-associated TREM2 R47H variant also showed similar but much less severe effects (Kleinberger et al., 2014). Therefore, routinely proteolysis of TREM2 and release of sTREM2 might suggest a potential paracrine or

autocrine function of sTREM2 in regulating microglial activities and perhaps other cell types in the brain as well.

Under the context of AD, people then started to investigate the relevance of CSF sTREM2 in AD. It has been consistently found that the CSF sTREM2 level is positively associated with ageing, and in AD patients associated with CSF total-tau and phosphorylated-tau in AD patients (Henjum et al., 2016; Heslegrave et al., 2016; Piccio et al., 2016; Suarez-Calvet et al., 2016a; Suarez-Calvet et al., 2016b). A few studies showed CSF sTREM2 levels but not plasma sTREM2 were significantly higher in AD patients than in healthy controls (Heslegrave et al., 2016; Piccio et al., 2016; Suarez-Calvet et al., 2016a). Investigation of the temporal sequence of various AD marker changes showed that the CSF sTREM2 change in AD followed Aβ deposition and alterations in CSF Aβ and total-tau, but was concurrent with neurodegenerative changes such as hippocampus volume and cognitive performance decline, suggesting the CSF sTREM2 change as an event occurring at early symptomatic stages of AD but after the initiation of cellular pathology (Suarez-Calvet et al., 2016a). However, controversial results were also reported as equivalent (Henjum et al., 2016) or lower CSF sTREM2 (Kleinberger et al., 2014) in AD cases compared to the control population. The inconsistency might be due to differences in the sample size, differences in ethnicity of populations, the case selection of different pathological stages, or the assays used for measurement. Even in the studies showing a significant CSF sTREM2 difference in AD versus controls, there was always large overlap between groups, suggesting sTREM2 in CSF might not be an ideal biomarker for AD diagnosis. However, it could still be a useful marker for assessing microglial status and inflammation in the brain, particularly in a subset of patients.

It remains unclear in terms of the exact physiological/pathological functions of sTREM2. Wu and colleagues found sTREM2 application promoted the survival of bone-marrow-derived macrophages via an anti-apoptotic effect, whether or not full-length TREM2 was constitutively expressed in these cells (Wu et al., 2015). A more recent study (Zhong et al., 2017a) also identified a

role of sTREM2 on microglial survival in primary cultures, independent of full-length TREM2/DAP12 expression, with a mechanism through affecting the Akt-GSK3β-β-catenin signaling pathway, suggesting that the previously reported influence of TREM2 on microglial survival was at least partially due to sTREM2. Additionally, they also found that sTREM2 augmented pro-inflammatory gene expression in microglia both *in vitro* and *in vivo*. Interestingly, sTREM2 bearing AD-associated R47H or R62H variants exhibited reduced anti-apoptotic and pro-inflammatory functions on primary microglia compared to WT sTREM2 (Zhong et al., 2017a), which might be one of the potential mechanisms underlying the 'pro-AD' effects of theses variants. Although the results might need more confirmation, it suggests microglia-released sTREM2 may serve as an effector for microglia themselves and play a role in regulating their survival and functions through an independent mechanism of the membrane-tethered-TREM2/DAP12 signaling.

Summary

Alzheimer's disease, the most common cause of dementia, threatens the whole society with its particular difficulty of early diagnosis and effective intervention. Scientific research since its first description has revealed some of the key components in AD pathogenesis such as Aβ dys-homeostasis as an early initial factor and tau pathology as a correlate to neurodegeneration and cognitive decline. However, there are still many details missing in this story, *e.g.* how Aβ becomes dysregulated given that it is normally produced in healthy brains, how Aβ pathology mechanistically leads to tau pathology, and how the brain homeostatic system reacts to and contributes to the signature pathology, *etc*. GWAS studies uncovering a variety of AD risk gene variants have placed a spotlight on the potential role of the innate immune system especially the brain resident microglia in the pathogenesis. In particular, TREM2, as one of the strongest risk genes expressed exclusively by microglial/myeloid cells in the brain, still retains secrecy for its precise biological functions but is likely to perform a regulatory role on microglia,

which requires intensive studies to reveal how it contributes to AD, and how this information could be utilized for drug discovery.

In this thesis, I established a scheme to investigate the importance of microglial GWAS hits for AD that is physiologically-relevant, specifically I developed a primary microglial culture model with acute *Trem2* knockdown, to study subsequent transcriptional changes in the microglia and also the microglial fate changes in response to pro- or anti- inflammatory stimuli. In particular, the effects were analyzed within a narrow time-window shortly after *Trem2* was knocked down to identify acute responses of microglia to *Trem2* knock-down and fate-switching stimuli, rather than developmental or chronic effects of complete *Trem2* ablation for weeks or months, which allows time for compensatory and homeostatic changes to cloud our results. I hypothesized that microglial *Trem2* expression might be very dynamic depending on various environmental cues in the brain. In the context of AD pathogenesis, accumulating stress with ageing or with other AD risk events could bring temporal or continuous changes, and direct or indirect to *Trem2* expression, which might affect microglial fine regulation in response to potential but still bi-directional AD initiative events. I found that acute knockdown of *Trem2* in primary microglia impaired anti-inflammatory or repair-related gene transcriptional changes, and identified that *Trem2* plays a suppressive role in preventing microglia becoming pro-inflammatory. I also validated the implication of TREM2 in microglial phagocytosis. Together, the results have highlighted an important aspect of TREM2 function that is important for dementia, and my data and model of study will allow opportunities for drug development.

Additionally, I characterized the microglial activation related to AD pathology in two lines of transgenic mouse models that mimic amyloid pathology and tau pathology respectively. Particularly, I compared these two models in the microglial gene expression levels by RT-qPCR and the microglial population changes by immunohistochemistry, in order to investigate the microglial reactions in response to different isoforms or stages of AD pathology. I found that the microglial activation followed the time course of the amyloid plaque

deposition in the amyloid mouse models, while the tau model presented microglial activation with a relative delay to the tangle development but with a more pro-inflammatory activation phenotype. More interestingly, although *Trem2* gene expression was higher in both models compared to the wildtype, the increase in *Trem2* in the tau mice is largely due to microglial proliferation as the ratio to *Aif1* expression is largely unchanged whereas in the amyloid mice the expression of *Trem2* in microglia increases as shown by an increased *Trem2:Aif1* ratio.

Notably, an obvious limitation of current transgenic mouse models is that they overexpress the genes of interest from artificial promoters and the transgenes insert randomly into the genome in multiple copies, which is apparently not true in human. However, these models are still useful for people to dissect the Aβ component of the AD pathology and thus to study the brain immune changes in response to Aβ dys-regulation and the neuronal changes at the molecular and synaptic levels. Very recently, the APP Knock-in mice were developed (Saito et al., 2014), in which APP is expressed from its native promoter and so expressed at the endogenous levels (e.g. not overexpressed) in the specific cells that normally express APP. This type of model, combined with manipulation of AD genetic risk factors, would likely provide a better animal model to mimic human AD. Unfortunately, for this thesis I did not have enough time to use the knock-in models.

Chapter 2

Materials and Methods

All mouse experiments were performed according UK Home office regulations under the Animals (Scientific Procedures) Act 1986 and UCL local ethical guidelines, and in agreement with the GlaxoSmithKline statement.

Mouse models

Both the *APP/PSEN1* and TauD35 mice used in this thesis were generated on a C57Bl/6 background by GlaxoSmithKline (UK). The *APP/PSEN1* mice are either homozygous or heterozygous transgenic for the human *APP* Swedish (K670N/M671L) mutation and *PSEN1* M146V mutation under the *Thy1* (Thy-1 T-Cell Antigen) promoter (Howlett et al., 2004; Matarin et al., 2015). The TauD35 mice are heterozygous transgenic for human microtubule-associated protein tau of P301L mutation under the CaMKIIα (Calcium/Calmodulin-dependent protein kinase II-alpha) promoter (Matarin et al., 2015; Joel, PhD dissertation, 2015).

All adult mice used were male for IHC and RT-qPCR. Mice were weaned at 21 days and then group-housed in individually ventilated cages under standard housing conditions with 12-hour light/dark cycle, environment enrichment, and *ad libitum* access to food and water. Housing materials were changed weekly. Age-matched C57Bl/6 mice housed under the same conditions were used as wildtype controls. Ear- and tail-samples were always collected for genotyping with standard PCR. For the TauD35 mice, an additional transgene copy number test was performed with TaqMan® qPCR

using uniquely designed TaqMan® primers/probes for the CaMKIIα promoter sequence by Stuart Martin (Head of the Molecular Biology Unit at UCL).

Primary microglial culture

Primary microglial cultures were generated from cerebral cortices and hippocampi of 1-3-day-old wildtype C57Bl/6 mice following an adapted protocol of Schildge et al. and Saura et al. (Saura et al., 2003; Schildge et al., 2013). For each independent preparation of primary microglial culture, brains of 4-6 pups from one litter of neonatal mice were dissected and pooled to make the cell suspension. On average, around 3,000,000 cortical and hippocampal cells per pup were obtained. Specifically, after decapitation, the brain was quickly collected and transferred to ice-cold HBSS. The cortices and hippocampi from each brain were then dissected, with all other brain regions, meninges, and blood vessels removed. Following mechanical and chemical (HBSS with 0.25% Trypsin) dissociation, cells were centrifuged, collected and seeded (at a density of 120,000 cells/cm^2) in poly-d-lysine coated flasks with a mixed glial culture medium (high glucose DMEM with 10% heat-inactivated Fetal Bovine Serum, 100 U/ml Penicillin and 100 µg/ml Streptomycin). Cells were cultured at 37°C in humidified 5% CO_2 / 95% O_2 air and the medium was changed every 3 days. After around 19-23 days when the mixed glial cells achieved confluency, a mild trypsinization method (incubation with DMEM with 0.05% Trypsin and 0.2 mM EDTA for 30-45 minutes) was applied to purify the primary microglia by removing the astrocytic cell layer. Isolated primary microglial cells were collected and seeded in poly-d-lysine coated 6-well plates or 24-well plates at a density of 40,000-100,000 cells/cm^2 depending on the following different experiments. Pure primary microglia were cultured under the same conditions as the mixed glial culture, and experiments were performed around 24 hours after isolation.

BV2 cell culture

BV2 cells, a murine microglial cell line, were kindly provided by Dr. Jennifer Pocock. Cells were cultured in medium containing DMEM with 10% heat-inactivated Fetal Bovine Serum, 2mM L-glutamine, 100U/ml Penicillin, 100µg/ml Streptomycin, and 1% Mycoplasma removal agent (AbD Serotec), and passaged every 2-4 days (avoiding confluency of more than 90%). Prior to experiments, BV2 cells were collected with Accutase (Sigma, A6964), and seeded on 6-well plates at a density of around 10,000 cells/cm^2 for testing siRNA transfection.

Culture treatments

siRNA treatment

Three siRNAs that target mouse *Trem2* (Ambion; siRNA No.1 sequences: sense 5'-CCCUCUAGAUGACCAAGAUtt-3', antisense 5'-AUCUUGGUCAUCUAGAGGGtc-3'; siRNA No.2 sequences: sense 5'-GCGUUCUCCUGAGCAAGUUtt-3', antisense 5'-AACUUGCUCAGGAGAACGCag-3'; siRNA No.3 sequences: sense 5'-GCACCUCCAGGAAUCAAGAtt-3', antisense 5'-UCUUGAUUCCUGGAGGUGCtg-3') and one non-targeting siRNA used as a control (Ambion, Catalog No. 4457287) were suspended in nuclease-free water to make 20 µM siRNA solutions and stored at -20°C. BV2 cells were used to test these three *Trem2* siRNAs and the siRNA No. 2 and No. 3 were selected for *Trem2* knockdown in primary microglia (See Chapter 3, figure 3.2 A).

Primary microglia were transfected with either *Trem2* siRNA or the non-targeting negative control siRNA using a transfection reagent Lipofectamine RNAiMax (Invitrogen), following the manufacturer's instructions. For 6-well

culture (used for the RNA study), 12.5 pmol siRNA with 3.75 µl Lipofectamine was applied per well; for 24-well culture (used for the protein study and phagocytosis assay), 2.5 pmol siRNA with 0.75 µl Lipofectamine was applied per well. The siRNA/Lipofectamine ratio used per well was 1 pmol siRNA : 0.3 µl Lipofectamine. Cells were harvested 72±2 hours after transfection.

LPS or IL4 treatment

For the microglial activation study, primary microglia transfected with either *Trem2* siRNA or the negative control siRNA were treated with 1 µg/ml LPS (Lipopolysaccharides; Sigma, L4391) around 3, 6, or 24 hours before harvest, or 20 ng/ml IL4 (Interleukin 4; PeproTech, 214-14) around 24 or 48 hours before harvest.

Phagocytosis assay

The phagocytosis assay using the pHrodo Green *E. coli* BioParticles Conjugate for Phagocytosis (Invitrogen, P35366) was adapted from the Invitrogen instructions and Kleinberger et al. (Kleinberger et al., 2014). In brief, purified primary microglia were cultured on 24-well plates at a density of around 50,000 cells/cm^2 (100,000 cells/well) and transfected with either *Trem2* siRNA or the negative control siRNA. After 72 hours, microglia were treated with 50 µg pHrodo-conjugated *E.coli.* per well for 1 hour at 37°C. Cells pre-incubated with 10 µmol Cytochalasin-D for 30min prior to the phagocytosis assay were used as a negative control. Cells were re-suspended off the plate with PBS after the assay, and then washed and collected in an ice-cold FACS buffer (PBS without $Ca^{2+/}Mg^{2+}$, with 0.5% BSA, 0.05% Sodium Azide and 2 mM EDTA). Collected microglia were assessed (10,000 cells counted per sample) by flow cytometry (FACSCalibur running CellQuest Pro; Becton Dickinson, UK) with excitation at 488 nm and emission at a range of 500-535 nm. Following identification of single microglial cells

with the expected size and granularity by forward (FSC-H) versus side (SSC-H) scatter of light, microglia with different amounts of phagocytosed fluorescent *E.coli* and thus with different levels of fluorescent intensity were plotted and analyzed using Flowing software (developed by Perttu Terho, Turku Centre for Biotechnology, Finland; www.flowingsoftware.com).

Molecular biology and immunohistochemistry

Mouse brain tissue extraction for gene expression analysis

Mouse brains were rapidly dissected on ice right after decapitation, and hippocampi were then collected, snap frozen on dry ice and stored at -80°C. Prior to RNA purification, hippocampi were homogenized using a homogeniser in QIAzol RNA lysis reagent (Qiagen) and total RNA was isolated with miRNAeasy columns (Qiagen) following manufacturer's instructions, RNA was aliquoted and stored at -80°C.

Primary microglia lysing for gene expression and protein analysis

For gene expression analysis, primary microglia were washed with ice-cold PBS three times and then lysed in ice-cold QIAzol RNA lysis reagent. Lysed cells were snap frozen on dry ice and stored at -80°C. Prior to RNA purification, the samples were homogenized using a 1ml syringe and a G21 needle. Total RNA was isolated using a miRNAeasy columns (Qiagen) following manufacturer's instructions, RNA was aliquoted and stored at -80°C.

For cellular protein lysing, primary microglia were washed with ice-cold PBS three times and then lysed in 2X Laemmli dye. Lysed cells were boiled at 95°C in a heating block for 5 minutes before storage at -20°C.

For ELISA, conditioned primary microglial media were collected and centrifuged to remove cell debris, and then stored at -20°C.

RNA purification and cDNA preparation

Total mRNA from the each sample was purified with the miRNeasy Mini Kit (Qiagen) following manufacturer's instructions. The quality and concentration of RNA was assessed with a NanoDrop Spectrophotometer (Thermo Scientific), with the A_{260}/A_{280} ratio typically around 2. RNA samples were aliquoted and stored at -80°C before use.

The same amount of RNA from each sample was first treated using DNase I (Amplification Grade, Invitrogen) plus RNaseOUT (Invitrogen). The reverse transcription reaction was then performed using the High Capacity cDNA Reverse Transcription Kit with RNase Inhibitor (Applied Biosystems) following the manufacturer's instructions, in parallel with a negative control lacking the reverse transcriptase. The cDNA samples were stored at -20°C.

Primer design and test

Primers were designed to span at least two exons and tested for homology against the entire transcriptome using Primer-BLAST (NCBI) and ordered from Eurofins MWG Operon. All primers were tested for specificity by performing a standard PCR reaction and resolving the products on a 3% agarose gel with ethidium bromide, followed by a quantitative RT-PCR reaction to obtain the linearity range for primers, calculate primer efficiency and test primer specificity using a "melt-curve" analysis.

RT-qPCR

The cDNA samples were tested in triplicates with a reverse-transcriptase (RT) lacking control in a 96-well plate using a CFX96 system (BioRad), with each 20 µl reaction containing the cDNA dilution, 0.25 µM of forward and reverse primers, and SYBR Green PCR Master Mix (Bio-Rad). Cycling conditions were: 95°C-3 min, 40 cycles of [95°C-10 sec, 58°C-30 sec and 72°C-30 sec], and then 72°C-5 min. A melt curve was generated by heating from 60 to 90°C with 0.5°C increments and 5 sec dwell time. All RT-qPCR reactions were checked for a single peak with the "melt-curve" analysis signifying a single PCR product. The raw cycle threshold (CT) values of target genes (mean of the triplicates for each sample) were normalized to *Rps28* or *Aif1* CT values for each sample depending on different experiments.

ELISA of secreted TNF-alpha by primary microglia

The TNF-alpha levels in the primary microglial supernatants were quantified using Quantikine® Mouse TNF-alpha ELISA kit (R&D Systems, MTA000B), following the manufacturer's instructions. In general, equal volumes of cell supernatants together with provided buffer were loaded in duplicate to the ELISA microplate, and incubated for 2 hours at room temperature. Following five times of washing, they were then incubated with the Horseradish peroxidase conjugated mouse TNF-alpha for another 2 hours at room temperature. The microplate was washed again and incubated with a Substrate solution prepared with chromogen (tetramethylbenzidine) and hydrogen peroxide for 30 minutes, before addition of a Stop solution with hydrochloric acid. Then the colour was read at 450 nm using a plate reader (BioTek, EL800) and the TNF-alpha concentrations in microglial supernatants were calculated from the standard curve. To account for the differences in the cell number between different wells of microglia, cell lysates were collected parallel with the supernatants from the same wells and then tested for a housekeeping protein HSPA9 (heat-shock protein 9) by Western blot, which

was used for normalization of TNF-alpha levels. The normalization factors were created by setting the density measure for the HSPA9 band of the negative control as 1 and calculating the ratios of the density measures for other samples versus the negative control. Then the TNF-alpha ELISA raw data were normalized to the normalization factor for each sample.

Cytokine proteome profile

The relative differences of 40 different cytokines / chemokines in primary microglial supernatants were tested with the Proteome Profiler Mouse Cytokine Array Panel A (R&D Systems, ARY006), following the manufacturer's instructions. The nitrocellulose membranes with spotted capture antibodies were washed in provided buffer and then blocked for 1 hour at room temperature. Membranes were next incubated with supernatant samples (for each treatment condition, 50µl of supernatants from 4 independent preparations were pooled together) mixed with a cocktail of biotinylated detection antibodies overnight at 4°C. Following washing three times, membranes were sequentially incubated with Streptavidin-HRP and chemiluminescent detection reagents. The chemiluminescence signal density was quantified by use of ImageLab software (v5.2, BioRad). To account for the differences in the cell number between different wells of microglia, cell lysates were collected parallel with the supernatants from the same wells and then tested for a housekeeping protein HSPA9 by Western blot, which was used for data normalization.

Western blotting of HSPA9 in primary microglia

Cellular protein samples from primary microglia were loaded onto 15% polyacrylamide gels and resolved by sodium dodecyl sulfate polyacrylamide gel electrophoresis (SDS-PAGE). A molecular weight ladder (BioRad) was

used for band identification. Then proteins were transferred to a 0.45μm nitrocellulose membrane (BioRad) by wet electro-transfer overnight.

Membranes were washed in Tris-buffered saline (TBS; 30 mM NaCl and 30 mM Tris [pH 7.4]) for 10 minutes, and then blocked in TBS with 0.1% Tween-20 (TBST) and 5% non-fat milk for 1 hour at room temperature. Membranes were then probed with a monoclonal HSPA9 antibody (BioLegend, MMS-5164, raised from mouse) that was 1/1000 diluted in blocking buffer overnight at 4°C. Following three washes with TBST, membranes were then incubated with a Horseradish peroxidase conjugated secondary antibody specific to mouse (Jackson ImmunoResearch) that was 1/10,000 diluted in blocking buffer for 1 hour at room temperature. Membranes were finally washed 3 more times, and the Horseradish peroxidase signals were then revealed with enhanced chemiluminescence detection (ECL, BioRad). Image acquisition and densitometric analysis was performed using ImageLab (v5.2, BioRad).

Mouse brain section preparation for immunohistochemistry

Mice were transcardially perfused with PBS, followed by 4% paraformaldehyde (PFA), under deep anaesthesia with Euthatal. Intact brains were removed, post-fixed in 4% PFA for 24 hours. Brains were then transferred into 30% sucrose for cryoprotection and sectioned (transverse to the hippocampus) to 30 μm sections using a frozen microtome (Leica). Serial sections were collected ~720 μm apart, and stored in PBS with 0.02% Sodium Azide. For each batch of immune-staining, a minimum of 3 sections were used for each mouse.

Immunohistochemistry

Free-floating sections were permeabilized with 0.3% Triton-X 100 in PBS and blocked with blocking solution (8% horse serum in PBS with 0.3% Triton-X 100) for 1 hour at room temperature. Primary antibodies (listed in Table 2.1) were diluted in blocking solution and sections were incubated with the diluted primary antibody overnight at 4°C. Sections were then washed with PBS-Triton-X100 three times and incubated for 2 hours at room temperature in appropriate secondary antibody dilutions in blocking solution. After three washes with PBS and staining with DAPI (1:10,000), sections were mounted on SuperFrost Plus slides (Fisher) with Fluoromount G (Scientific Biotech) and stored at 4°C until imaging.

Immunocytochemistry

Primary microglia plated on poly-d-lysine coated coverslips were fixed with 2% PFA for 15 minutes at room temperature, followed by five washes with PBS. Coverslips were then stored in PBS with 0.02% Sodium Azide at 4°C. Prior to immune-staining, coverslips were washed in PBS for 10 minutes and blocked for 1 hour at room temperature with 8% horse serum diluted in PBS with 0.125% Triton-X 100. Coverslips were then incubated overnight at 4°C with IBA1 antibody (Wako, 019-19741) 1:1000 diluted in the blocking solution. After primary antibody incubation, coverslips were washed three times with PBS and then incubated for 2 hours at room temperature in the secondary antibody dilution in blocking solution. After three washes with PBS and staining with DAPI (1:10,000), coverslips were mounted on SuperFrost Plus slides (Fisher) with Fluoromount G (Scientific Biotech) and stored at 4°C until imaging.

Table 2.1

Primary Antibody	Target	Supplier	Dilution
IBA1	C-terminus of IBA1 (ionised calcium-binding adaptor 1)	Wako, 019-19741	1: 500
CD68	Mouse macrosialin	BioRad, MCA1957	1: 500
MHC-II	Mouse major histocompatibility complex class II, I-A and I-E subregion-encoded glycoproteins	eBioscience, 14-5321	1: 200

Table 2.1. Primary antibodies used in the present study. Details of their corresponding antigens, as well as suppliers and dilution used are indicated.

Imaging and analysis

As *APP/PSEN1* mice at late stages showed heavy accumulation of microglia around plaques, which made it difficult to analyze the IBA1 and CD68 co-staining with an epifluorescent microscope, we instead used a two-photon confocal microscope (Olympus BX50WI) with a 60X oil immersion objective and Olympus FluoView software 300, to image the IBA1 and CD68 staining in sections from *APP/PSEN1* mice and age matched wildtypes. Images (300μm x 300μm area) were taken in the DG (the inner blade) and CA1 regions of hippocampus by a z-stack scanning (around 16μm thick, 2μm steps). Images were analyzed with ImageJ software for microglial counting. Three sections were used to calculate the mean for each animal.

For the *APP/PSEN1* and TauD35 MHC-II staining and the TauD35 IBA1/CD68 co-staining, sections were imaged using an EVOS® FL Auto Cell Imaging System (Life technologies). Images of the whole hippocampal region were taken under a 20X objective by area-defined serial scanning. Images were then analyzed with Adobe PhotoShop CS6 software. For the IBA1 and CD68 staining in TauD35 mice, an area of 360μm x 360μm was defined in the DG (the inner blade) and CA1 regions of hippocampus for cell counting. For the MHC-II staining in both *APP/PSEN1* and TauD35 mice, quantification of all positive cells in the whole hippocampal region was performed. For comparison of microglia in the CA1 layers amongst *APP/PSEN1* and TauD35 mice, an area of 240μm x 120μm was defined for quantification in each layer of the hippocampal CA1 region. Three sections were used to calculate the mean for each animal.

Coverslips were imaged using an EVOS® FL Auto Cell Imaging System (Life technologies) under a 20X objective. Two coverslips per sample were used and three fields of view (480μm x 360μm) per coverslip were taken. $IBA1^+$ cells and DAPI were counted with Adobe PhotoShop CS6 software and the microglial purity was calculated as a percentage of the IBA1 cell counts versus the DAPI counts in the same field of view.

Statistics

Data are shown as Mean ± SEM. The sample size (n) represents the number of independent experiments for Chapter 3 and the number of mice for Chapter 4 and 5. All statistics were performed using Microsoft Excel and Prism v6.2 (Graphpad). For the primary microglial gene expression changes with *Trem2* knockdown versus the non-targeting siRNA control, single gene expression level was normalized as a percentage of the control group within each independent microglial culture preparation, and then a one-sample t-test was conducted for statistical analysis. For the LPS or IL4 treatment experiments,

to assess the impacts of *Trem2* knockdown and LPS/IL4 treatment on the gene expression, each sample was normalized as a percentage of the non-targeting siRNA, non-LPS/IL4 treated control within each independent microglial culture preparation, and then two-way ANOVAs were conducted with multiple comparisons when appropriate. For the phagocytosis experiment, paired t-test was used to compare the *Trem2* knockdown group and the non-targeting siRNA control group (samples from the same microglial culture preparation were paired). For other experiments, differences between two group means were analyzed using Student t-tests, while two-way ANOVAs (with multiple comparisons when appropriate) were used to compare data with multiple factors, such as age and genotype. Differences were considered significant if $p<0.05$.

Chapter 3

Acute knock-down of *Trem2* in primary microglia impairs phagocytosis and anti-inflammatory functions

Introduction

TREM2 is predominantly expressed by microglia in the brain and implicated in neurodegenerative diseases, particularly in AD, but not exclusively. In this thesis, I developed a strategy to investigate the role of microglial genes that have been shown to have risk factor variants in GWAS studies expressed in microglia using primary cultures and acute knock-down of gene expression using RNAi. I then used this strategy to explore the effects of acute *Trem2* expression deficiency on primary microglia at the transcriptional and functional levels, especially when polarized towards the pro-inflammatory or anti-inflammatory phenotypes.

Evidence from *in vitro* studies has accumulated to support the role of TREM2 in inhibiting inflammation and phagocytosis. It was firstly reported in a study using primary microglia transduced with flag-tagged TREM2 that cross-linking of TREM2 stimulated microglial chemotaxis and phagocytosis of fluorescent beads (Takahashi *et al.*, 2005). They also showed that *Trem2* knock-down via lentiviral strategy increased pro-inflammatory gene expression and decreased phagocytosis of labeled apoptotic neuronal membranes in the primary microglia stressed with co-culture of apoptosis-induced primary neurones. TREM2 was also found to inhibit LPS-induced pro-inflammatory markers up-regulated in primary alveolar macrophages *in vitro* (Gao *et al*., 2013) and the BV2 microglial cell line (Zhong *et al.*, 2015). With particular respect to AD,

phagocytosis of Aβ was found to be impaired due to reduced mature TREM2 cell surface expression in studies with primary microglia from *Trem2* knockout mice and *Trem2* mutated microglial cell lines (Kleinberger *et al.*, 2014; Xiang *et al.*, 2016). Recently, it was further shown that apolipoproteins acted as ligands of TREM2 to facilitate microglial phagocytosis of Aβ and apoptotic neurons (Atagi *et al.*, 2015; Yeh *et al.*, 2016). In general, it suggests that *Trem2* deficiency exacerbates microglial pro-inflammatory activation in response to various stimuli, and accompanied by impaired phagocytosis.

In this thesis, I not only further validated the effects of *Trem2* deficiency on microglial phagocytosis and pro-inflammatory responses, but I also particularly studied its effects on microglial polarized to the anti-inflammatory phenotype. The current studies have not addressed the anti-inflammatory roles of TREM2 well, and I decided to test these functions in the primary microglia. Importantly, I employed the primary microglial culture from wild type mice and induced acute *Trem2* knock-down, after the microglia developed normally *in vivo* allowing us to study more direct effects of TREM2, not diluted by compensatory changes that may occur during chronic *Trem2* inhibition, as in *Trem2* knock-out studies. This system also allowed investigation of the regulation of microglial *Trem2* expression upon different stimulations, and the effects of temporal *Trem2* decreased expression on a variety of microglial fates assessed by gene expression and functional assays. In order to understand further mechanisms regulated by TREM2, I also initiated experiments to identify novel pathways that are affected by TREM2 in this model.

Hypotheses and aims

1. It is hypothesized that *Trem2* expression is dynamically regulated in microglia to adjust for different functional requirements in response to different stimuli. Aim: using LPS and IL4, to induce pro- and anti-inflammatory activation of microglia, and investigate the *Trem2*

expression change along with the time course of stimulation.

2. *Trem2* deficiency, even acutely induced, could result in microglial gene expressional profile and functional changes. Aim: to inhibit *Trem2* acutely using RNAi to investigate the effects of *Trem2* deficiency on microglial gene expression and phagocytosis.
3. TREM2 suppresses pro-inflammatory functions of microglia, and supports anti-inflammatory roles. Aim: to investigate whether the *Trem2* deficiency result in impairment or dys-regulated microglial pro- and anti- inflammatory responses using LPS and IL4 as stimulators of these fates.

Results

Establishment of an in vitro model of acute Trem2 knock-down

To specifically elucidate the implications of acute *Trem2* deficiency in robustly developed microglia, I established an *in vitro* model where primary microglia collected from P1-3 newborn mice (after normal embryonic development) were kept in mixed glial cultural conditions to fully develop for ~21 days before isolation and acute *Trem2* knock-down (figure 3.1 A). The generation of primary microglia is described in detail in the 'Materials and Methods' chapter.

To induce acute *Trem2* knock-down, a siRNA against *Trem2* was applied accompanied with Lipofectamine RNAiMax ~24 hours after pure microglia were isolated from the mixed glial culture **(the knock-down group)**. Cells in the same plate treated with a non-targeting siRNA and Lipofectamine were used as a control **(the control group)**. Primary microglia were harvested ~72 hours after siRNA was applied for analysis. To induce classical pro-inflammatory activation or alternative anti-inflammatory activation, cells were treated with LPS or IL4 at certain time points before harvest (figure 3.1 A).

The purity of our primary microglial culture was validated (97.22±0.32%) via immunocytochemistry by IBA1 and DAPI double-staining (figure 3.1 B). Additionally, consistent with Saura and colleagues' description (Saura *et al.*, 2003), the majority of the microglia showed a typical elongated morphology (bipolar or unipolar), with a small proportion of amoeboid as well.

In order to validate the capacity of the microglial culture to be polarized in the direction of either pro- or anti- inflammatory phenotype, LPS or IL4 was applied and gene expression of typical pro-inflammatory (*Tnf* and *Il1b*) or anti-inflammatory (*Arg1* and *Tgfb1*) genes was analyzed via RT-qPCR (figure 3.1 C). Microglia without LPS expressed low transcriptional levels of *Tnf* and *Il1b*; while with LPS treatment we observed a remarkable increase in the mRNA levels of *Tnf* and *Il1b* (presented as early as 3 hours after LPS application, and consistently >600-fold up-regulation for *Tnf* and >4000-fold for *Il1b* at 24 hours). In contrast, IL4 treatment induced a significant time-dependent up-regulation of the *Arg1* and *Tgfb1* expression (figure 3.1 C). *Arg1* expression, undetectable in our non-stimulated microglia, reached levels well above detection threshold at 24 hours and by 48 hours expression levels had further doubled. Tgfb1 expression showed around 150% up-regulation at 24 hours and 200% at 48 hours. These expected changes in *Tnf* and *Il1b*, and *Arg1* and *Tgfb1*, validate that LPS and IL4 can be used in this system of primary microglia to promote a pro-inflammatory and anti-inflammatory fate respectively.

Figure 3.1

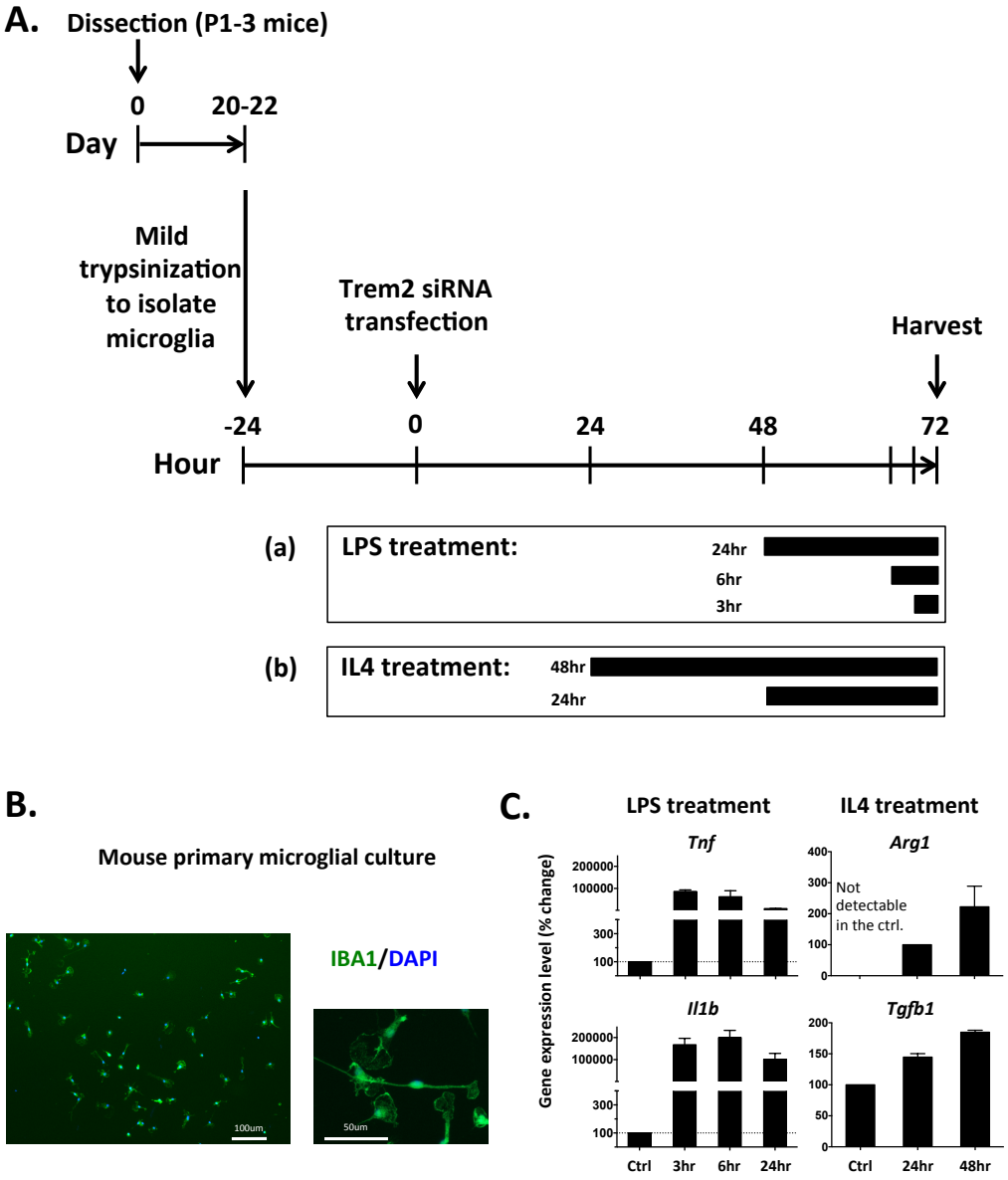

Figure 3.1. Establishment of our *in vitro* primary microglial model of acute *Trem2* knock-down. (A) Schedule of the *in vitro Trem2* knock-down model. **(B)** Primary microglia were stained with IBA1 and DAPI. The purity of microglia was calculated as the percentage of IBA1 positive cells relative to all nuclei visualized by DAPI staining. A higher-magnification image showed the morphology of microglia *in vitro*. **(C)** Pro- and anti-inflammatory gene expression up-regulation in primary microglia with LPS or IL4 treatment respectively. Gene expression in each condition was calculated as a percentage versus that in the control cells within the same experiment. N = 3-6 independent experiments. Data shown as Mean ± SEM.

Acute Trem2 knock-down and subsequent transcriptional changes

To determine the efficiency of different *Trem2* siRNA sequences, *in vitro* tests using BV-2 cells were first performed. Transfected cells were sampled at 24 and 48 hours and assessed for *Trem2* expression levels by RT-qPCR (Figure 3.2 A). As expected, BV-2 cells with the non-targeting siRNA showed substantial *Trem2* mRNA expression at 24 hours, which further increased at 48 hours as the cells proliferated in culture. I tested three different siRNA sequences, and identified one siRNA (Sequence 2) that was highly effective, with >80% knock-down of *Trem2* transcription compared to the control. I thus decided to use this siRNA sequence in the following primary microglia experiments. The next effective siRNA against *Trem2* was Sequence 3, giving 50-60% knock-down of *Trem2*; this second siRNA was used to confirm key findings in the primary microglia were dependent on the levels of *Trem2* expression.

Although the microglial purity of the primary culture was as high as ~97%, I noticed a substantial loss in the microglial number after *Trem2* knock-down, which could result in a decrease of the proportion of microglia in the culture. As a potential measure of altered microglial proportions in culture, *Aif1* mRNA levels were also found to be largely decreased in the knock-down cells compared to the control, which however this was not observed in BV2 cells (figure 3.2 B). Therefore, to normalize the effect of the microglial proportion change in the cultures on the microglial mRNA levels, I use *Aif1* as the housekeeping gene to normalize the gene expression of microglia.

The *Trem2* knock-down in the primary microglia performed consistently well (figure 3.2 C), and an average of 71.27±1.01% decrease in the *Trem2* expression was obtained. To understand the genetic pathways regulated by TREM2, I then investigated the subsequent gene expression changes, if any, in the *Trem2*-knock-down microglia. I searched for genes that we previously found to be potentially implicated in AD in the same genetic network as TREM2 following a microarray study of AD mouse models (Matarin *et al.*, 2015), or genes that played an important role in microglial maintenance and

homeostasis. As the raw gene expression levels of the primary microglia showed a substantial variation among different batches of microglial preparations, I analyzed the relative changes compared to the control group within each preparation. Among the genes investigated, the *C1qa* expression level was not significantly changed in the knock-down group; however, I found that there was a significant down-regulation of the expression of genes *Cd68*, *Csf1r*, *Igf1*, *Spi1*, and *Pi3kcg*, albeit only by a small percentage, at 72 hours after siRNA transfection (figure 3.2 D).

Furthermore, to elucidate whether the gene expressional changes were due to *Trem2* knock-down or any off-target effects of the transfection, I performed an independent trial using an alternative *Trem2* siRNA sequence (Sequence 3). This alternative siRNA produced around 60% knock-down in the primary microglia (figure 3.3 A). I tested the expression change of two major genes I found significantly affected by *Trem2* knock-down using the first siRNA – *Igf1* and *Csf1r*. As shown in figure 3.3 B, the *Igf1* expression was consistently significantly down-regulated by both siRNAs in the model, and related to the levels of *Trem2* expression. While the significant *Csf1r* down-regulation I saw previously was not observed here, I did see the same trend of a decrease (figure 3.3 B), the lack of significance is likely due to a small sample size (n=3 independent cell preparations in combination with the small effect size). Overall, the two independent siRNA sequences against *Trem2* produced similar results suggesting that this RNAi approach to study TREM2 function is capturing at least some of the effects of TREM2 with limited non-specific effects of using RNAi. In total, acute *Trem2* knock-down produced a slight but significant change in the gene expression profile of microglia, which might result in a shift of microglial functional phenotype.

Figure 3.2

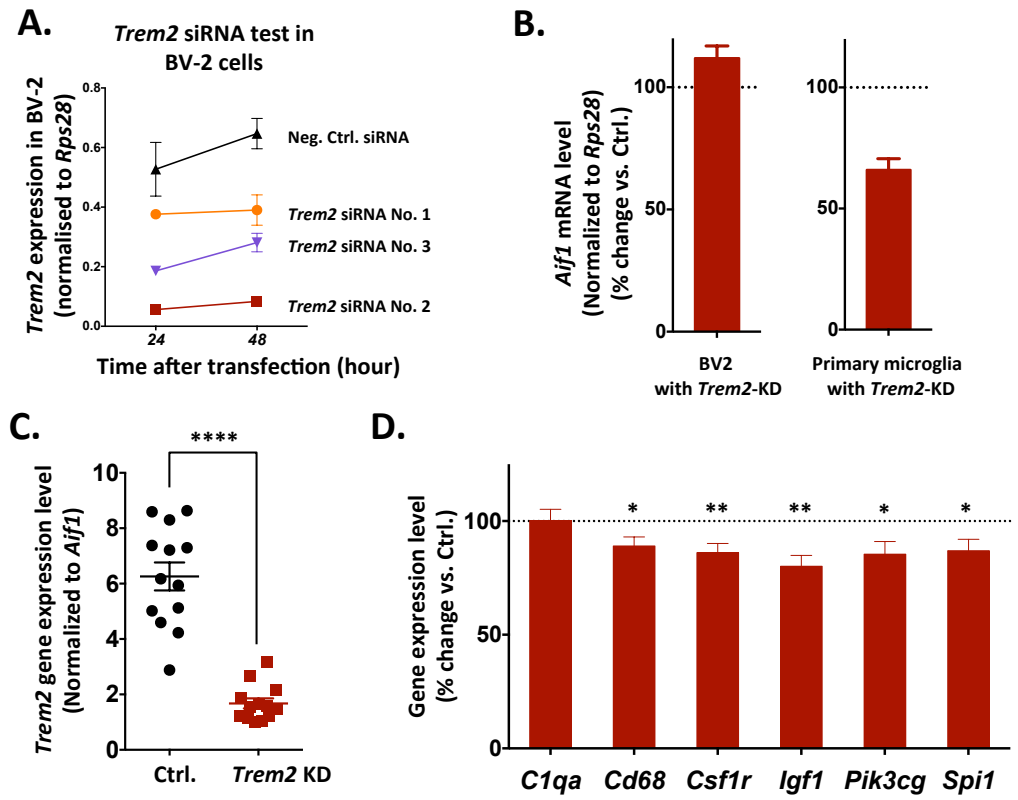

Figure 3.2. *Trem2* knock-down (>70%) and its influences on gene expression in primary microglia. (A) *Trem2* siRNAs were tested in BV2 cell culture (N=3). The siRNA No. 2 was chosen for the following *in vitro* acute *Trem2*-knock-down experiments due to its high knock-down levels. Key results were also tested with siRNA No. 3. **(B)** With *Trem2* KD there was a dramatic decrease in *Aif1* mRNA levels in primary microglia, which was not observed in the BV2 cell line. In order to account for any microglial cell loss after *Trem2* KD, the expression level of all other microglial genes was normalized to *Aif1*. **(C)** *Trem2* efficiency was tested with RT-qPCR at 72 hr after transfection. *Trem2* mRNA levels showed a 71.27±1.01% decrease. **(D)** Significant microglial gene expression changes relative to Control were observed at 72 hr after *Trem2* siRNA transfection. The mRNA levels of individual genes were first normalized to *Aif1*, and then the relative percentage change in KD was calculated versus Control from the same batch of cell preparation. N=13 independent cell preparations. Data shown as Mean ± SEM. One-sample t-test; * $p<0.05$, ** $p<0.01$.

Figure 3.3

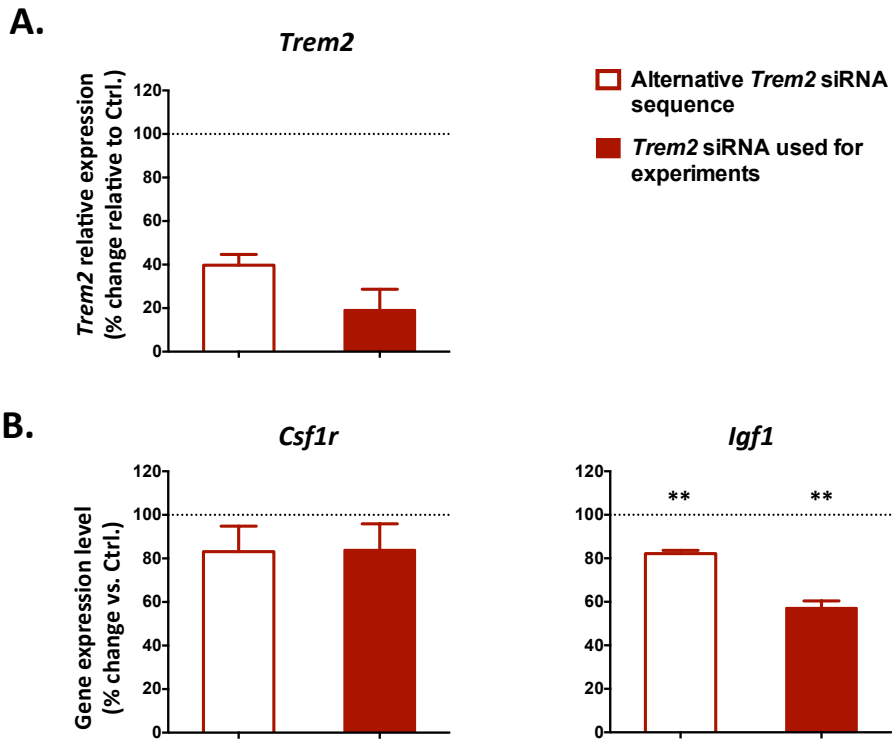

Figure 3.3. Effects of an alternative *Trem2* siRNA to validate the gene expression changes resulting from *Trem2* knock-down. (A) An alternative siRNA sequence (No. 3 from Figure 3.2A) was transfected into the primary microglia, and the previously employed siRNA (No. 2 from Figure 3.2A) was also used with cells from the same batch of preparation so that a comparison could be performed. Both siRNAs produced stable *Trem2* KD relative to Control when analyzed at 72 hours after transfection. (B) Two major genes we found to be affected by acute *Trem2* KD in the previous Figure 3.2 were analyzed via RT-qPCR in the alternative-siRNA-treated microglia. The *Igf1* downregulation was replicated in both conditions treated with either the alternative siRNA or the first siRNA, while *Csf1r* was not significantly changed by *Trem2* KD in this trial although a similar decreased trend was observed. N=3 independent experiments. Data shown as Mean ± SEM. One-sample t-test; ** $p<0.01$.

Attenuated phagocytosis of microglia with Trem2 knock-down

I then investigated if acute *Trem2* knock-down resulted in any functional change in the primary microglia, such as phagocytosis. Previous studies have already shown impaired phagocytosis in the primary microglia isolated from *Trem2* knockout mice and cell lines transfected with FTD-like or AD associated *TREM2* mutations (Kleinberger *et al.*, 2014). Here I investigated if acutely induced *Trem2* deficiency via RNAi in primary microglia affected the phagocytic activity. A phagocytosis assay was performed around 72 hours after siRNA transfection, testing the ability of microglia to phagocytose pHrodo (pH-sensitive fluorescent dye) conjugated *E. coli* and quantification of the microglia containing the fluorescent bacteria by fluorescence-activated cell sorting (FACS). As a negative control, phagocytosis was inhibited with Cytochalasin D (a potent inhibitor of actin polymerization) before addition of *E. coli*. We found that microglia with *Trem2* knocked down showed a significant reduction (~48.1±9.1%) of phagocytosis compared to the non-targeting siRNA treated microglia (figure 3.4).

Figure 3.4

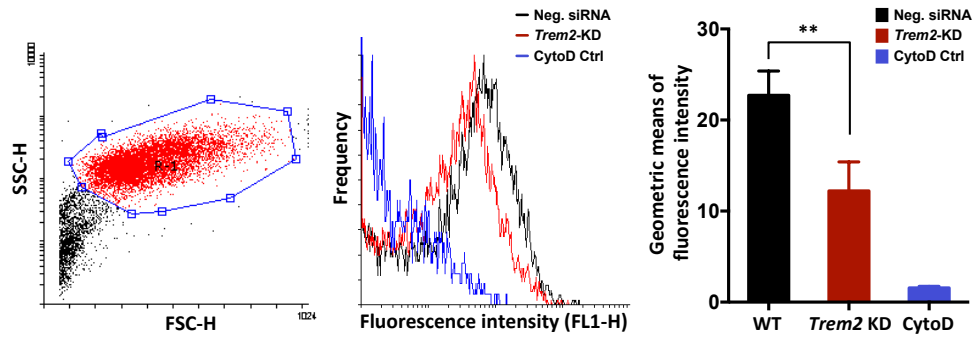

Figure 3.4. Impaired phagocytosis in primary microglia with acute *Trem2* knock-down. Primary microglia were transfected with *Trem2* siRNA or non-targeting siRNA for 72 hr, and then a phagocytosis assay was performed using pHrodo conjugated *E. coli* and the number of microglia containing fluorescence was quantified by FACS. As a negative control, phagocytosis was inhibited with 10 mM cytochalasin D 30 min before addition of *E. coli.* **Left and middle:** a representative experiment. **Left:** forward (FSC-H) versus side (SSC-H) scatter of light to allow identification of single microglial cells of the expected size and granularity (shown within the blue gate). **Middle:** frequency of microglia containing different levels of phagocytosed fluorescent bacteria. **Right:** Microglia with *Trem2* knocked down showed significant reduction (~48.1±9.1%) of phagocytosis. N=3 independent experiments. Data shown as Mean ± SEM. Paired t-test (paired within each culture preparation); ** $p<0.01$.

LPS stimulation dramatically suppresses Trem2 gene expression in primary microglia.

To begin to investigate how *Trem2* expression is regulated, microglia were stimulated with LPS to induce classical pro-inflammatory responses. I first found that, in the control cells, LPS treatment induced dramatic down-regulation of *Trem2* expression (figure 3.5 A), which was consistent with the previous findings shown with primary mixed glial cell culture and peritoneal macrophage cell cultures (Schmid et al., 2002). The time course analysis showed that the *Trem2* expression dropped to as low as around 40% of the non-stimulated cells from as early as 6 hours after LPS addition, and even lower at below 10% by 24 hours. This suggests that pro-inflammatory conditions might inhibit microglial *Trem2* expression and possibly functions as well, which might result in a temporary '*Trem2* deficiency' in microglia.

TNF-alpha and IL-1β are two typical pro-inflammatory markers that are upregulated in microglia upon LPS stimulation. The expression levels of *Tnf* and *Il1b* highly increased in our LPS-treated microglia from as early as 3 hours after LPS application. To investigate whether *Trem2* regulates this pro-inflammatory state in microglia, I knocked down *Trem2* expression and did not see significant changes in such upregulation of *Tnf* or *Il1b* at the transcriptional level (figure 3.5 B). This result was not surprising, and supported the finding that microglial *Trem2* expression was largely inhibited upon LPS stimulation. I further investigated if the protein level of TNF-alpha released from the microglia in response to LPS was affected by acute *Trem2* knock-down. Different from the transcriptional results, ELISA analysis of the microglial-conditioned medium showed that the production of TNF-alpha was significantly higher in the LPS treated *Trem2*-knock-down group than the control group with LPS (figure 3.6; $p<0.01$, Two-way ANOVA followed by Sidak's *post hoc* test). Collectively these findings show that pro-inflammatory stimuli such as LPS can suppress *Trem2* expression, and that by inhibiting *Trem2* expression the microglial cell can take on a stronger pro-inflammatory status, in this case producing more secreted TNF-alpha protein when *Trem2* expression is knocked down by RNAi.

Figure 3.5

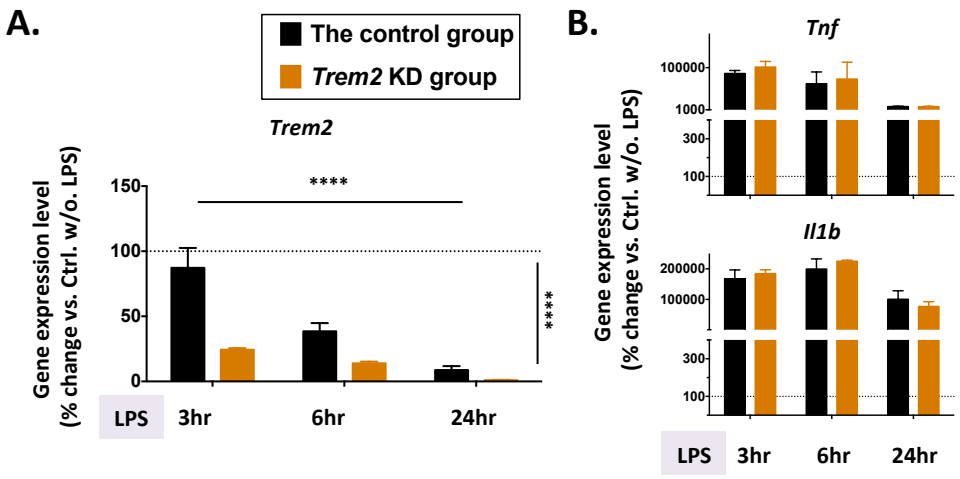

Figure 3.5. Remarkable *Trem2* suppression induced by LPS stimulation and no significant effects of *Trem2* knock-down on the pro-inflammatory gene upregulation. (A) *Trem2* gene expression showed a dramatic time-dependent decrease in the primary microglia with LPS stimulation. Gene expression levels were calculated as percentage changes relative to Control without LPS treatment from the same batch of culture preparation (dotted line at 100% representing levels of *Trem2* expression in Control without LPS). **(B)** *Tnf* and *Il1b* expression, as examples of pro-inflammatory genes, were largely up-regulated in primary microglia after LPS application. There was no significant difference between *Trem2* KD and Control.

N=3 (3hr), 3 (6hr), and 5 (24hr) independent microglial preperations. Data shown as Mean ± SEM. Two-way ANOVA followed by Sidak's *post hoc* test if there was significant interaction; Significant main effects of LPS incubation time and *Trem2*-KD indicated by horizontal and vertical lines respectively, post hoc test significance marked above individual groups, * $p<0.05$, ** $p<0.01$, *** $p<0.001$, **** $p<0.0001$.

Figure 3.6

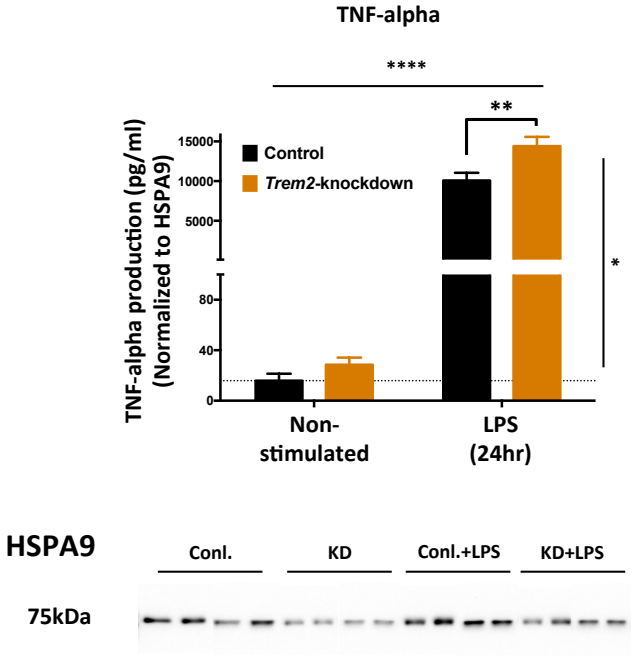

Figure 3.6. Increased TNF-alpha release from *Trem2* deficient primary microglia in response to LPS. ELISA analysis of the microglial conditioned medium showed that the TNF-alpha levels in the medium was significantly higher in the LPS-treated *Trem2*-KD group than in the LPS-treated Control group. As there was a potential change in the cell number under conditions of LPS or *Trem2* siRNA treatment, HSPA9 was employed as a housekeeping protein to normalize the TNF-alpha ELISA data. Cells in each well were harvested in 150µl Laemmli buffer, and then 20µl cell lysates of each well were loaded for HSPA9 Western blot analysis. The density values of bands were used to create normalization factors for TNF-alpha analysis. N=4 independent microglial preparations. N = 4 independent experiments. Data shown as Mean ± SEM. Two-way ANOVA followed by Sidak's *post hoc* test if there was significant interaction; Significant main effects of LPS treatment and *Trem2*-KD indicated by horizontal and vertical lines respectively, *post hoc* test significance marked above individual groups, * $p<0.05$, ** $p<0.01$, **** $p<0.0001$.

The expression levels of the microglial genes, which was tested in the previous section for *Trem2*-knock-down effects (figure 3.2), were also analyzed in response to the LPS conditions (figure 3.7). Genes such as *C1qa*, *Cd68 Csf1r*, and *Igf1,* showed a similar pattern of significant time-dependent down-regulation in the microglia with LPS stimulation. Expression of the *Spi1* transcription factor in the microglia with LPS showed at least a 2-fold increased level compared to that in the control group, which was observed to start as soon as from 3 hr after application, and maintain until at least 24 hr. *Pik3cg* was also up-regulated with LPS, but only observed at the very early stages (3 hr) of the LPS treatment. The gene expression changes caused by *Trem2*-knock-down, which I observed previously (figure 3.2 D), were masked in the LPS-treated cells, which is not unexpected given that LPS is strongly suppressing *Trem2* expression.

These data together suggested that microglia polarized to the classical pro-inflammatory phenotype exhibited largely suppressed *Trem2* gene expression, which in turn could inhibit TREM2-related functions. *Trem2* deficiency seemed to produce limited effects on the pro-inflammatory activation of microglia, although there is some evidence to suggest that inhibiting *Trem2* expression promoted a stronger pro-inflammatory response, particularly the levels of secreted TNF-alpha were significantly increased.

Figure 3.7

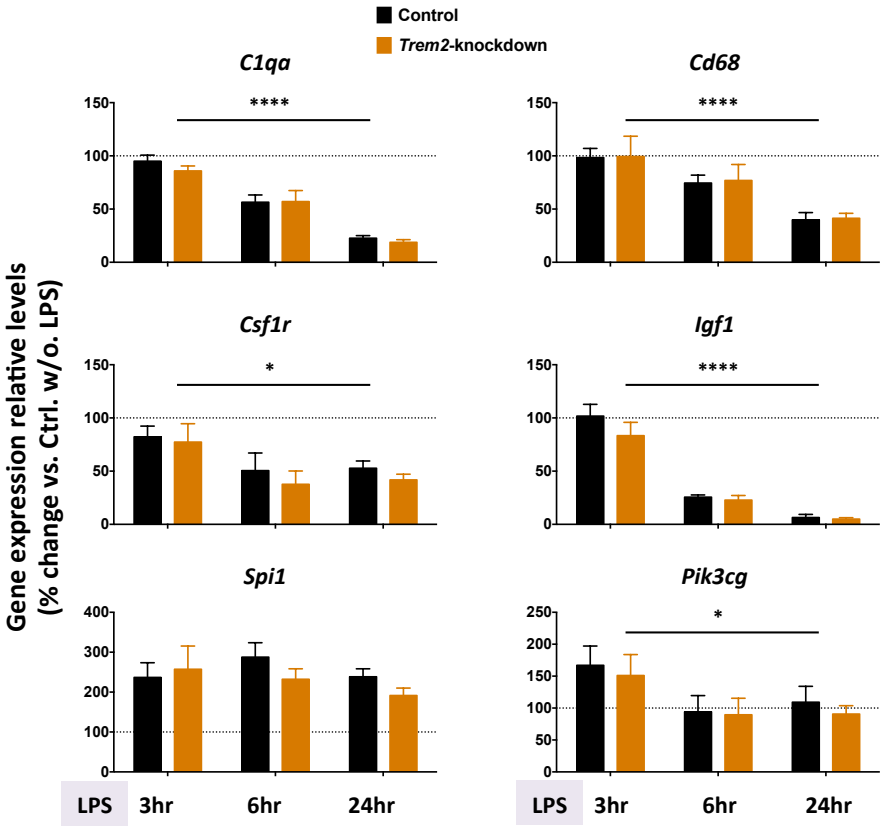

Figure 3.7. Changes of microglial gene expression in primary microglia with LPS. Microglial *C1qa*, *Cd68*, *Csf1r*, and *Igf1* expression showed similar time-dependent decreasing patterns in response to LPS treatment, although with different kinetics. *Spi1* expression showed around 2-fold up-regulation in response to LPS, which was observed to start at least from 3 hr after application and maintain at that level until 24 hr. *Pi3kcg* was also up-regulated with LPS, but only observed at the very early stage (3 hr) of LPS treatment. *Trem2* KD did not significantly affect the expression changes of these genes in response to LPS stimulation.

N=3 (3hr), 3 (6hr), and 5 (24hr) independent experiments. Gene expression levels were normalized to *Aif1* levels within samples, and then calculated as percentage changes relative to Control without LPS treatment from the same batch of culture preparation. Data shown as Mean ± SEM. Two-way ANOVA; Significant main effects of LPS incubation time and *Trem2*-knock-down indicated as horizontal and vertical lines respectively, no interactions between these two factors for all the genes in the figure here; * $p<0.05$, ** $p<0.01$, *** $p<0.001$, **** $p<0.0001$.

Trem2 is involved in microglial anti-inflammatory responses with IL4

Next I studied the effect of acute *Trem2* knock-down on the alternative anti-inflammatory activation of microglia. IL4 was applied to the cells with either siRNA against *Trem2* or the non-targeting siRNA and cells were analyzed at 24 hours and 48 hours after IL4 addition. I first found that *Trem2* expression exhibited a significant time-dependent up-regulation in response to IL4 treatment (figure 3.8 A). At 24 hours after IL4 application, the *Trem2* expression was still comparable to that of the non-stimulated control group, while at 48 hours it rose to 149.5±17.1% of the control. The *Trem2* knock-down group also showed a similar pattern in response to IL4, but as expected with significant lower levels than the control group.

I next investigated two anti-inflammatory markers *Arg1* and *Tgfb1* (figure 3.8 B). The *Arg1* gene expression was undetectable under the non-stimulated conditions by RT-qPCR. Upon IL4 treatment, expression was observed, and both the control and the knock-down groups showed a significant time-dependent up-regulation, and in particular, the *Trem2*-knock-down group exhibited significant lower *Arg1* up-regulation compared to the control group ($p<0.01$ for the main effect of IL4 treatment time, $p<0.05$ for that of *Trem2* knock-down, no significant interaction, Two-way ANOVA). Similarly, the *Tgfb1* expression also showed a time-dependent increase with IL4 stimulation, and a trend towards a significant effect of *Trem2* knock-down on such *Tgfb1* up-regulation ($p<0.001$ for the main effect of IL4 treatment time, and $p=0.059$ for that of *Trem2* knock-down, Two-way ANOVA). In total, acute *Trem2* knock-down attenuated the microglial anti-inflammatory gene up-regulation in response to IL4.

Furthermore, the gene expression levels of pro-inflammatory markers *Tnf* and *Il1b* were analyzed (figure 3.8 C). Both markers were expressed at relatively low levels in the non-stimulated control conditions, which were further decreased modestly with IL4 treatment. Significant differences between the control and the knock-down microglia were only observed in the *Il1b* levels ($p<0.01$ for the main effect of IL4 treatment time, $p<0.05$ for that of *Trem2*

knock-down, no significant interaction, Two-way ANOVA). The tendency for elevated Il1b with *Trem2* knock-down suggests that *Trem2* may be required to suppress pro-inflammatory function in response to anti-inflammatory cues.

Next to understand which genetic pathways are regulated by TREM2 in anti-inflammatory conditions I investigated the expression of the genes tested in previous sessions under the IL4 conditions (figure 3.8). The *C1qa* gene expression, which was not affected by *Trem2* knock-down in the non-stimulated state (figure 3.2 D), was upregulated in response to IL4 stimulation (~150-200% of the level in non-stimulated conditions), although there was no significant time-dependent change. Two-way ANOVA analysis showed a lower trend in the knock-down group than the control group under the IL4 conditions ($p=0.055$), and particularly a significant interaction between IL4 treatment and *Trem2* knock-down ($p=0.034$). Sidak's *post hoc* analysis displayed a significantly lower *C1qa* expression in the knock-down group than the control at 48 hours after IL4 application ($p=0.029$). The *Csf1r* gene expression under the IL4 condition, which upregulated by a similar percentage to *C1qa*, was found to be significantly lower in the knock-down group than in the control group ($p=0.029$, Two-way ANOVA). In contrast, the genes *Cd68* and *Igf1*, previously found to be downregulated by *Trem2* knock-down, showed significant time-dependent upregulation with IL4 treatment and no significant effect of *Trem2* knock-down was observed any more. Also, the gene expression of *Spi1*, *Pik3cg*, and another two AD-associated microglial genes *Abi3* and *Plcg2* were not significantly affected by *Trem2* knock-down under the IL4 condition. These data together suggested that the effect of *Trem2* expression on the microglial gene expression profile might be different depending on the activation phenotype of microglia, with higher levels of *Trem2* expression in response to anti-inflammatory phenotypes, and *Trem2* manipulation modifying the expression of a subset of genes increased with anti-inflammatory stimuli.

Figure 3.8

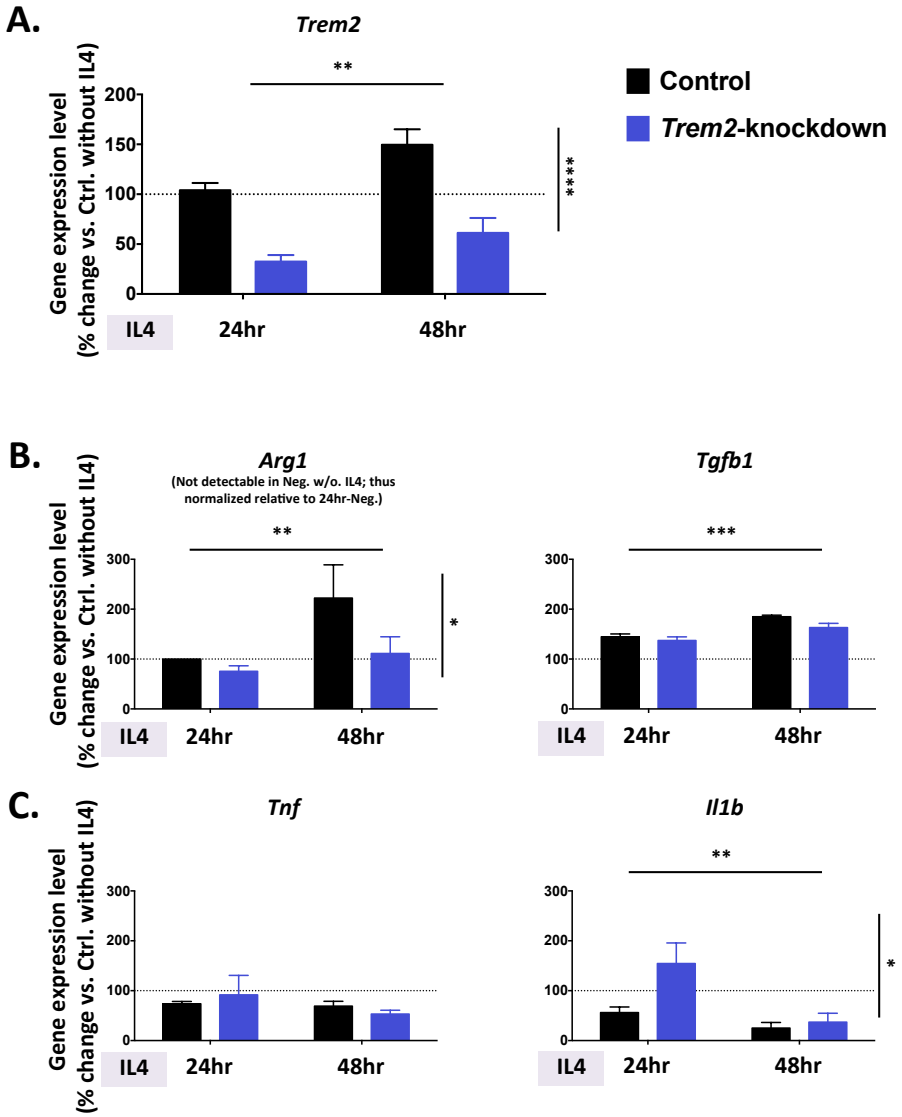

Figure 3.8. TREM2 is involved in the microglial anti-inflammatory response. **(A)** *Trem2* gene expression showed a significant time-dependent increase in primary microglia with IL4 stimulation. **(B)** *Arg1* and *Tgfb1*, as markers for the anti-inflammatory response, showed significant up-regulation with time after IL4 application. *Trem2* KD significantly decreased *Arg1* expression compared to Control. **(C)** Expression of the pro-inflammatory gene *Il1b* was inhibited with time after IL4 application; however, KD group was significantly higher than Control. No significant difference was observed for the *Tnf* expression. N= 6 (24 hr) and 4 (48 hr) independent experiments. Data shown as Mean ± SEM. Two-way ANOVA; Significant main effects of IL4 incubation time and *Trem2*-KD indicated as horizontal and vertical lines respectively, no interactions between these two factors for all the genes in the figure here; * p<0.05, ** p<0.01, *** p<0.001, **** p<0.0001.

Figure 3.9

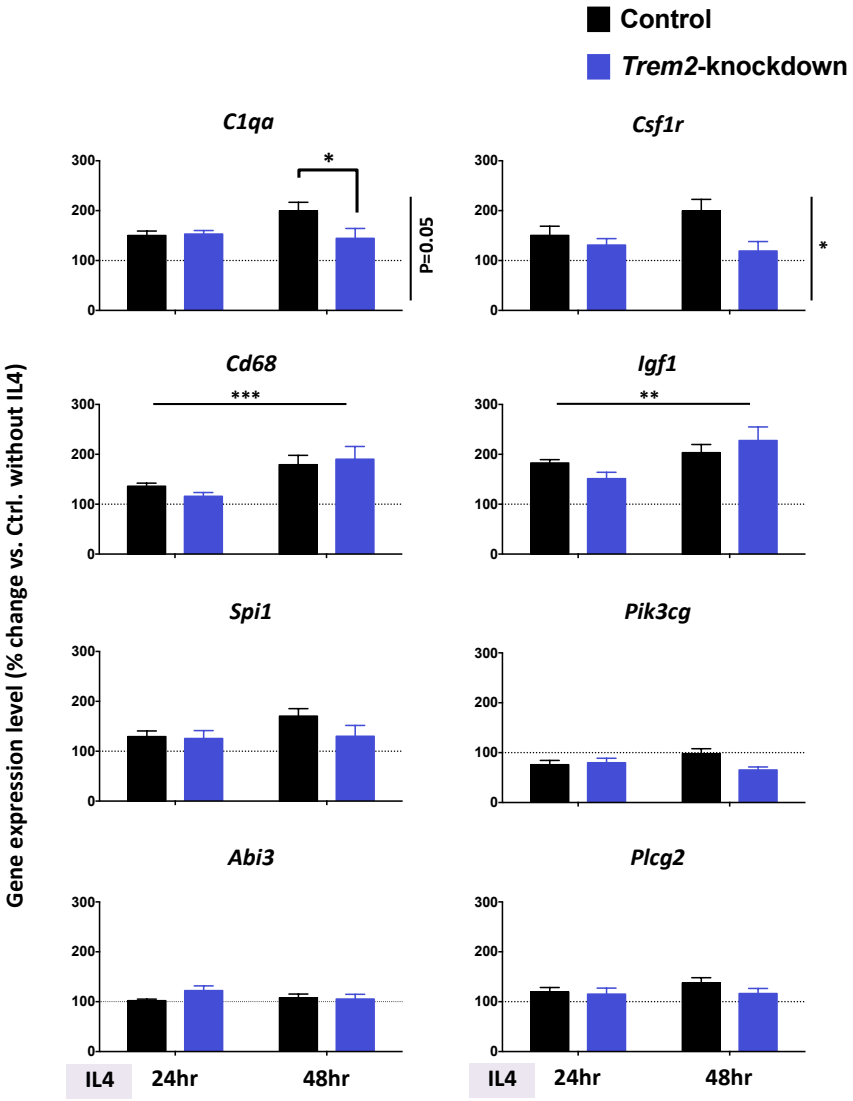

Figure 3.9. Gene expression changes in primary microglia with IL4 treatment. *C1qa, Cd68, Csf1r*, *Igf1*, *Plcg2,* and *Spi1* expression was found to be up-regulated with IL4 (determined by one-sample t-test). *Csf1r* was significantly lower in KD compared Control. There was also a significant interaction between IL4 treatment and *Trem2* KD for *C1qa* expression; Sidak's *post hoc* tests showed *C1qa* expression level was significantly lower in KD at 48 hr after IL4 application.

N= 6 (24 hr) and 4 (48 hr) independent experiments. Data shown as Mean ± SEM. Two-way ANOVA followed by Sidak's *post hoc* test if there was significant interaction; Significant main effects of IL4 treatment time and *Trem2*-knock-down indicated by horizontal and vertical lines respectively, *post hoc* test significance marked abov individual groups, * $p<0.05$, ** $p<0.01$, *** $p<0.001$, **** $p<0.0001$.

Effects of acute Trem2 knock-down on the cytokine and chemokine release of microglia in response to LPS or IL4

In order to identify further and potentially new pathways affected by acute *Trem2* knock-down on microglial LPS or IL4 induced activation, I used a Cytokine Array (a membrane-base sandwich immunoassay that allows us to detect a series of cytokines in parallel) to initially screen for cytokines and chemokines released from knock-down or control microglia stimulated with LPS or IL4. The conditioned culture supernatant samples of the same condition were mixed in equal volumes from four independent experiments, and performed the array in parallel. The raw data were normalized to the western blot signals of GRP75, a housekeeping protein, to account for the difference in the cell number among different conditions. With this array, we were able to test up to 40 different cytokines, although not all cytokines showed detectable signals. A summary of the cytokines / chemokines is listed in Table 3.1 and 3.2. What can be noticed is that most of the cytokines tested showed much higher levels in response to the LPS than in response to the IL4 so that they could not be analyzed at the same exposure time. Thus I only compared the *Trem2*-knock-down and control groups with the same stimulation.

The cytokine array probed with LPS-treated microglia showed dramatic signals of various pro-inflammatory cytokines such as TNF-alpha, CCL5, CXCL2, and CXCL10, suggesting the array was working well. The effect of *Trem2* knock-down on the cytokines released in response to LPS appeared modest (Table 3.1). As a control, this cytokine array panel also included TNF-alpha, for which we saw a 140-150% significant increase in LPS-treated *Trem2*-knock-down microglia versus LPS-treated control microglia using ELISA (Figure 3.6), compared to the 1.51-fold increase in TNF-alpha levels in the LPS-treated knock-down microglia versus LPS-treated control microglia using the cytokine array (Table 3.1), confirming the validity of this cytokine array panel. Besides TNF-alpha, we also found a series of cytokine / chemokines showing >1.3-fold (but <2-fold) increase in the LPS-treated knock-down microglia than the LPS-treated control microglia, such as CCL2,

CCL3, CCL4, CCL5, CXCL1, CXCL10, CXCL12, CXCL13, TIMP-1 and IL1-RA, while other cytokines detected in this condition showed comparable levels between knock-down and control groups. As we mixed the n=4 samples in the experiment, we could not perform statistics. The next step in these experiments would be to perform ELISAs on these top altered cytokines using the n=4 samples individually to enable us to confirm the cytokine array results using statistics.

As the cytokine signals were consistently much lower in the IL4-stimulated microglial medium than the LPS-treated, I had to increase the exposure time of detection to obtain analyzable signals. Different from the LPS cohort, I did observe more remarkable differences in some of the cytokines between the IL4-treated knock-down and the control groups (Table 3.2). The most potently increased chemokine was CXCL1, which showed a 6-fold change in the IL4-treated *Trem2* knock-down microglia compared to the IL4-treated control microglia. Also, CXCL10 and TIMP-1 production in IL4-treated microglia showed substantial difference (around 3-fold) between the knock-down and control groups. Furthermore, there was an array of cytokines / chemokines showing over 2-fold increase in the knock-down group compared to the control, such as CCL5, CXCL2, CXCL12, CXCL13, IL-1α and IL-1RA, and over 1.5-fold increase, such as CD54 and CCL2. Some classical pro-inflammatory markers detected in the LPS condition, such as IL-6, TNFα, and G-CSF, were not detectable in the IL4-treated microglia.

In total, my collective data provides strong evidence that acute *Trem2* knock-down affected the microglial cytokine release in response to the anti-inflammatory factor IL4, while its effects on the LPS-induced cytokine release seem relatively modest so far.

Table 3.1

Microglia with LPS for 24 hours

Cytokine/ Chemokine	Full name	Fold change (*Trem2* KD/Ctrl.)
CCL5	Regulated Upon Activation, Normally T-expressed, and Presumably Secreted; RANTES	**1.66**
CCL2	Monocyte Chemotactic Protein 1; MCP-1	**1.63**
CCL4	Macrophage Inflammatory Protein 1-beta; MIP-1β	**1.62**
CCL3	Macrophage Inflammatory Protein 1-alpha; MIP-1α	**1.58**
CXCL13	B-lymphocyte Chemoattractant; BLC	**1.51**
TNFα	Tumor Necrosis Factor, Alpha	**1.51**
CXCL1	Keratinocyte-derived Chemokine; KC	**1.50**
TIMP-1	Tissue Inhibitor of Metalloproteinase 1	**1.43**
CXCL12	Stromal Cell-derived Factor 1; SDF1	**1.42**
IL-1RA	Interleukin 1 Receptor, Alpha, Type I	**1.41**
CXCL10	Interferon-gamma-inducible Protein 10; IP10	**1.36**
IL-1α	Interleukin 1-Alpha	1.26
G-CSF	Granulocyte Colony-stimulating Factor	1.24
IL-6	Interleukin 6	1.08
CXCL2	Macrophage Inflammatory Protein 2; MIP2	1.06
CCL12	Monocyte Chemotactic Protein 5; MCP-5	0.72
sICAM (CD54)	Intercellular Adhesion Molecule 1	0.72

Table 3.1. Changes caused by acute *Trem2* knock-down in the cytokine and chemokine secretion in response to LPS stimulation. Microglial culture conditioned media samples of the same condition from 4 independent experiments were equally mixed, and a parallel cytokine array was performed to determine the difference between *Trem2* KD and Control microglia in response to LPS. The fold-change was listed as the average intensity of duplicate spots for *Trem2* KD relative to Control microglia. Cytokines /chemokines with >1.3-fold-change were in red.

Table 3.2

Microglia with IL4 for 48 hours

Cytokine/ Chemokine	Full name	Fold change (*Trem2* KD/Ctrl.)
CXCL1	Keratinocyte-derived Chemokine; KC	**6**
TIMP-1	Tissue Inhibitor of Metalloproteinase 1	**3.06**
CXCL10	Interferon-gamma-inducible Protein 10; IP10	**3.01**
CXCL13	B-lymphocyte Chemoattractant; BLC	**2.64**
IL-1α	Interleukin 1-Alpha	**2.41**
CXCL12	Stromal Cell-derived Factor 1; SDF1	**2.38**
CXCL2	Macrophage Inflammatory Protein 2; MIP2	**2.37**
CCL5	Regulated Upon Activation, Normally T-expressed, and Presumably Secreted; RANTES	**2.23**
IL-1RA	Interleukin 1 Receptor, Alpha, Type I	**2.12**
sICAM (CD54)	Intercellular Adhesion Molecule 1	**1.85**
CCL2	Monocyte Chemotactic Protein 1; MCP-1	**1.64**
CCL12	Monocyte Chemotactic Protein 5; MCP-5	0.89
CCL4	Macrophage Inflammatory Protein 1-beta; MIP-1β	0.86
CCL3	Macrophage Inflammatory Protein 1-alpha; MIP-1α	0.75
G-CSF	Granulocyte Colony-stimulating Factor	-
IL-6	Interleukin 6	-
TNFα	Tumor Necrosis Factor, Alpha	-

Table 3.2. Changes caused by acute *Trem2* knock-down in the cytokine and chemokine secretion in response to IL4 stimulation. Microglial culture conditioned media samples of the same condition from 4 independent experiments were equally mixed, and a parallel cytokine array was performed to determine the difference between *Trem2* KD and Control microglia in response to IL4. The fold-change was listed as the average intensity of duplicate spots for *Trem2* KD relative to Control microglia. Cytokines /chemokines with >1.3-fold-change were in red.

Summary

This chapter of the thesis focuses on studying two aspects, firstly, identifying the cellular functions of TREM2 in regulating different microglial activation phenotypes, and secondly, investigating how *Trem2* and other important microglial factors are regulated in response to pro-inflammatory and anti-inflammatory factors. I established an *in vitro* primary microglial model with acute *Trem2* knock-down via RNAi strategy. I found that acute *Trem2* knock-down induced significant down-regulation of an array of microglial genes, such as *Igf1* and *Csf1r*, and impairment of phagocytosis. Furthermore, I showed that *Trem2* expression was largely down-regulated in microglia with the M1 pro-inflammatory stimulus LPS, but up-regulated with treatment with the M2 anti-inflammatory cue IL4. *Trem2* deficiency produced only a limited effect on microglial pro-inflammatory responses, although there was some evidence that *Trem2* suppressed TNF-alpha secretion in response to LPS. In contrast, the M2 alternative phenotype expression in microglia was attenuated in *Trem2*-knock-down microglia. Additionally, *Trem2* knock-down also induced a higher level of chemokine secretion in response to LPS or IL4, which might suggest an increased signaling from microglia for activation and infiltration of other cell types such as endothelial cells and peripheral immune cells. Overall my data suggest that TREM2 plays an important role in microglial functions in inflammation resolution and suppression. In humans, accumulated pro-inflammatory stimuli might result in prolonged suppressed *Trem2* expression and function, which leads to a similar influence to that of acute *Trem2* knock-down in the model.

Chapter 4

Microglial gene expressional differences in transgenic mouse models of Amyloid-beta pathology versus Tauopathy

Introduction

The important role of TREM2 in regulating microglial gene expression and function *in vitro has been investigated*. Then the next question would be whether microglial *Trem2* expression changes in response to different components of AD pathology *in vivo*. In this chapter, I characterized the microglial gene expression changes by RT-qPCR in transgenic models of amyloid or tau pathology. I particularly investigated the *Trem2* gene expression related to the Aβ or tau pathology development in these mice. The mouse models were described in details in the Methods and Materials chapter.

Recent genome-wide association studies have identified a number of gene variants that influence AD risk, and are related to microglia. Examples of genes that contain SNPs and regulate innate immune cell functions in human AD from independent studies are *TREM2, CD33, PLCG2 and ABI3* (Griciuc et al., 2013; Guerreiro et al., 2013b; Jonsson et al., 2013; Malik et al., 2013; Sims et al., 2017), and consistently these genes were also found to show significantly increased expression in our previous www.Mouseac.org study in the *APP/PSEN1* amyloid mouse models as plaques started to deposit (Matarin *et al.*, 2015). In our study, we performed microarray and network analysis using the same models to examine the gene expression profile associated with either Aβ or tau pathology. *Trem2* showed strikingly increased

expression (around 6-fold) in our amyloid mouse models, and formed a hub gene within a network of genes representing the immune system, also containing Plcg2, Abi3 and microglial genes like *Aif1* and *Cd68*. The expression of this module of immune genes showed an impressive correlation of 0.97 with the amyloid pathology, which suggests that *Trem2* and the module of genes, of which *Trem2* is a member, are key drivers of the amyloid pathology. The spectacular increase in the expression of this immune module in supported by significant increases in the number of microglia in our *APP/PSEN1* mice by immunohistochemistry.

However, at the time of that study we were not aware that the tau mice constituted two lines of mice with different transgene copy numbers and this would have increased the variation at any age tested. In this thesis I compared amyloid mouse models with different levels of pathology (high pathology homozygous *APP/PSEN1* mice and medium pathology heterozygous *APP/PSEN1* mice) to tau mouse models with different levels of pathology (high pathology high transgene-copy-number Tau mice and low pathology low transgene-copy-number Tau mice), to specifically investigate the expression changes of microglial genes in different activation states via RT-qPCR.

Pathology progression in the mouse models

The amyloid mice used here are two sublines of an *APP/PSEN1* mouse model – homozygous and heterozygous mice. The HO-*APP/PS1* mice start to show diffuse amyloid plaques around 2 months, but only from 4 months they tend to show true dense-core plaques in the hippocampus (Howlett *et al.*, 2008; Howlett and Richardson, 2009; Matarin *et al.*, 2015). The plaque deposition then further develops, and until 18 months of age most of the HO-*APP/PS1* mouse hippocampus is found covered with a huge amount of Aβ deposition (hence high amyloid pathology). The HE-*APP/PS1* line (Cummings et al., 2015; Matarin et al., 2015) shows a similar but slower pattern of Aβ

pathology development, with mature plaques starting to development around 8 months (hence medium amyloid pathology). No obvious neuronal loss is reported in this amyloid model, whereas a study from our lab shows early synaptic changes (Cummings *et al.*, 2015).

The tau model, TauD35, is a novel tauopathy model generated by GlaxoSmithKline (Matarin *et al.*, 2015). Zelah Joel first characterized the tau tangle progression in this model (Joel 2015, PhD dissertation). At 4 months of age, neither the low-TAU nor the high-TAU line shows obvious neurofibrillary tangles, except some diffuse neuronal soma and processes staining with CP13, a phosphorylated tau (specific to phosphorylated serine 202) antibody. The high-TAU mice start to show sparse tangles in the hippocampus at around 8 months, and the pathology then progresses at an aggressive rate, with a heavy tangle load at 12 months and significant neuronal loss and brain volume reduction at 18 months (hence high Tau pathology). At around 18 months they present with severe symptoms such as reduced bodyweight, heavy breathing, akinesia, piloerection, and kyphosis, and culled for ethical reasons. The low-TAU line, however, only shows very few tangles in the hippocampus at 13 months. At 24 months of age, the low-TAU mice do exhibit comparable tau tangle burden compared to the 13-month high-TAU, while the number of tangles to neurones ratio is lower probably due to the beginning of neuronal loss in the 13-month high-TAU mice.

Aims

1. To characterize the expression of typical microglial genes (general microglial, pro-inflammatory, and anti-inflammatory) in the hippocampus along with the Aβ or tau pathology development in the transgenic mice by RT-qPCR.
2. To estimate the average microglial *Trem2* expression levels in the hippocampus of both models.

Results

Microglial gene expression changes in the hippocampus of wildtype mice along with ageing

Before addressing the question of the effects of AD-related pathology, I investigated the microglial gene expression changes in the hippocampus of wildtype mice along with normal ageing. I studied by RT-qPCR the gene expressional levels in the mouse hippocampus of two microglial marker genes *Aif1* and *Cd68*, two pro-inflammatory markers *Tnf* and *Il1b*, two anti-inflammatory markers *Arg1* and *Tgfb1*, and one of the recently revealed AD-associated gene *Trem2*. As shown in figure 4.1, the most commonly used pan-microglial marker *Aif1* expression showed a significant increase with ageing in the mouse hippocampus ($p<0.0001$, One-way ANOVA), with a ~3.9-fold increase at 12 months and a ~2.8-fold increase at 18 months compared to that at 4 months (4m vs. 12m, $p<0.0001$; 4m vs. 18m, $p<0.01$; 8m vs. 12m, $p<0.01$; Tukey's *post hoc* test). Interestingly, I also observed a significant decrease of *Aif1* expression level from 12 months to 18 months ($p<0.05$). AD-associated gene *Trem2* also showed significant expression increases with ageing ($p<0.01$), with an increase of ~1.7-fold at 12 months and ~1.9-fold at 18 months respectively compared to the level at 4 months of age (4m vs. 12m and 18m, $p<0.01$; One-way ANOVA followed by Tukey's *post*). Additionally, the expression levels of *Cd68* ($p<0.001$), *Tnf* ($p<0.01$), and *Tgfb1* ($p=0.014$) in the wildtype hippocampus was shown to be increased with age as well, with *Cd68* starting to show statistic significance from 12 months while *Tnf* and *Tgfb1* only showing significance at 18 months. *Il1b* and *Arg1* gene expression did not significantly change with age. In general, there was an increase of a subset of microglial gene transcripts in the wildtype mouse hippocampus with normal ageing that was not specific to certain state of microglia (e.g. pro- or anti-inflammatory), which became detectable at around 12 months of age.

Considering that the cDNA used for RT-qPCR analysis was generated from the RNA pool of the whole mouse hippocampus that included all cell types, the increase of microglial transcripts with ageing might be partially, if not

completely, due to an expansion of the microglial population in the hippocampus, rather than a simple indicator of microglial gene expression profile changes with age. To neutralize this factor to some extent, I used the pan-microglial marker *Aif1,* instead of *Rps28* that is expressed by all cell types, as the housekeeping gene to re-analyze the RT-qPCR data with the assumption that the average *Aif1* transcription level shows little change in the microglial population with ageing. As in this thesis I was particularly interested in *Trem2* expression and functional implications, I re-analyzed *Trem2* by normalizing to *Aif1* instead of *Rps28* (figure 4.1 B). Interestingly, it was found that, there was a significant decrease with age in the *Trem2* (normalized to *Aif1*) level in the mouse hippocampus ($p<0.0001$, One-way ANOVA). Similar to the increase of microglial transcripts in the hippocampus with age, this decrease started to show statistic significance at 12 and 18 months compared to younger ages (4m vs. 12m, $p<0.0001$; 4m vs. 18m, $p<0.01$; 8m vs. 12m, $p<0.01$; Tukey's *post hoc*). Also there was a slight but significant recovery from 12 months to 18 months ($p<0.01$). Strictly speaking, it is to some extent oversimplified to use this approach to analyze the microglial gene expression, as in the brain microglia may show various subgroups with different gene expressional signatures and thus different functional phenotypes. But still, such decrease with age might suggest 1) *Trem2* expression decreases in each single microglial cell with age, 2) a reduced proportion of microglia with substantial *Trem2* expression compared to other microglial phenotypes with relatively low *Trem2* expression, or 3) a difference in the *Aif1* expression level between microglia. Additionally, the recovery of the *Trem2*/*Aif1* ratio from 12 months to 18 months also appeared interesting, which might need follow up to further investigate.

Figure 4.1

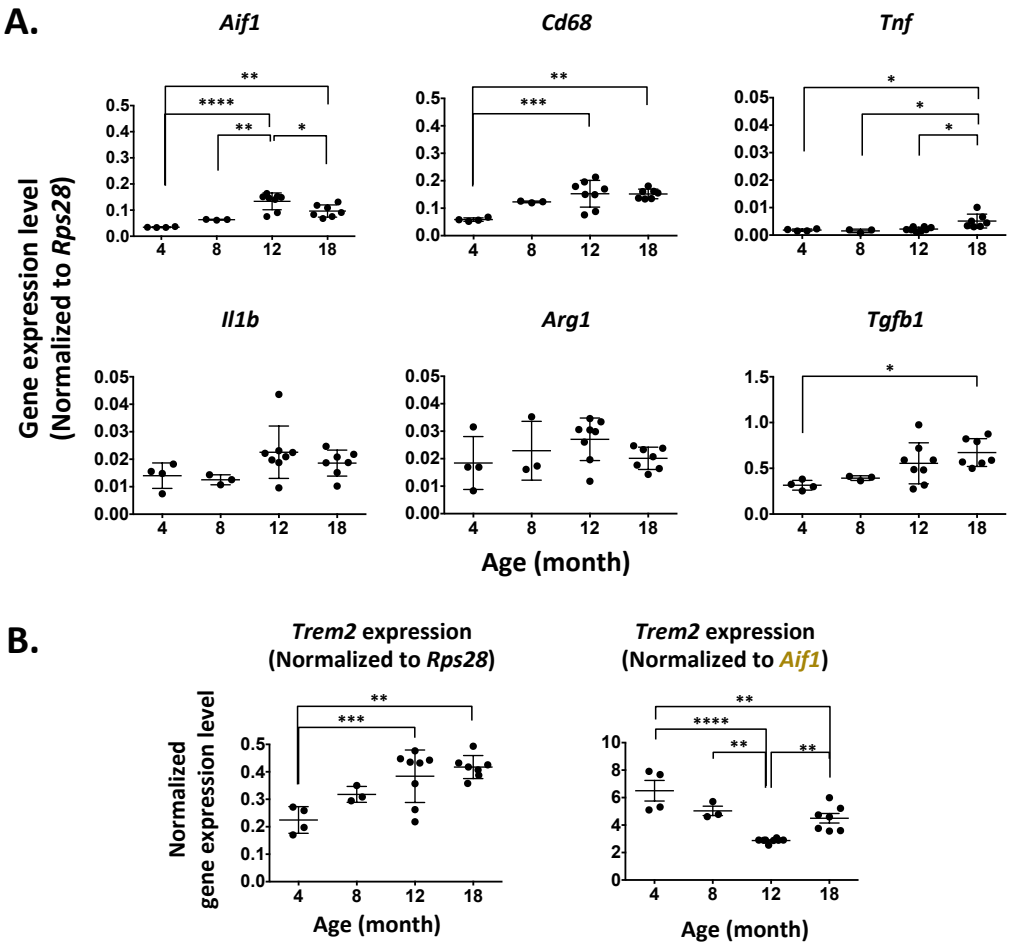

Figure 4.1. Increase of microglial gene transcripts in wildtype mouse hippocampus with normal ageing. (A) Significantly increased transcript levels of various microglial genes with ageing in wildtype mouse hippocampus were observed, as measured by RT-qPCR and normalized to a housekeeping gene *Rps28*. **(B)** *Trem2* transcript level (as measured by RT-qPCR and normalized to *Rps28*) showed a significant increase in wildtype hippocampus with ageing as well; However, when normalized to a pan-microglial marker gene *Aif1*, *Trem2* expression showed a significant decrease with ageing.

N=4 (4 months), 3 (8 months), 8 (12 months), and 7 (18 months) mice. Data shown as Mean ± SEM. One-way ANOVA followed by Tukey's *post hoc* tests if there was significant interaction, * $p<0.05$, ** $p<0.01$, *** $p<0.001$, **** $p<0.0001$.

Microglial gene expression changes in the amyloid or tau pathology mouse models

In order to investigate the microglial gene expression at different stages of Aβ or tau pathology, I employed two amyloid model lines of different pathology progression rates (homozygous and heterozygous *APP/PSEN1* mice) and two TauD35 lines (high-transgene-copy (high-TAU) and low-transgene-copy (low-TAU) mice), with the wildtype data shown in figure 4.1 as the age-matched control. Again I analyzed the same microglial genes with the previous section by RT-qPCR. As shown in figure 4.2 A, *Aif1*, *Cd68*, and *Trem2* all showed increased expression in the hippocampus of the mouse models along with pathology progression (significant main effects of both Genotype and Age and interaction; Two-way ANOVA followed by Tukey's *post hoc* tests). Specifically, for the amyloid models, HO-*APP/PSEN1* mice started showing significant increase compared to age-matched wildtype mice from about 8 months (the stage when mature amyloid plaques developed), which further kept rising with age; while in HE-*APP/PSEN1* the significant increase started to be evident from 12 months, corresponding to a slower rate of Aβ deposition than HO-*APP/PSEN1*. For the tau model, the up-regulation of these genes started to be significant from 12 months in high-TAU mice, while there was no significant difference from the wildtype across all age groups in low-TAU mice. Particularly, the high-TAU mice showed consistently significantly lower *Trem2* levels than the HO-*APP/PSEN1* mice across 8-18 months of age. Then I analyzed pro-inflammatory genes *Tnf* and *Il1b* expression levels in the models (figure 4.2 B). These two genes also showed significant changes among different ages and genotypes, and a significant interaction allowing us to perform *post hoc* tests. For the amyloid models, significant increase of *Tnf* expression was only observed in the homozygous mice, starting from 12 months and maintaining statistical significant until 18 months, the *Il1b* expression was not significantly different from the wildtype though. For the tau models, again only high-TAU but not low-TAU showed significant increased *Tnf* and *Il1b* expression at 12 months and 18 months. Particularly, the *Il1b* expression in the 18-month high-TAU was significantly higher than the HO-*APP/PSEN1* mice ($p<0.01$), although the *Tnf* expression level was not

significantly different between these two genotypes. Additionally, the fold changes of these two pro-inflammatory genes in the mouse models versus wildtype appeared to give a lot of variation among mice, *e.g.* the *Tnf* expression in 12-month HO-*APP/PSEN1* mice was about 3-10 fold of that in age-matched wildtype mice, and 5-48 folds at 18 months of age, suggesting a high inter-animal variability with respect to the inflammatory states in the brain. Next we tested anti-inflammatory genes *Arg1* and *Tgfb1* expression (figure 4.2 C). *Arg1* did not show significant changes across ages or genotypes by Two-way ANOVA. *Tgfb1* did show significant main effects of both age ($p<0.0001$) and genotype ($p<0.01$), but no significant interaction. Taken together, both Aβ and tau pathology development induced increased microglial transcripts in the mouse hippocampus, although this might be due to an expansion of microglial population. Also, the tau mice at late stage of pathology appeared to show higher pro-inflammatory gene expression, such as *Il1b*, than the amyloid mice at the same age.

Figure 4.2

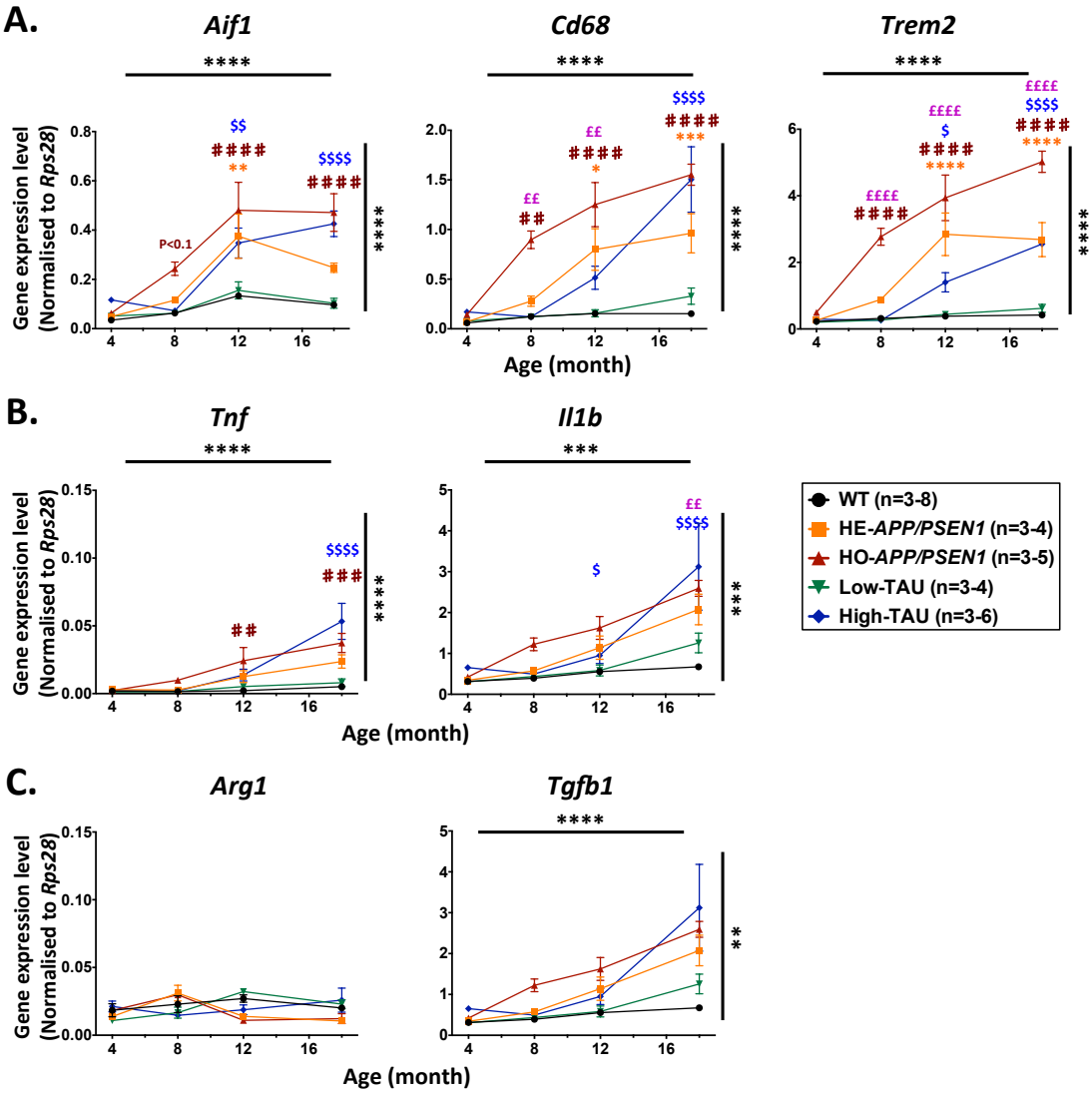

Figure 4.2. Changes of microglial gene transcripts in the hippocampus of amyloid or tau mouse models with age. (A) Significant gene expression increase of *Aif1*, *Cd68* and *Trem2* compared to age-matched wildtypes (same data with figure 4.1) was observed in both amyloid and tau models. **(B)** Significant *Tnf* expression was observed in HO-*APP/PSEN1* and high-TAU mice at relatively middle-late stages of the pathology progression, while the *Il1b* expression was only found to be significantly higher in the high-TAU line at middle-late stages. **(C)** Time-dependent increased *Tgfb1* expression in both types of models without significant interaction between genotype and age. No significant change in *Arg1* expression between models and wildtypes.

N=3-8 (wildtype), 3-4 (HE-*APP/PSEN1*), 3-5 (HO-*APP/PSEN1*), 3-4 (low-TAU), and 3-6 (high-TAU) mice per group. Data shown as Mean ± SEM. Two-way ANOVA followed by Tukey's *post hoc* test if there was significant interaction; horizontal and vertical lines for significant main effects of age and genotypes respectively, * for *post hoc* test significance HE-*APP/PSEN1* versus WT, ♯ for HO-*APP/PSEN1* versus WT, **$** for high-TAU versus WT, and £ for high-TAU versus HO-*APP/PSEN1*.

To neutralize the influence of the microglial population expansion, I again re-analyzed *Trem2* expression by normalizing to *Aif1* rather than *Rps28* (figure 4.3 A). Two-way ANOVA showed that both the age and genotype had significant main effects on the *Trem2* (normalized to *Aif1*) levels in the mouse hippocampus ($p<0.0001$), and also there was a significant interaction between the two factors ($p<0.01$) suggesting a genotype-dependent *Trem2* expression pattern with age. Further Tukey's *post hoc* tests suggested that only the Aβ models, but not the tau models, exhibited significantly increased *Trem2* compared to age-matched wildtype mice, with HO-*APP/PSEN1* and HE-*APP/PSEN1* starting around 8 and 12 months respectively and maintaining until at least 18 months. Additionally, high-TAU mice at 4 months showed significant lower *Trem2* than the wildtype ($p=0.011$), which gradually normalized with ageing but still significantly lower than age-matched *APP/PSEN1*. As a comparison, the *Cd68* expression was re-analyzed by normalizing to *Aif1* as well (figure 4.3 B). Different from *Trem2*, although there were significant main effects of genotype ($p<0.01$) and age ($p<0.0001$), no significant interaction was observed by Two-way-ANOVA, suggesting the changing pattern of the magnitude differences between genotypes compared to the wildtype with age was not significantly different between the Aβ and tau models. Overall, the results suggest a highly up-regulated microglial *Trem2* expression in the amyloid model as the Aβ deposition developed, despite the increased microglial number in the hippocampus. However, in the tau mice, I did not observe convincing *Trem2* increase relative to the *Aif1* levels, possibly suggesting a lack of *Trem2* up-regulation in the context of individual microglial cell.

Figure 4.3

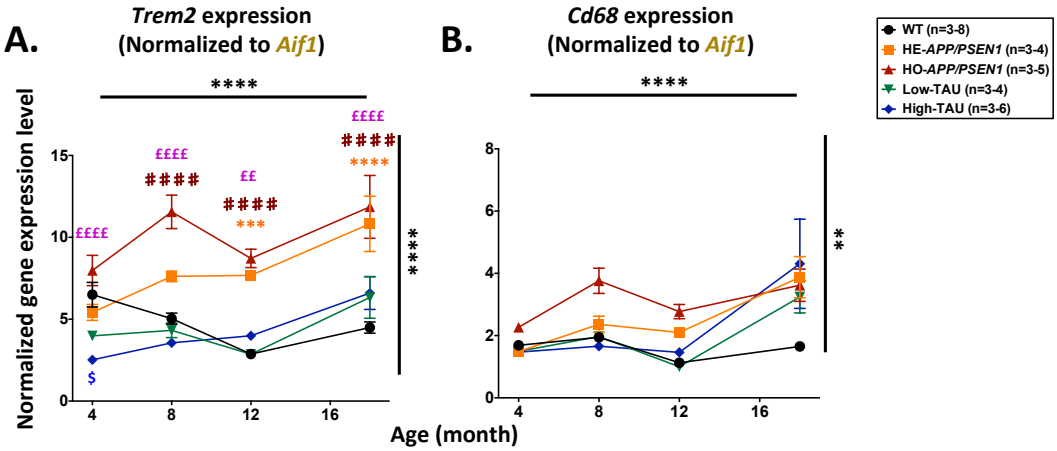

Figure 4.3. Microglial *Trem2* and *Cd68* expression relative to *Aif1* levels in the hippocampus of amyloid or tau mouse models. (A) *Trem2* (normalized to *Aif1* rather than *Rps28*) expression in each mouse hippocampus was analyzed and showed a significant increase relative to the WT in the amyloid models along with pathology development, but not in the tau models. However, at 4 months of age high-TAU exhibited a significant lower *Trem2* expression compared to the WT. **(B)** Significant changes of the *Cd68* (normalized to *Aif1*) expression among ages ($p<0.0001$) or genotypes ($p<0.01$), while no significant difference in the changing pattern between amyloid and tau models was found. Two-way ANOVA followed by Tukey's *post hoc* tests if there was significant interaction between age and genotype effects.

N=3-8 mice per group. Data shown as Mean ± SEM. Two-way ANOVA followed by Tukey's *post hoc* test; horizontal and vertical lines for significant main effects of age and genotypes respectively, * for *post hoc* test significance HE-*APP/PSEN1* versus WT, ♯ for HO-*APP/PSEN1* versus WT, **$** for high-TAU versus WT, and £ for high-TAU versus HO-*APP/PSEN1*.

Summary

I characterized the expression of a series of microglial genes in the hippocampus of the amyloid and tau models by RT-qPCR. An increase of microglial gene transcripts (*Aif1*, *Cd68*, *Trem2*, *Tnf*, and *Tgfb1*) with ageing was found in the hippocampus of the wildtype mice, potentially suggesting increased microglial number and/or increased microglial activation with normal ageing. Furthermore, referring to the time course of pathology development in these models previously reported from our group (Cummings *et al.*, 2015; Matarin *et al.*, 2015; Joel 2015, PhD dissertation), the general microglial genes transcripts increased closely following the amyloid plaque progression in the amyloid mice, while in the tau mice it was relatively delayed compared to the tangle development. With respect to the pro-inflammatory genes, they only showed significant upregulation at late stages of established pathology in both types of models. Especially for *Il1b*, its level in 18-month high-TAU was significantly higher than age-matched HO-*APP/PSEN1*. More importantly, although increased *Trem2* transcripts were observed in the hippocampus of both models, different models showed significantly different *Trem2* expression when it was normalized to microglial marker gene *Aif1* to neutralize the influence of the microglial number changes in the hippocampus. The *Trem2* level normalized to *Aif1* was highly increased with age in the amyloid mice compared to the tau model and the wildtype, suggesting a highly upregulated microglial *Trem2* expression specifically induced in the amyloid mice with pathology development.

Chapter 5

Microglial similarities and differences in transgenic mouse models of Amyloid-beta pathology versus Tauopathy – Histology

Introduction

Accumulated and activated microglia are important features of AD pathology, which has been described in both human patients and transgenic mouse models. Highly up-regulated MHC-II (HLA-DR) expression in the microglia, especially those accumulating in the vicinity of amyloid plaques in human AD brains (Itagaki et al., 1989; McGeer et al., 1987; Perlmutter et al., 1992; Rogers et al., 1988; Styren et al., 1990), particularly indicates an activated phenotype in response to Aβ pathology of AD. In addition to the interaction between microglia and plaques, the microglial interaction with tau pathology has recently started being investigated as well, while the relationship between microglia and tau pathology remains to be further studied. *In vitro* research has shown that both tau oligomers and fibrils can induce microglial activation and promote pro-inflammatory cytokine production (Morales et al., 2013). Consistently, in a tau (P301S) mouse model microglial activation was observed before neurofibrillary tangles developed (Yoshiyama et al., 2007), suggesting a role of pre-tangle tau species in activating microglia. More importantly, activated microglia appear to promote the onset and progression of tau pathology in a human tau mouse model (Maphis et al., 2015), which might suggest a potential link between Aβ pathology and tau pathology in AD progression.

In chapter 4, I have characterized the microglial gene expression in our amyloid models and tau models, in which it was showed a more closely associated microglial genes up-regulation with Aβ pathology and a potential difference in the microglial *Trem2* expression regulation between the amyloid and tau models. Additionally, I observed a potentially more pro-inflammatory state in the tau model than the amyloid model at the stage when both expressed high load of pathology. In this chapter, by immunohistochemistry, I further characterized the microglial proliferation and activation in different regions of the hippocampus of mice exhibiting different pathology stages, with a particular emphasis on analyzing the similarities and differences between the amyloid mice and the tau mice.

Unfortunately, I did not manage to find a mouse TREM2 antibody with high specificity. I tested in total 4 commercially available TREM2 antibodies with our *Trem2*-knocked-down BV2 cell samples by Western blot, none of which showed sufficient specificity.

Aims

1. To investigate the microglial expansion/proliferation and activation in different regions of the hippocampus related to the pathology in the models by immunohistochemistry.
2. To compare and contrast the microglial parameters between the amyloid and the tau models.

Results

Microglial activation in the hippocampus of an APP/PSEN1 mouse model

In order to characterize further microglial proliferation and activation in AD-related mouse models I used immunohistochemistry. Here I immune-stained serial sections (30μm thick, around 720μm apart, transverse to the hippocampus) from frozen-fixed brains of HO-*APP/PSEN1* and wildtype mice at 4 and 12 months, which represented the early and late stages of the Aβ deposition, with CD68 and IBA1 targeting antibodies. IBA1 (ionized calcium binding adaptor molecule 1), which is encoded by gene *Aif1* and in the brain is specifically expressed in microglia (Imai et al., 1996; Ito et al., 1998), is widely used as a marker for all microglia regardless of activation. CD68 (macrosialin) is a lysosomal glycoprotein highly expressed by monocytes and tissue macrophages (Holness and Simmons, 1993; Saito et al., 1991), and is commonly used as a marker for microglial phagocytic activities.

To quantify the total microglia in the dentate gyrus (DG) and CA1 regions of hippocampus I produced a z-stack image using confocal microscopy (figure 5.1). As shown in figure 5.1 C, IBA1-positive cells, representing the whole microglial population, showed a significant increased number (around 5-fold change) in 12 month HO-*APP/PSEN1* DG ($p<0.0001$) and CA1 ($p<0.001$) regions compared to age-matched wildtype mice (Two-way ANOVA followed by Tukey's *post hoc* tests). Also, I noticed that the microglia number in both DG and CA1 of the 4-month HO-*APP/PSEN1* was actually ~2-fold of that in the wildtype; although no statistic significance was obtained (in DG, $p=0.86$; in CA1, $p=0.33$), probably due to a small sample size ($n=2$ for 4-month HO-*APP/PSEN1*) and thus lack of statistic power, it still retained the possibility of a potential increase in the microglia number in the HO-*APP/PSEN1* mice at this age.

I further quantified the CD68-positive cells in the same regions of the brain. I

observed a proportion of microglia (IBA1-positive cells) with obvious CD68, mainly represented as spreading or clustered or vesicular signals in the cytoplasm or closely underneath the cell membrane. Quantification showed that both DG ($p<0.001$) and CA1 ($p<0.01$) regions had significantly more CD68-positive microglia in 12-month HO-*APP/PSEN1* mice than wildtype mice (Two-way ANOVA followed by Tukey's *post hoc* tests). At 4 months of age, I did not observe a significant difference between HO-*APP/PSEN1* and wildtype mice. As the total microglial number increased significantly in the 12-month HO-*APP/PSEN1* model, the increased number of CD68-positive microglia was not surprising. Next, to further understand the phenotype change of microglia at the cellular level, I analyzed whether the percentage of CD68-positive microglia in the whole microglial population also changed in the HO-*APP/PSEN1* compared to the wildtype (figure 5.1 D). Two-way ANOVA suggested that there was no significant difference between HO-*APP/PSEN1* and wildtypes; however, the age did exhibit a significant main effect (in DG, $p=0.034$; in CA1, $p=0.0012$), with significantly increased percentage of CD68-positive microglia in the 12-month mice compared to 4-month mice in both DG and CA1 hippocampal regions. Overall, the HO-*APP/PSEN1* mice showed significant expansion of the microglial population in the hippocampus, following the amyloid plaque deposition. The percentage of activated CD68-positive microglia in the total microglial population showed an age-dependent increase in the hippocampus, while there was no significant difference between wildtype and HO-*APP/PSEN1.*

Figure 5.1

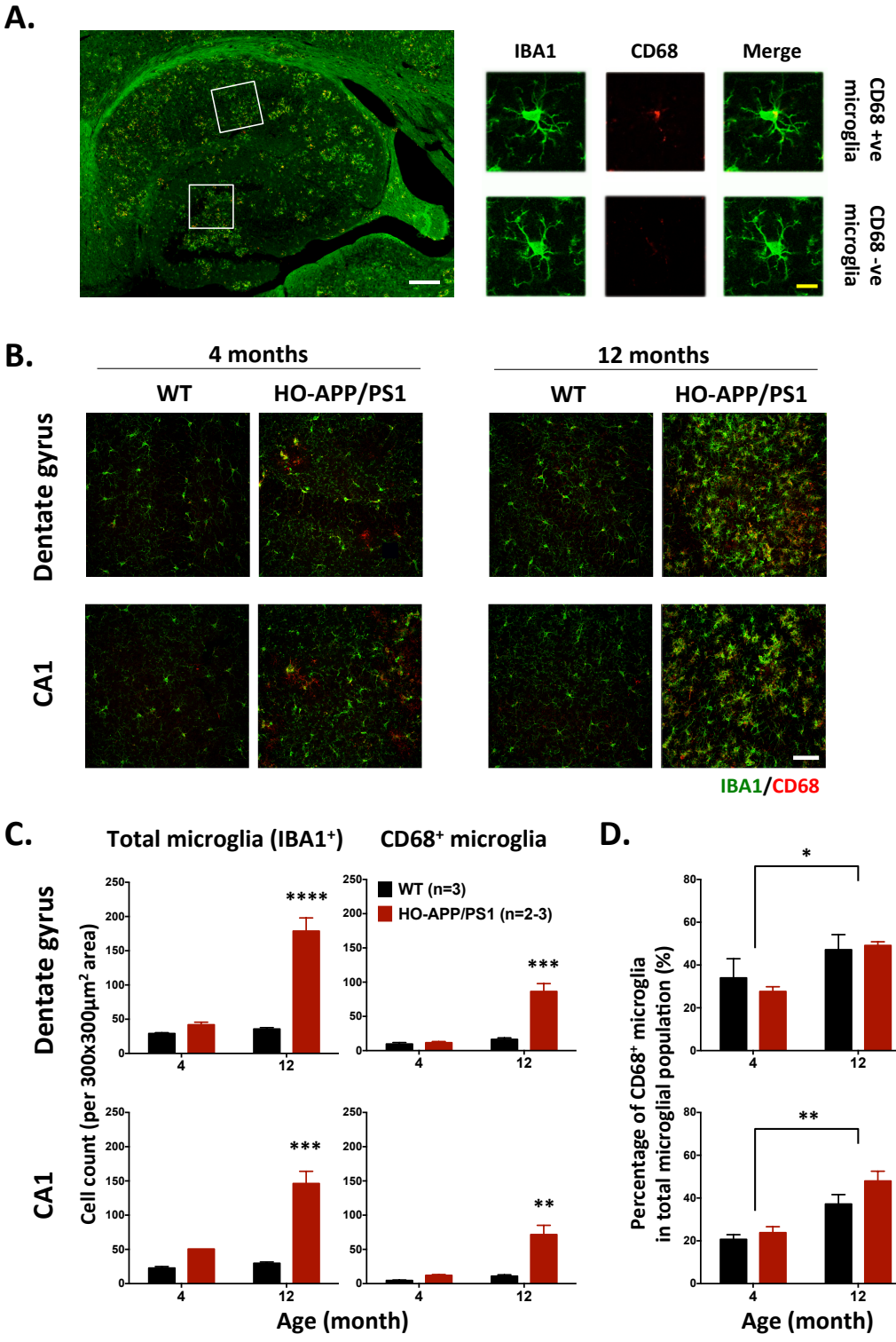
A.
IBA1
CD68
Merge
CD68 +ve microglia
CD68 -ve microglia
B.
4 months
12 months
WT
HO-APP/PS1
WT
HO-APP/PS1
Dentate gyrus
CA1
IBA1/CD68
C.
Total microglia (IBA1+)
CD68+ microglia
WT (n=3)
HO-APP/PS1 (n=2-3)
Dentate gyrus
CA1
Cell count (per 300x300µm2 area)
****
***
***
**
Age (month)
D.
Percentage of CD68+ microglia in total microglial population (%)
*
**
Age (month)

Figure 5.1. Microglial activation in the hippocampus of the amyloid mouse model. (A) Left panel: An overall low-magnification image to show the transverse hippocampus of a 12-month HO-*APP/PSEN1* mouse. The white boxes showed the areas of interest employed for confocal imaging and quantification. Scale bar: 200μm. **Right panel:** Representative $CD68^+$ microglia and $CD68^-$ microglia. Scale bar: 10μm. **(B)** Representative images of hippocampal dentate gyrus and CA1 regions in the brain sections from 4- and 12- month HO-*APP/PSEN1* and wildtype mice double stained using IBA1 (green) and CD68 (red), imaged with confocal microscopy and quantified with ImageJ. Scale bar: 50μm. **(C)** Significantly higher numbers of both total microglia (determined by $IBA1^+$ cells) and $CD68^+$ microglia were observed in the HO- *APP/PSEN1* mice at 12 months compared to the wildtype. **(D)** The percentage of $CD68^+$ microglia in the total microglial population showed no significant difference between the WT and HO- *APP/PSEN1*, but there was a significant increase with age.

N=3 mice per group, except for 4-month HO-*APP/PSEN1* with n=2 (3 sections per mouse). Data shown as Mean ± SEM. Two-way ANOVA followed by Tukey's *post hoc* test if there was significant interaction; horizontal and vertical lines for significant main effects of age and genotypes respectively, * $p<0.05$, ** $p<0.01$, *** $p<0.001$, **** $p<0.0001$.

To further investigate the activation status of microglia, I studied mouse MHC-II expression in the *APP/PSEN1* mouse model versus the wildtype. MHC-II (Major Histocompatibility Class II) molecules generally present antigens to immune cells, which thus elicit adaptive immune responses, and the MHC-II up-regulation in microglia accompanies more pro-inflammatory activation. I first tested co-staining of IBA1 and mouse MHC-II in the brain sections of HO-*APP/PSEN1* and wildtype mice, and found all MHC-II positive cells found in the brain parenchyma were IBA1-positive as well (figure 5.2 A), suggesting MHC-II was predominantly expressed by brain-resident microglia/ macrophages, and perhaps peripherally infiltrated myeloid cells, if any. I investigated the MHC-II expression in the hippocampus across different ages by immunohistochemistry. Surprisingly I found that, in the wildtype mice even at very old ages (30 months), there was no detectable MHC-II staining in the brain parenchyma, except a group of positive cells found in the choroid plexus. However, in both homozygous and heterozygous *APP/PSEN1* brains, I did observe a subgroup of microglia with substantial MHC-II signals, which started from around 12 months of age and particularly, only represented a small proportion of the total microglia (figure 5.2 B). Additionally, there was a high inter-animal variability in the number of MHC-II-positive microglia in the brain, and between the 12-month HO- and HE- *APP/PSEN1* mice, which exhibited a substantial difference in the amyloid plaque load, quantification of the MHC-II positive microglia in the whole hippocampus did not show a significant difference (student t-test).

In total, it suggests that there is significant expansion of microglia in the amyloid mouse models, which is probably due to increased proliferation of microglia in response to Aβ deposition. However, the ‘activation’ phenotype of the microglial population does not seem to have a comparable change relative to the level of microglia number increase, as represented by unchanged proportion of CD68-positive microglia and only a small group of MHC-II positive microglia at the middle-late stages of Aβ deposition.

Figure 5.2

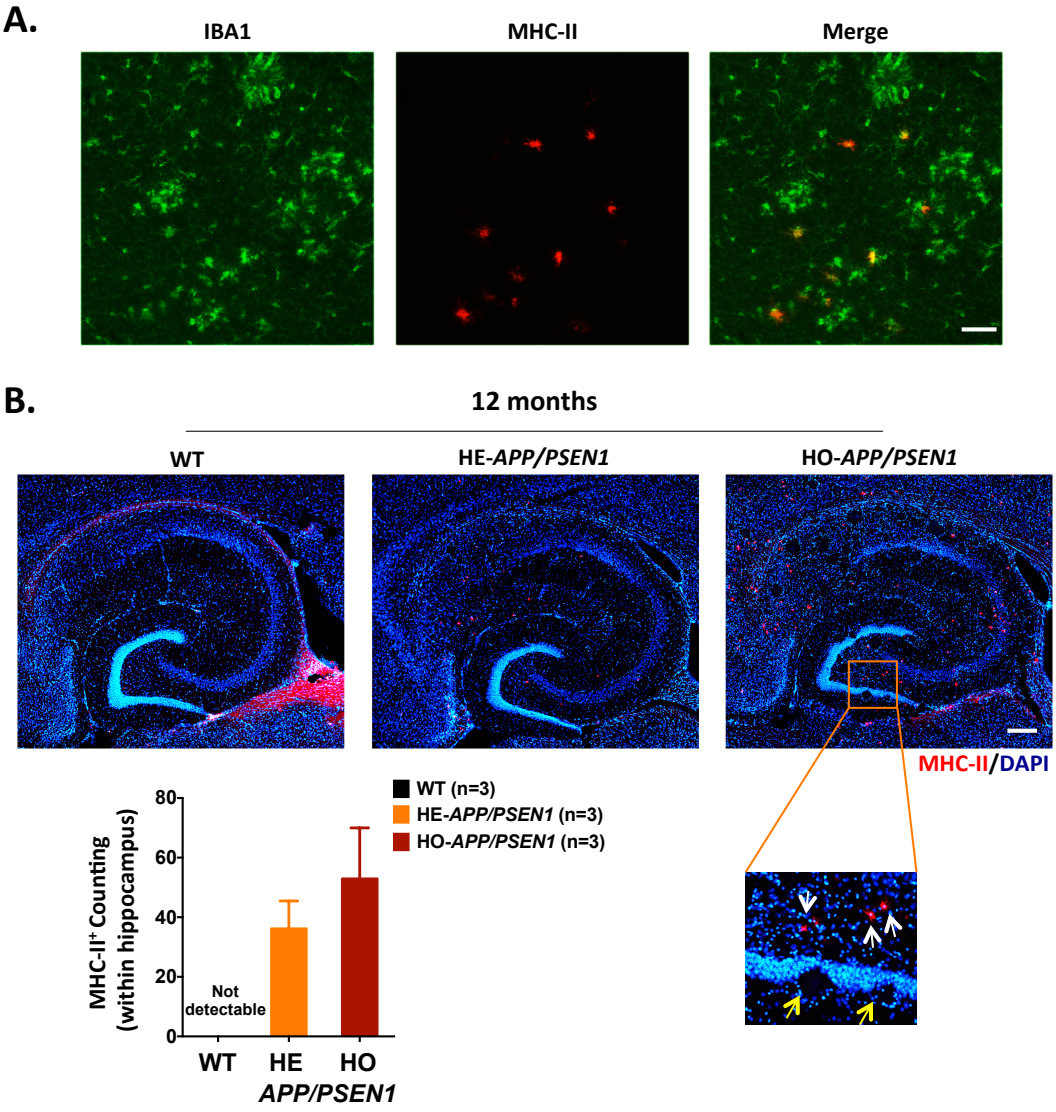

Figure 5.2. MHC-II expression in the hippocampus of *APP/PSEN1* mice at 12 months. **(A)** IBA1 and MHC-II double-staining showed a subgroup of microglia (IBA1$^+$) were MHC-II$^+$ in the brain parenchyma of the 12-month *APP/PSEN1* mice. All MHC-II$^+$ cells were also IBA1$^+$. Scale bar: 50μm. **(B) Top:** Representative images showing microglia expressing MHC-II in the whole hippocampus. MHC-II was not observed in the brain parenchyma of WT mice except in the choroid plexus. 4-month and 12-month HE- and HO- *APP/PSEN1* were analyzed and MHC-II expression in the brain parenchyma was only observed in the 12-month mice. The distribution showed a random pattern without obvious association with plaques. The area in the orange box was zoomed to show examples of MHC-II$^+$ microglia (white arrows) and plaque area (the hole-like area without DAPI, indicated with yellow arrows). Scale bar: 200μm. **Bottom:** Comparison of the MHC-II$^+$ microglial number in the area of the whole hippocampus between 12-month HE- and HO- *APP/PSEN1* mice. No significant difference was found (Unpaired Student t-test). N=3 mice per group (3 serial sections (around 720μm apart) per mouse). Data shown as Mean ± SEM.

Microglial changes in the hippocampus of a tau model

Next I studied the microglia number and activation by immunohistochemistry in the TauD35 mouse models. I employed the high-TAU and low-TAU mice with wildtype mice at the ages of 4 and 12 months. Again I first investigated the IBA1 and CD68 expression in the hippocampus of the brain (figure 5.3). Quantification of total microglia (IBA1-positive) showed that in both DG and CA1 regions of the hippocampus, both the transgene copy number (DG, $p<0.001$; CA1, $p<0.01$) and the age (DG, $p<0.0001$; CA1, $p<0.001$) exhibited significant main effects on the microglia number, with a significant interaction as well (DG, $p<0.001$; CA1, $p<0.01$; Two-way ANOVA). Tukey's *post hoc* tests suggested a significantly increased microglia number in the hippocampus of the 12-month high-TAU mice than age-matched wildtypes (DG, $p<0.0001$; CA1, $p<0.01$), while no significant difference was observed between 4-month high-TAU and wildtype mice or between 12-month low-TAU and wildtype mice. In terms of CD68-positive microglia, I observed a similar pattern of changes to the IBA1 quantification in the TAU model. There were significant effects of both the transgene copy number (DG, $p<0.0001$; CA1, $p<0.001$) and the age (DG, $p<0.0001$; CA1, $p<0.0001$) that showed a significant interaction as well (DG, $p<0.0001$; CA1, $p<0.001$; Two-way ANOVA). Following Tukey's *post hoc* tests showed again a significant increase of CD68-positive microglia in the hippocampus of the 12-month high-TAU mice ($p<0.0001$ in both DG and CA1). Again, I analyzed the percentage of CD68-positive microglia in the total microglial population (figure 5.3 D). In both DG and CA1 regions of the hippocampus, I observed a significant increase in the CD68-positive microglia proportion with age regardless of the genotype (both DG and CA1, $p<0.0001$; Two-way ANOVA), which was consistent with our previous results for the *APP/PSEN1* section. However, different from the Aβ model, I did find a significantly elevated CD68-positive microglia proportion in the TAU model than the wildtype (DG, $p=0.03$, CA1, $p=0.06$ (trend); Two-way ANOVA), which seemed more evident in the 12-month high-TAU compared to the wildtype.

Figure 5.3

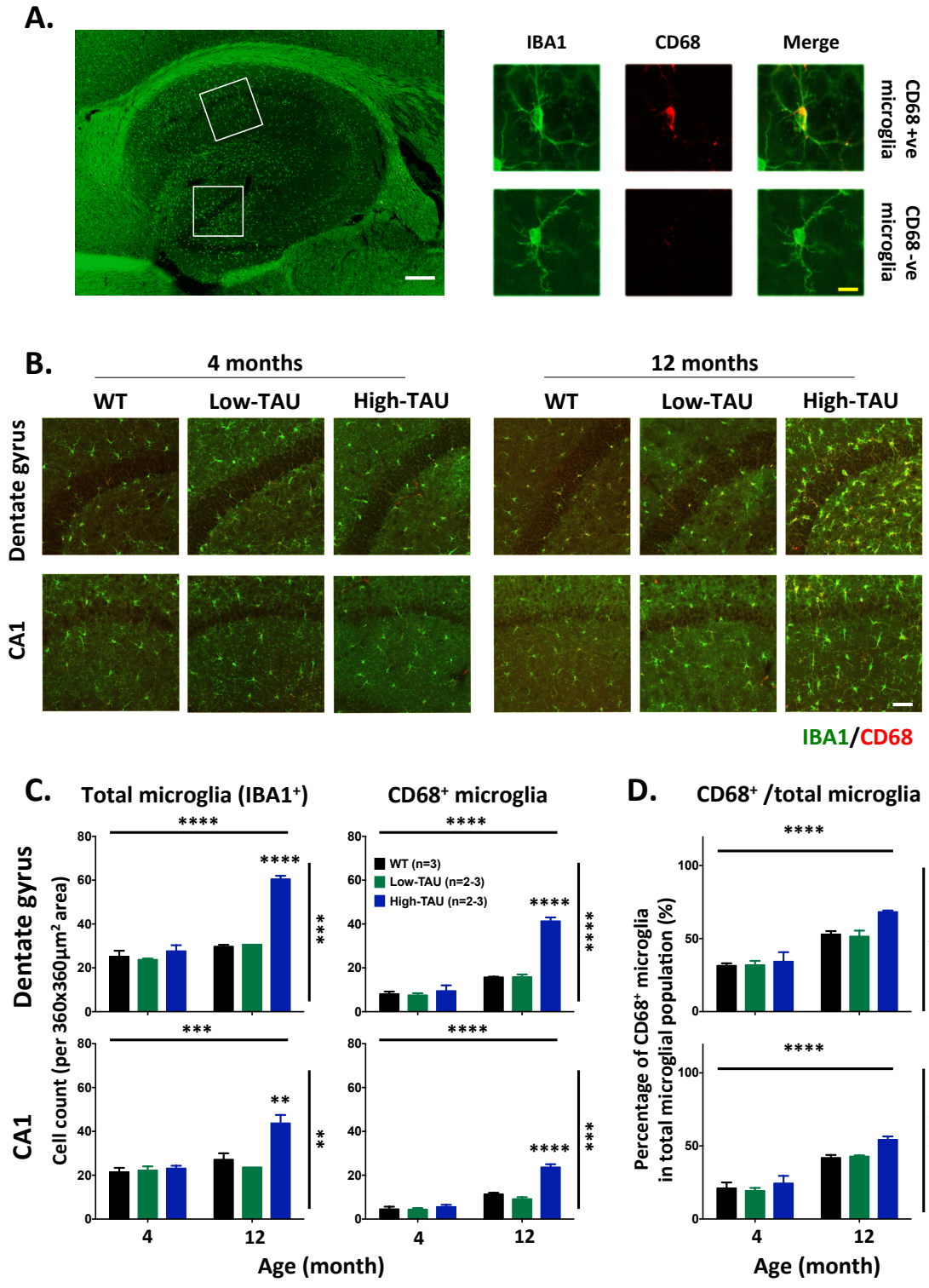
A.
IBA1
CD68
Merge
CD68 +ve microglia
CD68 -ve microglia
B.
4 months
12 months
WT
Low-TAU
High-TAU
WT
Low-TAU
High-TAU
Dentate gyrus
CA1
IBA1/CD68
C.
Total microglia (IBA1+)
CD68+ microglia
Dentate gyrus
CA1
Cell count (per 360x360µm² area)
WT (n=3)
Low-TAU (n=2-3)
High-TAU (n=2-3)
Age (month)
D.
CD68+ /total microglia
Percentage of CD68+ microglia in total microglial population (%)
p=0.06
Age (month)

Figure 5.3. Microglial activation in the hippocampus of the tau model. **(A) Left panel:** An overall low-magnification image to show the transverse hippocampus of a 12-month high-TAU mouse. The white boxes showed the areas of interest employed for imaging and quantification. Scale bar: 200μm. **Right panel:** Representative $CD68^+$ microglia and $CD68^-$ microglia. Scale bar: 10μm. **(B)** Representative images of hippocampal dentate gyrus and CA1 regions from 4 and 12 months wildtype, low-TAU, and high-TAU mice, stained with IBA1 (green) and CD68 (red), imaged with an epifluorescent microscope and quantified with ImageJ. Scale bar: 50μm. **(C)** Significantly higher numbers of both total microglia (determined by $IBA1^+$ cells) and $CD68^+$ microglia in the high-TAU mice at 12 months compared to the wildtype. **(D)** The percentage of $CD68^+$ microglia in the total microglial population was compared between genotypes and ages. Both the age and the transgene copy number showed significant main effects.

N=3 mice per group except for the 12-month high-TAU and 12-month low-TAU with n=2 (3 sections per mouse). Data shown as Mean ± SEM. Two-way ANOVA followed by Tukey's *post hoc* test if there was significant interaction; horizontal and vertical lines for significant main effects of age and genotypes respectively, * $p<0.05$, ** $p<0.01$, *** $p<0.001$, **** $p<0.0001$.

I then examined the pro-inflammatory MHC-II expression in the tau models as well. At 4 months of age, neither high-TAU nor low-TAU mice showed detectable MHC-II in the brain parenchyma by immunohistochemistry. However, at 12 months, high-TAU mice showed a group of MHC-II positive microglia in the hippocampus and cortex, while the low-TAU at 12 months still showed no detectable MHC-II positive microglia (figure 5.4 A). Importantly, the distribution of this group of MHC-II positive microglia in the hippocampus was distinct compared to the Aβ model, with a substantial number of cells accumulated in the *stratum lacunosum-moleculare* (SLM) layer adjacent to the hippocampal sulcus. Additionally, I immuno-stained with MHC-II antibody in the 24-month low-TAU mice to investigate whether they would show MHC-II signals in the brain at this stage, and I did observe a subgroup of microglia that were MHC-II positive. The 24-month low-TAU mice showed comparable tau tangle number in the hippocampus to the 12-month high-TAU; however, there was a potential but not statistically significant neuronal loss in the 12-month high-tau mice that was not observed in the 24-month low-TAU (Joel, PhD dissertation 2015). We thus proposed that these stages represented the potential period of the progression from tauopathy to neurodegeneration. Comparison between the 12-month high-TAU and 24-month low-TAU showed a strong trend of a significantly higher number of the MHC-II positive microglia in the 12-month high-TAU (figure 5.4 B; $p=0.056$, Student t-test), although the sample size was low and further clarification is necessary.

In total, microglial expansion and activation in the hippocampus was observed in 12-month high-TAU that was at the stage with severe tau tangle development. Different to the amyloid model, the tau mice not only showed a strong increase in the total microglial number, but also a significant increase in the proportion of CD68-positive microglia (representing high phagocytic activity and widely used as a marker for microglial activation). In addition, the MHC-II positive microglial/myeloid cells that were evident in both amyloid and tau models at middle-late stages, showed a particularly different distribution in the tau mice from the *APP/PSEN1* model.

Figure 5.4

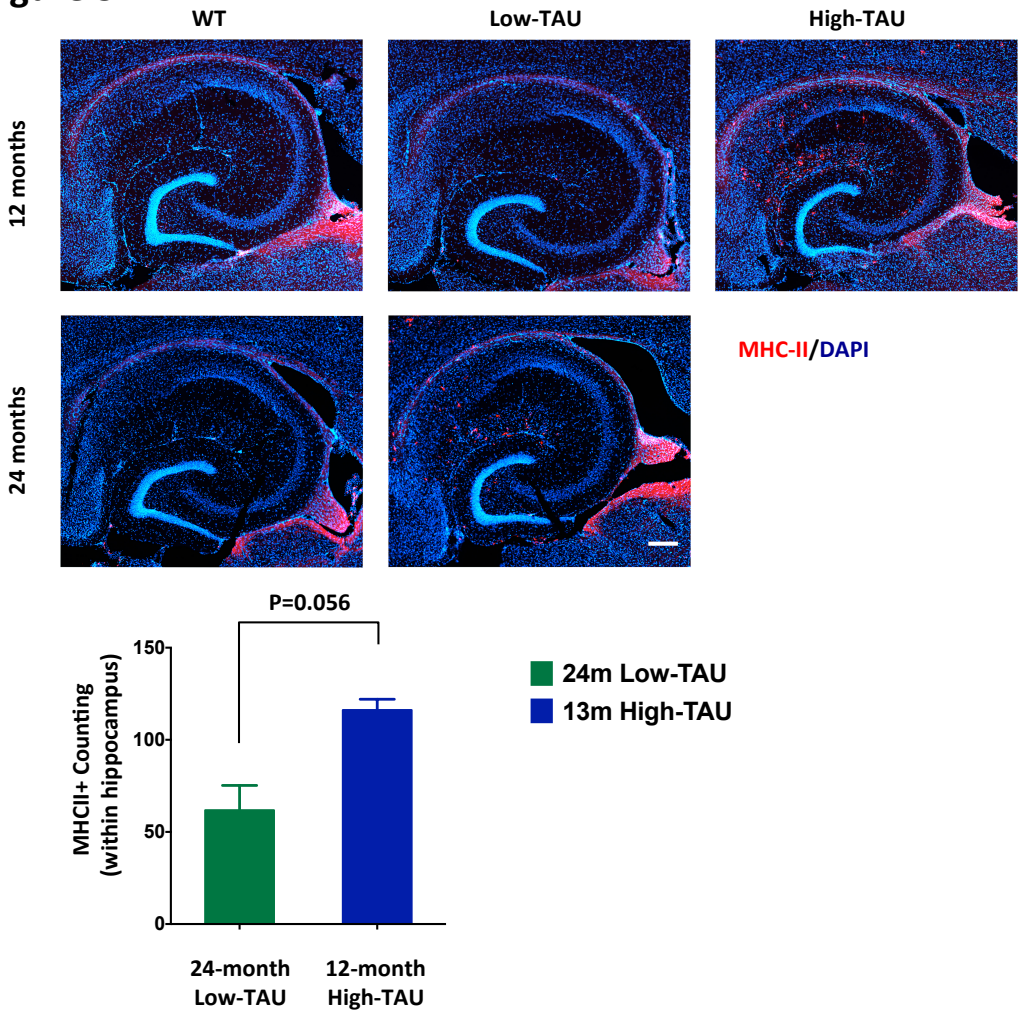

Figure 5.4. MHC-II expression increase in the hippocampus of 24-month low-TAU and 12-month high-TAU mice. Top: Representative images showing microglia expressing MHC-II in the hippocampus. MHC-II expression was investigated using immunohistochemistry in 4-, 12-, and 24-month old mice. MHC-II staining was visible from 12 months in high-TAU mice and 24 months in low-TAU mice. The MHC-II^{+} microglia tend to have a higher density in the *stratum lacunosum-moleculare* (SLM) region. Scale bar: 200µm**. Bottom:** Comparison of the MHC-II^{+} cell number between 24-month low-TAU and 12-month high-TAU mice in the total hippocampus. N=2-3 mice per group (3 sections per mouse). Data shown as Mean ± SEM. Unpaired student t-test; p=0.056.

Microglial expansion in different layers of the hippocampal CA1 region in the tau mice

As the MHC-II positive cells in the tau model showed an accumulation in the CA1 SLM layer, I wondered whether the total microglial distribution amongst different regions of the hippocampus was changed in different mouse models. I analyzed the microglia number by IBA1 staining in different layers of the hippocampal CA1 region in the wildtype, HO-*APP/PSEN1*, HE-*APP/PSEN1*, high-TAU, and low-TAU mice at 12 months of age (figure 5.5). I did observe a significant interaction between the effects of different genotypes and different CA1 layers (genotype, $p<0.0001$, CA1 layer, $p<0.0001$, interaction, $p<0.001$; Two-way ANOVA followed by Tukey's *post hoc* test). Specifically, the HO-*APP/PSEN1* showed dramatic increase of microglial number in all four CA1 layers compared to the wildtype. The HE-*APP/PSEN1* mice at this age only showed significantly increased microglia number in the SLM and SR (*stratum pyramidale*) layers, with a level falling between the homozygous line and the wildtype. However, regarding the high-TAU mice, a significant increase in the microglial population was only observed in the SLM layer, with an over 2-fold level of that in the wildtype mice. Additionally, there was a strong trend towards a significant increase in the SO (*stratum oriens*) layer in the high-TAU versus the wildtype ($p=0.055$). Taken together, the microglial distribution in the amyloid mice mainly depends on the plaque deposition (as shown by clustered microglia around plaque-like areas), and thus in the HE-APP/PS1 mice at 12 months, a higher microglia number was shown in the layers where plaques first develop in the CA1 region. However, in the tau model, there is a dramatic higher microglial density in the SLM layer where the perforant pathway fibers from the entorhinal cortex form synapses with the CA1 pyramidal neurons.

Figure 5.5

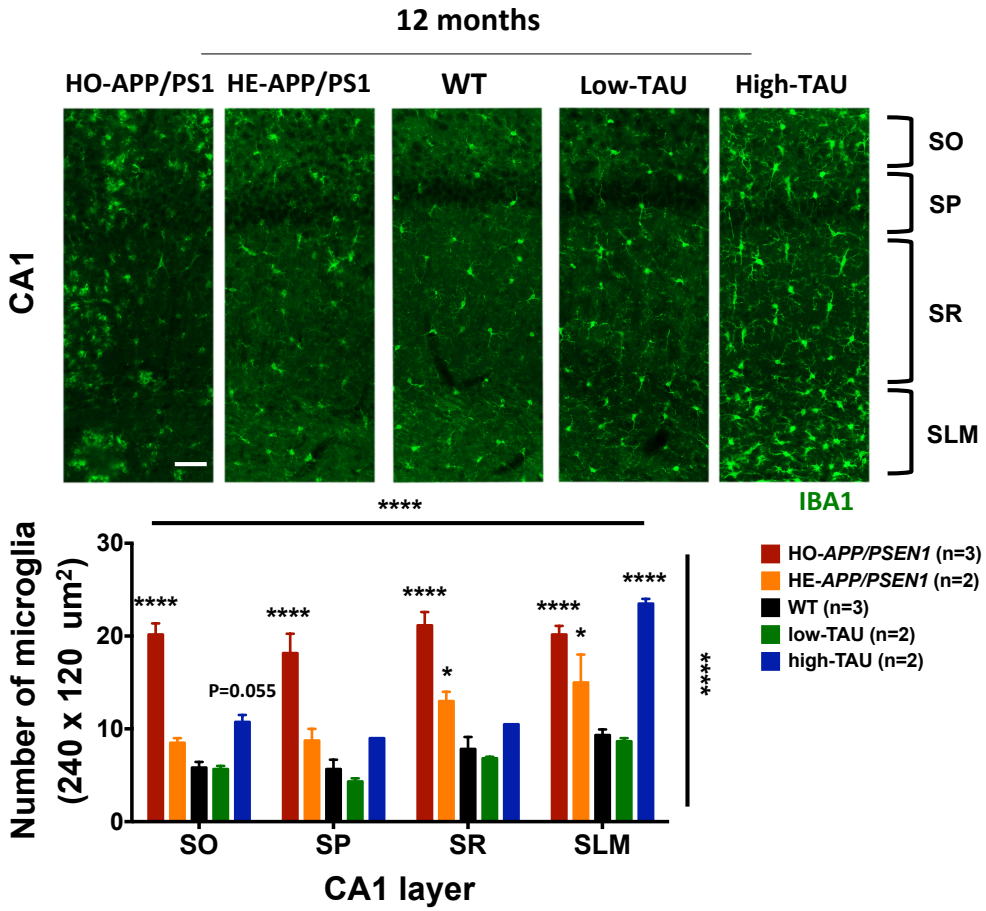

Figure 5.5. Microglial distribution in the hippocampal CA1 layers of the amyloid model and the tau model at 12 months. Upper: Representative images showing microglia by IBA1 staining in the CA1 region of the hippocampus. The layers from top are SO (*stratum oriens*), SP (*stratum pyramidale*), SR (*stratum radiatum*) and SLM (*stratum lacunosum-moleculare*). Scale bar: 50μm. **Lower:** Significantly increased microglial density in all 4 CA1 layers in the HO-APP/PS1, in the SR and SLM regions in the HE-APP/PS1, and in the SLM layer in the high-TAU mice. N=2-3 animals per group (3 sections per mouse). Data shown as Mean ± SEM. Two-way ANOVA followed by Tukey's *post hoc* test if there was significant interaction; horizontal and vertical lines for significant main effects of layers and genotypes respectively, * p<0.05, *** p<0.001, **** p<0.0001.

Summary

Both models showed obvious microglial expansion along pathology development using immunohistochemistry. However, the activation phenotype seemed different between the amyloid and the tau models. First, there was a significant increase in the CD68-positive microglial proportion in the tau models compared to the wildtype, while the amyloid mice only showed expansion of the total microglial population. Second, in the tau mice there was more substantial MHC-II expression in the hippocampus. The amyloid mice did show MHC-II positive cells as well, but it was only a very small group of cells, especially considering the highly increased microglial population at that stage. Third, the distribution of microglia in the hippocampus changed in the tau mice, with much higher microglial density in the SLM layer of CA1 region, while the microglial density in the SP region, mainly with CA1 pyramidal neuronal cell bodies where tau tangles accumulate, did not show much changes compared with the wildtype. Importantly, these similarities and differences in microglial numbers, activation and hippocampal regional localization provide us with important information on how microglia respond to different aspects of pathology associated with Alzheimer's disease, and how microglia may contribute to the pathology.

Chapter 6

Discussion

Alzheimer's disease, the most common cause of dementia, threatens society at many levels with its particular difficulty of long progression, late diagnosis and lack of effective intervention. Recently, GWAS studies uncovering a variety of immune-related gene variants as AD risk factors, such as *TREM2*, *CD33*, *ABI3*, and *PLCG2* (Griciuc et al., 2013; Guerreiro et al., 2013b; Hollingworth et al., 2011; Jonsson et al., 2013; Malik et al., 2013; Naj et al., 2011; Sims et al., 2017), have placed a spotlight on the potential role of the innate immune system especially the brain resident microglia in AD pathogenesis. In particular, TREM2, a myeloid cell transmembrane protein only first identified in the early 21st century and revealed as one of the strongest AD risk genes, still retains secrecy for its precise biological functions. But it is likely to perform a regulatory role for microglia, which requires intensive studies to reveal its functions and contributions to AD, as well as allowing us to understand enough of the driving mechanisms to enable effective drug targeting.

In this thesis, I have focused on the cellular functions of TREM2 in microglia, using an *in vitro* primary microglial model with acute *Trem2* knockdown by RNAi strategy. This approach can readily be applied to study the many other microglial-expressed genes recently discovered to be associated with AD and other neurodegenerative conditions. In the past few years, there have already been a variety of *in vitro* studies that have shed light on some aspects of the TREM2 biological functions on microglia or macrophages, and the most promising conclusion is about the involvement of TREM2 in phagocytosis and restricting inflammatory responses (as discussed in Chapter 1). In chapter 3 of this thesis, I not only further validated the effects of *Trem2* deficiency on these functions in a physiologically relevant system, primary microglia, but I

also particularly studied its effects on general microglial gene expression and microglia polarized to the M2 alternative activation phenotype, also known as 'anti-inflammatory and tissue repairing' functions. Particularly, my results suggest that TREM2 is involved in regulating the microglial IL4 signaling pathway that further up-regulates *Trem2* expression, which could be an important pathway interacting with the TREM2 signaling in microglia and a potential drug-targeting pathway for compensating TREM2 deficiency. Further investigation on potential downstream steps influenced by TREM2 is needed. Additionally, I employed the primary microglial culture from wild type mice and induced acute *Trem2* knockdown after the microglia developed normally *in vivo,* allowing us to study more direct functions of TREM2, not diluted by compensatory changes that may occur during chronic *Trem2* inhibition, as in *Trem2* knock-out studies.

Secondly, in chapter 4 and 5, I utilized two lines of transgenic mouse models that mimic either the amyloid or the tau pathology development of AD, to investigate the differences in microglial phenotypes in the context of different aspects or stages of AD pathogenesis. By studying this topic, I have furthered the importance of targeting differential microglial pathways and functions depending on the different time points of therapeutic intervention in AD. Particularly, I have emphasized divergent microglial *Trem2* expression changes in response to amyloid or tau pathology in these mice, which enables us to analyze the dynamic and multiple contributions of TREM2 implicated in AD pathology progression.

Trem2 gene expression divergently regulated by microglial inflammatory states in vitro

I found *Trem2* expression was differentially regulated under different microglial inflammatory conditions in our *in vitro* model. In steady-state microglia, without either LPS or IL4 treatment, *Trem2* expression was consistently detected in our primary microglial model, although there was a

substantial variation in the expression levels between different preparations of cells, which might reflect biological variability between different litters of mice and differences in the microglial status due to a technical variation during experiment. With LPS stimulation, our model exhibited a robust pro-inflammatory response, as measured by strong up-regulation of *Tnf* and *Il1b*, and importantly, *Trem2* gene expression was largely suppressed, which started between 3 and 6 hours after LPS application and quickly reached >90% decrease by 24 hours. This finding is consistent with previous studies showing that LPS down-regulated *Trem2* expression in microglia or macrophages *in vitro* and *in vivo* (Owens et al., 2017; Schmid et al., 2002; Turnbull et al., 2006; Zheng et al., 2016). Moreover, Owens and colleagues showed that treatment with pro-inflammatory mediators engaging other TLRs, rather than TLR4, which is recognized by LPS, also suppressed *Trem2* expression in the BV2 cell line, albeit with slight different potency (Owens et al., 2017). This suggests that the *Trem2* down-regulation is not specific to LPS-TLR4 signaling but perhaps a common event occurring in microglial classical activation induced by various pro-inflammatory stimuli.

Mechanistically, it was found that LPS-induced *Trem2* down-regulation in the BV2 cell line was dependent on activation of NF-κB (Owens et al., 2017; Zhong et al., 2017b). I found in the *in vitro* model that the *Trem2* transcriptional suppression started between 3 and 6 hours after LPS treatment, which occurred later than up-regulation of pro-inflammatory genes *Tnf* and *Il1b* that are directly regulated by NF-κB activation. The suppression of *Trem2* expression might thus be through an indirect regulatory mechanism of NF-κB. Scientists have already found that *Trem2* expression was suppressed by miRNA-34a that was induced by NF-κB (Alexandrov et al., 2013; Bhattacharjee et al., 2016; Zhao et al., 2013). Therefore, negative regulation of *Trem2* expression might be one of the modulating mechanisms of microglia to adjust to various functional requests.

In contrast to LPS, IL4 stimulation that induces typical M2 alternative activation, involved in inflammation suppression and tissue repair, resulted in up-regulation of *Trem2* expression in the *in vitro* model. I noticed a consistent

increase (to around 150% levels of non-treated cells) in the *Trem2* transcriptional levels at 48 hours after IL4 treatment. But at 24 hours after stimulation, the mRNA levels of *Trem2* were not significantly different from the baseline *Trem2* expression, consistent with a recent study published by Owen and colleagues showing that 24-hour IL4 treatment did not affect *Trem2* expression in primary microglia or the BV2 cell line (Owens et al., 2017), although they did not investigate whether longer IL4 treatment could increase *Trem2* expression. Conclusively, IL4-induced microglial alternative activation is accompanied by increased *Trem2* expression, but it occurs with an apparent delay compared with the induction of typical M2 genes. IL4 signals through IL4Rα that predominantly activates STAT6, which plays a central role in inducing M2 genes expression (Gordon and Martinez, 2010; Luzina et al., 2012; Nelms et al., 1999). A study with *Stat6*-knockout mice shows that the presence of STAT6 is sufficient but not necessary for macrophage *Trem2* expression induction (Turnbull et al., 2006). Also considering the markedly delayed *Trem2* mRNA increases observed in the *in vitro* model, I propose that the *Trem2* up-regulation is not the direct target regulated by transcription factor STAT6, but is due to some other events induced at relatively later stages of the IL4 response, or one of the consequences of the inflammation suppressive effects mediated by IL4-induced inhibition of NF-κB-dependent transcription (Ohmori and Hamilton, 2000).

Taken together, microglia constitutively express *Trem2*. Pro-inflammatory stimuli like acute infection, elevated amyloid-beta, neuronal injury, or infiltrated pro-inflammatory mediators from periphery could induce down-regulation of microglial *Trem2* expression and subsequently decrease TREM2-related functions in microglia. This might reflect a physiological mechanism for microglia to adapt to the functional requirements under the inflammatory condition. Nevertheless, accumulated inflammation in the brain, which is often observed in aged brains, could cause sustained suppression of *Trem2* expression and thus an impairment of TREM2-dependent microglial functions. This might be one of the major mechanisms underlying TREM2 dys-function that contributes to sporadic AD progression with advanced age, since *TREM2*

loss-of-function variants associated with increased AD risk are extremely rare in frequency in humans.

In a previous collaborative study, we produced genome-wide gene expression data from different lines of mouse models mimicking either amyloid pathology or tau pathology in AD (Matarin et al., 2015). We identified a range of genes showing similar expression changing patterns in the amyloid model, with *Trem2* as a 'hub' gene in the network. To analyze the potential regulating factors for *Trem2* expression, we employed the top 50 genes in the network most similar to the change in *Trem2* expression and searched for transcription factor binding sites (performed by Dr. Evan Santo and Dr. Dervis Salih). We found that this group of genes contained significant enrichment ($p<0.01$) for 90 binding motifs for transcription factors from the TRANSFAC database (version February 2013; http://www.biobase.de), of which only eight transcription factors (*E2f2*, *Myc*, *Spib*, *Egr3*, *Egr1, Spi1, E2f4* and *Xbp1*) were expressed at the highest level in microglia in the mouse brain compared to other cell types, according to an online database (http://www.brainrnaseq.org) generated by Ben Barres and colleagues (Zhang et al., 2014). Of these eight transcription factors, only the SPI1 binding motif was present in the promoter region of *Trem2* (defined as 2.5 kb upstream of the transcription start site and 0.5 kb downstream of the transcription start into the first intron; figure 6.1 A), which was bound by transcription factor PU.1 and also potentially by SPIB. A previous study also suggested *TREM2* as a PU.1 target gene in the BV2 cell line (Satoh et al., 2014) and human monocytes (Huang et al., 2017). PU.1 is a key transcription factor required for myeloid cell development and functions, including microglia (McKercher et al., 1996). Particularly, it was found that *Spi1* (the gene encoding PU.1) overexpression or knockdown regulated expression levels of many AD risk genes in the BV2 cell line, and lower expression of PU.1 was associated with a decreased AD risk (Huang et al., 2017). All these thus suggest a potential role of PU.1 in *Trem2* expression regulation. However, in my *in vitro* model, *Spi1* expression was found to be up-regulated in both LPS- and IL4- treated conditions (figure 3.7 and 3.9), whereas *Trem2* expression was divergently regulated. Especially in the LPS condition, *Spi1* showed an over 2-fold up-regulation at all time points of

analysis, while *Trem2* was found to be largely down-regulated, suggesting PU.1 may not be the key regulator of *Trem2* expression in microglia. To investigate more specifically the role of PU.1 in *Trem2* expression regulation, I used an RNAi strategy to knockdown *Spi1* in the BV2 cell line (figure 6.1 B); Note, I tried to knock down *Spi1* in my primary microglial model but this caused severe cell death, which made it impossible to collect enough samples for analysis. I found in the BV2 cell line that, different from the *Csf1r* expression that was strongly inhibited by *Spi1* knock-down, the *Trem2* expression was not significantly changed, although there was a trend towards a decreased level ($p=0.094$; One-sample t-test). This is consistent with the findings by Huang and colleagues (Huang et al., 2017) that also showed *Trem2* expression was not significantly affected by *Spi1* overexpression or knockdown in BV2 cells. Therefore, PU.1 does not seem to play a central role in regulating *Trem2* expression levels in microglia either *in vitro* or in our mouse models of AD.

Figure 6.1

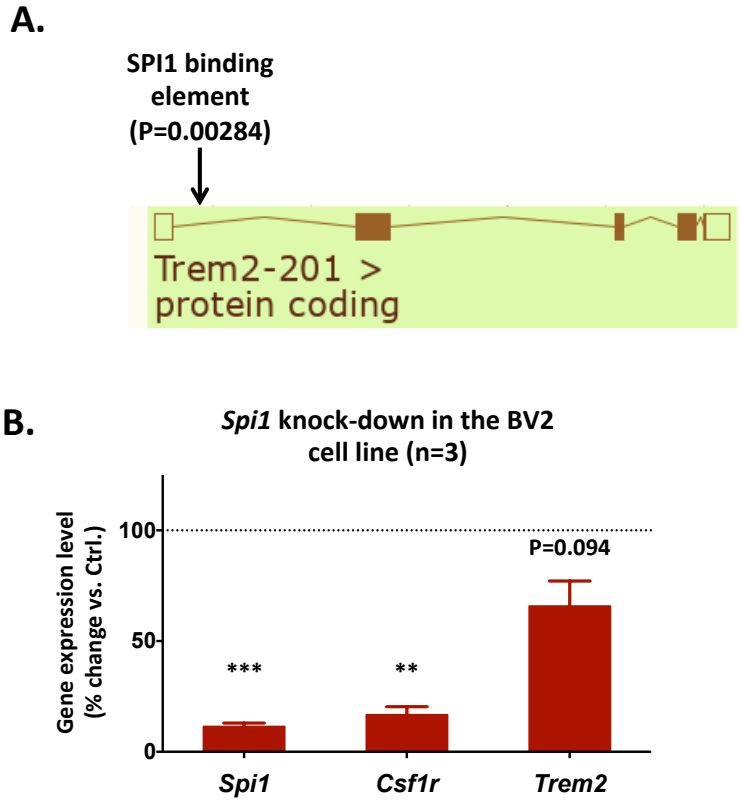

Figure 6.1. PU.1 is not the key regulator for *Trem2* expression in the BV2 cell line. (A) 50 genes (including *Trem2*) behaving most similarly in a microarray analysis with amyloid mouse models versus the wildtype (Matarin et al., 2015) were analyzed for potential transcription factor binding sites using the TRANSFAC database. There were 90 significantly enriched binding sites ($p<0.01$) for transcription factors, of which only 8 were expressed most by microglia in the mouse brain (http://www.brainrnaseq.org). Moreover, only the SPI1 binding site was present in the promoter region of the *Trem2* gene. **(B)** BV2 cells were treated with either *Spi1* siRNA or non-targeting siRNA for 48 hours, and analyzed for gene expression. *Spi1* levels were decreased by around 90%, and *Csf1r* showed over 80% down-regulation. However, the *Trem2* expression level was not significantly affected. N=3 independent experiments. Data shown as Mean ± SEM. One-sample t-test; ** $p<0.01$, *** $p<0.001$, **** $p<0.0001$.

Microglial basal gene expression changes resulting from *Trem2* expression deficiency, such as decreased *Igf1* expression levels

The next question is how loss of TREM2 expression affects microglial functions. To answer this question, I first examined if acute *Trem2* deficiency induced by RNAi influences gene expression in the primary microglia. Then we polarized microglia to either M1 classical or M2 alternative phenotypes to investigate if *Trem2* deficiency alters microglial activation.

To characterize the contribution of TREM2 to the normal microglial phenotype, I investigated the gene expressional changes in primary microglia with acute *Trem2* knockdown in regular microglial culture conditions. I found a significant decrease in the expression levels of a range of microglial genes such as *Cd68*, *Csf1r*, *Igf1*, *Pik3cg*, and *Spi1*. This effect appeared subtle – only a 10-20% decrease of expression of those genes was observed, especially compared to the strong knockdown (70%) of *Trem2* obtained. It suggests that *Trem2* deficiency may not strongly impair the baseline microglial state but only slightly shift the microglial phenotype, and in future studies we would employ microarray or RNA-seq to further investigate the effect of *Trem2* knockdown on the entire microglial transcriptome.

An important point which needs to be considered here is that *in vivo* microglia receive various regulatory signals from other brain cell types such as neurons (*e.g.* CX3CL1 and CD200) to maintain the normal microglial phenotype and surveillance abilities, and *in vitro* primary microglia have been shown to exhibit a significantly different transcriptional signature compared to the *in vivo* microglia (Butovsky et al., 2014). Also, CSF1 (or IL34), the ligand of CSF1R and a key survival factor for microglia (Elmore et al., 2014), was not added to our regular microglial culture medium. Although the mixed-glial-conditioned medium used to culture isolated primary microglia might still bear some of the trophic factors for microglial survival, there was still increasing cell death as the trophic factors were consumed. Therefore, the microglia at the point of

analysis may not exactly represent normal 'resting' microglial state but act more like a microglial phenotype in slightly stressed conditions, and thus the effects of *Trem2* deficiency we observed here actually reflect the implications of *Trem2* on slightly stressed and activated microglia rather than normal microglia in healthy brains. It still needs further study for whether such phenotype shifts also happen *in vivo* when *Trem2* expression or function is suppressed. A very recent paper has studied the microglial transcriptome in *Trem2* knock-out mice and found a wide range of genes slightly but significantly dys-regulated, a majority of which represent functions in microglial mobility and chemotaxis (Mazaheri et al., 2017). However, the knock-out mouse model with complete TREM2 loss likely contain some detrimental or compensatory/homeostatic responses indirectly due to TREM2 loss, especially during development, which may influence the estimation of TREM2 regulatory functions. Mice with disease-associated *TREM2* variants knocked-in or acute *Trem2* knock-down via e.g. oligonucleotide-based *in vivo* gene silencing may provide better *in vivo* models to study the direct regulating functions of TREM2 on microglia.

Among the down-regulated genes I observed in the *in vitro Trem2* knock-down model, *Igf1* is the most pronounced changed gene which was also validated with another independent *Trem2* siRNA. IGF1 is an important neurotrophic factor in the brain, mainly involved in neuroprotection, neurogenesis, synaptic plasticity maintenance, anti-inflammation and ageing (Fernandez and Torres-Aleman, 2012). In addition to its peripheral source from the liver, IGF1 is also produced locally in the brain. In general, microglia are the major source of IGF1 produced in the CNS whereas neurons constitute the main targets of IGF1 due to high expression of IGF1R, although it is found that IGF1 is only abundantly expressed by activated microglia during postnatal development, ageing or following brain injuries and plays a vital role in promoting neuronal survival (Fernandez and Torres-Aleman, 2012; Kohman et al., 2012; Thored et al., 2009; Ueno et al., 2013). In the *in vitro* model, as described above that it represents a slightly stressed and activated microglial phenotype, it is not surprising that I observe a relatively high *Igf1* expression in microglia. Both my findings and previous studies

(Arkins et al., 1995; Barrett et al., 2015; Suh et al., 2013; Wynes and Riches, 2003) show that *Igf1* expression is inhibited by pro-inflammatory stimuli and enhanced in M2 anti-inflammatory environments. Thus the *Igf1* expression decrease caused by *Trem2* deficiency may suggest a microglial phenotype shift towards M1 activation but away from M2, and a decrease of the pro-survival role on neurons.

The phenotype shift caused by *Trem2* knock-down made us curious about how *Trem2* deficiency affects microglia reactions in response to M1 pro-inflammatory or M2 anti-inflammatory stimuli. So I polarized our *in vitro* model to either M1 or M2 activation with LPS or IL4 application. However, an important issue about microglial activation *in vivo* has to be considered carefully. Different from microglia polarized to M1/2 states with purified LPS or IL4 stimuli *in vitro*, microglia *in vivo* never receive only one single stimulus to govern their activation states. Instead, they are modulated by mixed cues including various regulatory signals from local environment (e.g. from neurons and astrocytes) and exposure to emerged DAMPs (disease-associated molecular patterns) and cytokine stimuli, leading to a mixed, dynamic and context-dependent microglial phenotype *in vivo*. It has been clear that reactive microglia in diseased brains demonstrate a mixed phenotype with expression of both M1 and M2 markers, even at the single-cell level, rather than completely reproduce the phenotype obtained from *in vitro* polarization studies (Kim et al., 2016; Morganti et al., 2016). Therefore, it is apparently inappropriate to directly apply the *in vitro* phenotype to our interpretation of *in vivo* microglial activation. However, I propose M1 and M2 stimuli still represent part of the driving factors determining the range microglia fall in of the entire multidimensional continuum of microglial activation. Thus, to study the relevance of TREM2 in regulating microglial activation, I initially used the polarization experiments to dissect the reaction of microglia in response to either M1 or M2 stimuli and investigate the effects of *Trem2* deficiency in each direction.

Modestly amplified M1 pro-inflammatory activation of *Trem2*-deficient primary microglia in response to LPS

As discussed earlier, *Trem2* expression was largely suppressed in microglia with LPS stimulation, suggesting inhibition of TREM2-related functions in pro-inflammatory responses. I found that the M1 gene expression changes in response to LPS were not significantly different between the control group and the *Trem2* knockdown group, which was not surprising to us as the *Trem2* expression in the control group treated with LPS was suppressed to a comparable level to that in the knockdown group. However, I did observe a modest increase of the LPS-induced pro-inflammatory secreted marker TNFα at the protein level in the knockdown group compared to the control, by ELISA analysis of microglial supernatants. Furthermore, a cytokine array confirmed increased LPS-induced TNFα production (~1.5-fold) in the *Trem2*-knockdown microglia compared to the control. Previous studies using primary microglia, BV2 cells, or macrophage cultures have also shown that *Trem2* deficiency results in an elevated M1 response with pro-inflammatory stimuli, as measured by increased inflammatory cytokine production (Gao et al., 2013; Takahashi et al., 2005; Turnbull et al., 2006; Zhong et al., 2015). Therefore, constitutive expression and function of TREM2 may play a role in restraining the levels of microglial pro-inflammatory responses, although the underlying mechanisms are still unclear. My findings do not seem to suggest a strong effect at the transcriptional levels, as the pro-inflammatory marker mRNA increases did not show significant differences between the knockdown and control groups. The TREM2 signaling might instead affect the proteolytic cleavage and secretion of pro-inflammatory cytokines, which still needs further investigation.

Additionally, I found a range of pro-inflammatory chemokines such as CCL2, CCL3, CCL4, CCL5, CXCL1, CXCL13, *etc.* induced by LPS and showing a similar increasing trend to TNFα in the *Trem2*-knockdown microglia versus the control, none of which demonstrated more than a 2-fold change. Among all the cytokines / chemokines detected in the LPS-treated microglia by the

parallel proteome array, CCL5 was the factor with the highest detected signal, suggesting a high level of release from microglia in response to LPS, and particularly it showed over a 1.6-fold increase in the *Trem2*-knockdown group than the control. CCL5 (also known as 'Regulated on activation normal T cell expressed and secreted'; RANTES) is a pro-inflammatory chemokine mainly produced by T cells and antigen-presenting cells and in the brain by microglia, and it is known to induce migration and homing of classical lymphoid cells such as T cells and monocytes (Appay and Rowland-Jones, 2001; Hu et al., 1999). It was suggested to play an important role in CNS infiltration of T cells in a Parkinson's disease mouse model (Chandra et al., 2016), and besides its chemo-attractant role, it was also found to amplify microglial pro-inflammatory responses in vitro (Skuljec et al., 2011). Furthermore, CCL2 (also known as 'Monocyte chemotactic protein 1'; MCP-1), a key chemokine determining leukocyte infiltration in injured CNS (Babcock et al., 2003; Bose and Cho, 2013; Huang et al., 2001), was also produced around 1.6-fold higher in the *Trem2*-knockdown microglia than the control. Therefore, *Trem2*-deficient microglia, when encountering pro-inflammatory stimuli, appear to show stronger chemokine production involved in interactions between microglia and peripheral immune cells. In the context of brain injury, this might provide a promoting role in infiltration of peripheral immune cells.

Attenuated M2 alternative activation of *Trem2*-deficient microglia in response to IL4

The M2 alternative activation induced by IL4 treatment seemed to be affected more prominently by *Trem2*-deficiency. I found significantly reduced *Arg1* up-regulation and a trend of decreased *Tgfb1* up-regulation in *Trem2*-knockdown microglia with IL4. ARG1 and TGFβ1 are both important M2 markers. ARG1 (Arginase-1) in macrophages mainly functions as an enzyme to hydrolyze arginine to produce ornithine, which on one side promotes tissue repair through generation of polyamines and collagens and on the other side reduces nitric oxide production from iNOS through limiting intracellular

arginine availability (Yang and Ming, 2014). TGFβ1 promotes an inflammation suppressive function in microglia and enhances IL4-induced M2 activation of microglia through a MAPK-dependent pathway (Basu et al., 2002; Herrera-Molina and von Bernhardi, 2005; Suzumura et al., 1993; Zhou et al., 2012). Importantly, TGFβ1 has been recently found to be a key factor to retain a normal 'resting' microglial signature *in vivo* (Butovsky et al., 2014). Our findings suggest an attenuated M2 phenotype expression in *Trem2*-knockdown microglia, although *Trem2*-deficiency does not seem to completely block the IL4-induced expression of M2 markers. I thus propose TREM2 signaling may function in parallel to facilitate IL4-induced transcription changes. TREM2 signals through DAP12 or DAP10, which recruits SYK and initiates a cascade of downstream signaling events, such as PI3K activation, MAPK activation, and calcium mobilization (as discussed in Chapter 1). IL4 signaling mainly regulates M2 gene transcription through STAT6 activation in macrophages, but it also recruits IRS-1/2 to activate the PI3K pathway that is required for STAT6-dependent transcription changes (Gordon and Martinez, 2010; Rauh et al., 2005; Weisser et al., 2011). Additionally, p38 MAPK has also been suggested to be involved in IL4-induced M2 phenotype expression in macrophages (Jimenez-Garcia et al., 2015). Therefore, the PI3K and MAPK pathways activated by TREM2 signaling might provide a supportive intracellular environment to enhance the STAT6-dependent gene transcription induced by IL4, which is worth following up to confirm. However, the PI3K/Akt pathway, in the context of M2 activation, could be activated by multiple signaling pathways, such as direct IL4-IRS1/2 recruitment and IGF1 signaling as well, which is also up-regulated and suggested to contribute to IL4-induced M2 activation. All these pathways might coordinate together, and probably temporarily, to control the microglial anti-inflammatory phenotype.

Similar to LPS-treated microglia, I also observed an increase in the release of various cytokines / chemokines from the IL4-treated *Trem2*-knockdown microglia compared to the IL4-treated control microglia. Most of the altered chemokines overlapped with those found in LPS-treated cells, such as CCL5, CCL2, CXCL1, TIMP-1, CXCL12, CXCL10, *etc.,* although the absolute detected signal levels were lower than those from LPS-treated cells. However,

the fold change was much higher in the IL4 conditions, further suggesting a stronger effect of *Trem2*-deficiency on IL4 responses. The most prominently altered chemokine was CXCL1 (keratinocyte-derived chemokine; KC), which showed a 6-fold higher level in the IL4-treated knockdown group than the IL4-treated control group. Notably, in the LPS conditions, its release was also higher (around 1.5-fold of the control) in the *Trem2*-knockdown microglia. CXCL1 is a chemokine mainly expressed by macrophages, neutrophils and epithelial cells, and known as a chemoattractant for leukocyte recruitment (Baggiolini, 1998; Haskill et al., 1990). Previous studies have also suggested its potential relevance with AD. For example, its receptor CXCR2 was found to be expressed by hippocampal neurons and up-regulated in the neurites surrounding Aβ plaques in AD (Horuk et al., 1997). A study suggested that CXCL1 could trigger tau hyper-phosphorylation in mouse primary neurons through the ERK1/2 and PI3K pathway (Xia and Hyman, 2002). Also, CXCL1 could activate astrocytes and promote their cytokine and chemokine production (Luo et al., 2000). However, as endothelial cells rather than microglia are the major source of CXCL1 in the brain, it is still not clear whether *Trem2*-deficiency-induced microglial CXCL1 production increase is of any obvious functional relevance in the brain homeostasis and AD pathogenesis.

Overall so far, I have shown that acutely induced *Trem2* deficiency results in a slight but significant microglial gene expressional change, which might be associated with a more pro-inflammatory state of microglia and lead to less neuroprotective functions. With LPS stimulation, *Trem2* deficiency amplifies the pro-inflammatory response of microglia, albeit only modestly. With the IL4 application, however, microglial anti-inflammatory responses are considerably affected at least at the transcriptional levels. Additionally, *Trem2* deficiency leads to an enhanced chemokine secretion in both M1 and M2 conditions, which might suggest an over-reactive microglial response and potentially more infiltration of peripheral immune cells into the CNS.

Divergent *Trem2* expression and microglial gene expression profile between amyloid mice and tau mice

To characterize the differences in the microglial activation at different pathology stages of AD *in vivo*, I employed two lines of transgenic mouse models mimicking the amyloid pathology and the tau pathology respectively. I examined the microglial gene expression in the hippocampus of different aged mice to allow us to assess changes associated with different stages of disease. This allows us to investigate microglial reaction in response to different aspects of AD pathology, that being rising amyloid-beta and plaque deposition in APP/PSEN1 mice versus rising hyper-phosphorylated tau and neurofibrillary tangles in TauD35 mice. I identified three major stages in pathology development to analyze the similarities and differences between the two lines of mouse model, especially between the HO-*APP/PSEN1* and the high-copy TauD35 mice. First, at 4-8 months of age, when the *APP/PSEN1* mice started to develop mature dense-core Aβ plaque deposition in the hippocampus, with the heterozygous showing a slower rate than the homozygous, we observed that the expression levels of microglial genes such as *Aif1*, *Cd68*, and *Trem2* started to increase. In contrast, the TauD35 mice microglial genes still showed comparable expression levels to wildtype mice at this stage when the high-TAU model demonstrated a significant degree of phosphorylated tau in the hippocampus and started to develop neurofibrillary tangles. Secondly, at 12 months of age, when both *APP/PSEN1* mice and high-TAU mice exhibited a relatively heavy load of Aβ plaques or tangles in the hippocampus, the amyloid model showed further increased expression of these microglial genes, and the tau model just started to show the up-regulation. Thirdly, at 18 months, the HO-*APP/PSEN1* hippocampus was heavily covered by plaques and the high-TAU showed a significant neuronal loss. Not surprisingly, microglial genes expression further increased in both models. I also observed a significantly increased expression with age in the pro-inflammatory genes *Tnf* and *Il1b* and the anti-inflammatory gene *Tgfb1* in both models, but in general no overtly pro- or anti- inflammatory phenotype developed. It seemed that the amyloid model showed increasing microglial

gene expression following the progressing amyloid deposition; while in the tau mice there was a delay in the microglial gene response compared to the tangle development. One important point here is that the cDNA samples were generated from the whole hippocampus including all cell types, so the microglial gene expression changes might be partially due to an expansion of the microglial population. Also that some more subtle but significant microglial gene expression changes might be masked by using a whole hippocampal homogenate of mixed cell types.

Trem2 expression showed up-regulation along with pathology progression in both models, but the expression levels were consistently lower in the tau model than in the amyloid model. To further characterize the relative *Trem2* expression in microglia, we used *Aif1* as a reference to normalize it, to provide a measure of the average *Trem2* expression in the microglial population. I found, interestingly, the relative *Trem2* levels were getting significantly higher as amyloid pathology developed, whereas the tau mice only showed comparable relative *Trem2* expression levels to wildtype mice even at the late stage with severe neuronal loss. Although the *Trem2*/*Aif1* ratio does not exactly represent the *Trem2* expression level per microglia because of heterogeneity of the microglial population and potential *Aif1* expression differences, it still provides us with some information on the average *Trem2* expression in microglia. Moreover, as we described in our previous paper (Matarin et al., 2015), network analysis of the gene expression changes in these two lines of mouse models suggested *Trem2* as a hub gene with extremely high connectivity with other genes in the amyloid model, but not in the tau model. Therefore, we propose that in response to Aβ deposition microglial *Trem2* expression is up-regulated starting from early stages of pathology, which may play an important role in regulating the microglial activation. However, in the tau model, *Trem2* does not seem to be critically involved in regulation of microglial activation in response to tangles, and its exact expression level is not convincingly up-regulated despite an expansion of the entire microglial population. In a recently published study (Keren-Shaul et al., 2017), it was suggested that *Trem2* expression determined development of a protective disease-associated microglial activation

phenotype associated with plaques in the 5XFAD mouse model, further suggesting the central role of TREM2 in regulating robust microglial activation in response to amyloid pathology development.

To further confirm the difference in the microglial gene expression between the amyloid model and the tau model, we then employed the gene expression database (www.mouseac.org) generated in our previous study (Matarin et al., 2015) and presented further analysis of the microglial genes in the 18-month HO-*APP/PSEN1* and high-TAU mice, both at a late stage of pathology development. Genes expressed most abundantly in microglia were identified using the online database generated by Ben Barres and colleagues showing gene expression changes between different cell types of the mouse brain (http://www.brainrnaseq.org; Zhang et al., 2014). We then identified genes with more than 20% increases or decreases comparing wildtype to the amyloid or the tau mice (with $p<0.01$). We found considerable differences in the microglial genes both up-regulated and down-regulated between these two models (figure 6.2). This comparison further suggests a different microglial phenotype induced in the amyloid model versus the tau model.

Figure 6.2

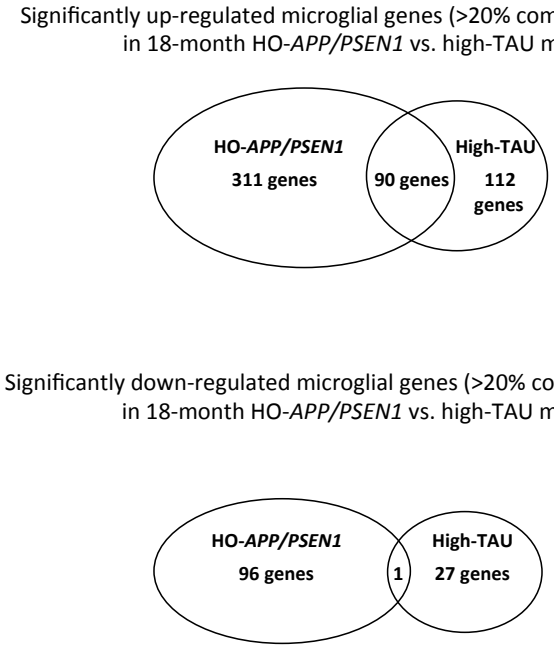

Figure 6.2. Genes with expression levels changed >20% in the HO-*APP/PSEN1* mice and the high-TAU mice at 18 months compared to wildtype mice. Venn diagrams depicting the overlap between genes increased or decreased >20% (ANOVA, $p<0.01$) within the hippocampus of the HO-*APP/PSEN1* and high-TAU animals at 18 months.

In brief, I have revealed the microglial gene expression reaction to amyloid versus tau pathology in mouse models, and particularly suggested a TREM2-involved early microglial activation in response to amyloid deposition. Such robust microglial activation associated with amyloid pathology development does not show an obvious pro-inflammatory state, and probably protects against further AD-related pathology progression and the transition to late stages of the disease, as the amyloid model does not show fully developed AD (tau tangles and neuronal death). However, the situation is different in human brains. The mouse models are always kept in a well-controlled pathogen-free environment, and so lacking a variety of modifiable environmental risk factors that humans are normally exposed to during ageing, such as type 2 diabetes, vascular diseases, smoking, and obesity. These factors are usually associated with an increased systemic inflammatory state, which could 'prime' microglia in the brain and cause exaggerated or

dys-regulated reactions to emerging AD-related pathology (Cunningham et al., 2009; Perry et al., 2007; Perry and Holmes, 2014). Such dys-regulated immune reactions might be a critical component in AD contributing to the progression from the stage of Aβ elevation to that of tau pathology and neurodegeneration.

Histology differences in microglia between amyloid and tau models

I then performed immunohistochemistry to further investigate the expansion and activation of the microglial population in the amyloid compared to the tau models. In the 4-month HO-*APP/PSEN1* mice, when mature plaques just started to develop, I did not observe a significant difference in the overall microglia number in the hippocampus compared to the wildtype mice. But that could be partially due to a small sample size of the 4-month HO-*APP/PSEN1* group. The mean microglia number of this group was actually around 1.4-fold of the wildtype in dentate gyrus and around 2-fold in CA1 region, suggesting microglia may potentially start to proliferate at this stage as amyloid plaques begin to be deposited. In future work we might be able to determine if this early proliferation is significant. I did find a highly increased number of total microglia and CD68-positive microglia in the hippocampus of the HO-*APP/PSEN1* model at 12 months, when they developed a relatively heavy plaque load. For the tau model, I did not observe any significant increase of microglia in the hippocampus at the pre-tangle (4-month low- and high-TAU) or early tangle (12-month low-TAU) stages, whereas in 12-month high-TAU mice, both total microglia and CD68-positive microglia showed significant increases compared to the wildtype. Additionally, I observed a slightly increased percentage of CD68-positive microglia in the entire microglial population in the hippocampus of 12-month high-TAU mice, while in the HO-*APP/PSEN1* mice this proportion did not show a significant difference from that in the wildtype. Interestingly, despite the genotype, I also observed an increase of the proportion of CD68-positive microglia with age. The increased

CD68 proportion possibly suggests an increased proportion of microglia with high phagocytic activity.

A pronounced difference in the microglia between the amyloid and tau models I observed was the distribution of microglia in the hippocampal CA1 region. I found a particularly increased microglia density in the SLM layer (*stratum lacunosum-moleculare*) of CA1 region in the 12-month high-TAU mice, whereas in the *APP/PSEN1* mice the density of microglia increased almost equally among all different layers of CA1. Moreover, the MHC-II positive microglia also tended to accumulate in this SLM region of the tau mice, suggesting a highly activated subgroup of microglia in this region. This is interesting because the SP (*stratum pyramidale*) layer, rather than the SLM layer, is the region with CA1 pyramidal neuronal cell bodies where tau tangles accumulate, which did not show much changes compared with the wildtype. The SLM is where the perforant pathway fibers from the entorhinal cortex form synapses with the CA1 pyramidal neurons. In human AD, tau pathology tends to progress from the entorhinal cortex to the hippocampus (Braak and Braak, 1991, 1997), suggesting a higher vulnerability of entorhinal neurons and a potential involvement of the synaptic pathways between entorhinal cortex and hippocampus in tauopathy progression. Trans-synaptic tau propagation from entorhinal neurons has been implicated with the tau mice harbouring human-tau restricted to the entorhinal cortex but showing detectable tau aggregates downstream in the synaptic circuit (de Calignon et al., 2012; Harris et al., 2012; Liu et al., 2012). Further research reveals that neuronal activity stimulates tau protein release from neurons (Pooler et al., 2013; Wu et al., 2016; Yamada et al., 2014). Moreover, it has been postulated that microglia take up tau proteins released from neurons and play a role in trans-neuronal tau propagation, suggesting they actively react to neuronally released tau (Asai et al., 2015; Wang et al., 2017). So it is possible that there is a higher level of released tau proteins from the perforant fibers in the SLM region, which drives microglial accumulation and activation here. Another possible cause might be potential neurite or synaptic damage in this region. The CA1 pyramidal neurons project distal apical dendrites to the SLM region, and 12-month high-TAU mice show a high load of tangles in the CA1

pyramidal neurons, which could result in degeneration of spines or dendrites. A few studies have shown dendritic dystrophy of cortical or hippocampal neurons in the rTg4510 tau (P301L) mice or the AAV-tau (P301L)-transfected mice, which is particularly pronounced in the distal apical parts (Crimins et al., 2012; Jaworski et al., 2011). Previous work in our lab (Joel 2015, PhD dissertation) has not found significant electrophysiological changes in the Schaffer collateral pathways in CA1 of the tau model at this stage, but we have not investigated the perforant pathway yet; except a significantly increased membrane potential in the CA1 pyramidal neurons, suggesting reduced ion channel opening that might be due to a dendritic regression induced membrane surface decrease.

Lack of strong MHC-II induction in the amyloid model compared to the tau model or human AD

MHC-II (Major Histocompatibility Class II) is a range of cell surface receptors involved in antigen presentation and the adaptive immune response elicitation, which is usually associated with up-regulated inflammation. I only found scattered MHC-II positive cells in the cortex and hippocampus of the *APP/PSEN1* mice with medium to heavy plaque loads, with a considerable variability in the number of the MHC-II positive cells between different mice. All MHC-II positive cells were also IBA1-positive, indicating they are predominantly microglia. This MHC-II positive subgroup seemed only to constitute a very small proportion of microglia in the *APP/PSEN1* mice at this stage with a highly expanded microglial population, whereas the tau model seemed to show more considerable MHC-II positive microglia. Surprisingly, I did not observe any MHC-II positive microglia in the brain parenchyma of wildtype mice at any age groups (4, 12, 24, and 30 months). A previous study with a different *APP/PS1* mouse model and a different MHC-II antibody also found that the number of MHC-II positive microglia only increased at late stages of Aβ pathology and showed a high inter-animal variability with no obvious correlation to the plaque amount (Gordon et al., 2002). This is

contrary to the findings in human patients. Early AD pathological reports (Itagaki et al., 1989; McGeer et al., 1987; Perlmutter et al., 1992; Rogers et al., 1988; Styren et al., 1990) show that AD patients exhibit highly increased MHC-II positive microglia, most clustering around plaques (and tangles, but not always). Additionally, they find scattered MHC-II immunoreactivity in the white matter of the non-demented control people, with a positive correlation with age (Perlmutter et al., 1992; Rogers et al., 1988; Styren et al., 1990). This difference between human and mice might be partially due to species differences, and/or different sensitivity of the antibodies. But another possibility perhaps is that the lack of 'microglial priming' factors in the mouse model compared to elderly people, as we discussed earlier, results in a robust and less-detrimental microglial phenotype represented by a relatively low level of MHC-II induction in response to Aβ pathology, while in human AD, for some reason the microglia fail to react appropriately but induce a more pro-inflammatory phenotype with high MHC-II expression, which might be an important component in downstream progression of the Aβ pathology. Particularly, an early study found that a group of non-demented elderly people showed a significantly lower number of MHC-II positive microglia compared to a group of age-matched AD patients despite the plaque load being comparable (Lue et al., 1996). Also, in a post-mortem study, researchers found that MHC-II levels in AD brains showed a negative relationship with the MMSE scores and a positive relationship with neuritic plaque and neurofibrillary tangle load, whereas in non-demented people the MHC-II levels only showed an insignificant or negative relationship with AD pathology, except a positive relationship with the diffuse plaque load (Minett et al., 2016). As we suggest *Trem2* up-regulation in the amyloid mouse model plays a central role in the microglial activation, it would be interesting to investigate whether microglial *Trem2* expression / function is to some extent correlated with the MHCII levels, and also whether the MHC-II levels are different in human AD with *TREM2* risk variants.

Conclusions

In this study, I established an *in vitro* primary microglia model that could be used to test the mechanism of action of the newly discovered microglial GWAS hits, which was validated here with acute *Trem2* knock-down. I found that TREM2 played an important role in microglial phenotype regulation. Specifically, besides validating phagocytosis impairment, acutely induced *Trem2* deficiency resulted in slight but significant microglial gene expression changes, suggesting a phenotype shift towards a pro-inflammatory state and away from an anti-inflammatory and neurotrophic state. *Trem2* deficiency in microglia modestly amplified the M1 classical activation in response to the pro-inflammatory stimulus LPS, and substantially impaired the M2 alternative activation in response to IL4. I also found that *Trem2* suppression led to enhanced expression of chemoattractants, especially for peripheral immune cells, perhaps suggesting an exaggerated microglial phenotype in response to stimuli and potentially increased driving force for leukocyte infiltration in the context of injured brains. Additionally, with respect to the regulation of *Trem2* expression, I found that a pro-inflammatory environment inhibited *Trem2* expression while anti-inflammatory cues enhanced *Trem2* expression, suggesting that TREM2 is functional in anti-inflammatory situations.

In a line of an amyloid mouse model, I observed an up-regulation of *Trem2* expression relative to the number of microglia from early stages of amyloid pathology, which was not found in the tau model that showed a more pro-inflammatory microglial phenotype. Together with our previous network analysis (Matarin et al., 2015), my findings suggest a potentially central role of *Trem2* up-regulation in coordinating a robust and balanced microglial reaction to amyloid pathology. Since we do not observe a fully developed AD pathology in the amyloid model (lacking tau tangles and neuronal death), I propose that enhanced TREM2 expression / function and lack of other environment 'microglial priming' factors experienced by humans outside of a mouse facility lead to a robust protective microglial activation (with low MHCII induction) accompanying the amyloid pathology, which prevents further

downstream development of AD. However, the *Trem2* inhibition due to the pro-inflammatory stimuli (as suggested by my *in vitro* work) might be prolonged in the context of human aged brains where various environmental risk factors could increase the baseline inflammation levels. Then such *Trem2* inhibition may impact upon microglial reactions to dys-regulated Aβ metabolism, which could be one of the microglial mechanisms contributing to AD pathogenesis, especially at the post- Aβ and pre-tangle stages.

It would provide great insights for drug discovery if we could expand the work described here showing that microglia respond differently in amyloid versus tau pathology environments by identifying the genetic network differences in the microglial populations to enable appropriate modulation of microglia with pharmacology. Also, in future work, it would be interesting to further study the role of Aβ-induced microglial activation in the link of Aβ driving the tau pathology in AD progression, and also the contribution of tau-induced microglial activation back to the Aβ pathology.

References

Aizenstein, H.J., Nebes, R.D., Saxton, J.A., Price, J.C., Mathis, C.A., Tsopelas, N.D., Ziolko, S.K., James, J.A., Snitz, B.E., Houck, P.R.*, et al.* (2008). Frequent amyloid deposition without significant cognitive impairment among the elderly. Arch Neurol *65*, 1509-1517.

Alexandrov, P.N., Zhao, Y., Jones, B.M., Bhattacharjee, S., and Lukiw, W.J. (2013). Expression of the phagocytosis-essential protein TREM2 is down-regulated by an aluminum-induced miRNA-34a in a murine microglial cell line. J Inorg Biochem *128*, 267-269.

Allcock, R.J., Barrow, A.D., Forbes, S., Beck, S., and Trowsdale, J. (2003). The human TREM gene cluster at 6p21.1 encodes both activating and inhibitory single IgV domain receptors and includes NKp44. European journal of immunology *33*, 567-577.

Appay, V., and Rowland-Jones, S.L. (2001). RANTES: a versatile and controversial chemokine. Trends Immunol *22*, 83-87.

Arkins, S., Rebeiz, N., Brunke-Reese, D.L., Biragyn, A., and Kelley, K.W. (1995). Interferon-gamma inhibits macrophage insulin-like growth factor-I synthesis at the transcriptional level. Mol Endocrinol *9*, 350-360.

Arriagada, P.V., Growdon, J.H., Hedley-Whyte, E.T., and Hyman, B.T. (1992). Neurofibrillary tangles but not senile plaques parallel duration and severity of Alzheimer's disease. Neurology *42*, 631-639.

Asai, H., Ikezu, S., Tsunoda, S., Medalla, M., Luebke, J., Haydar, T., Wolozin, B., Butovsky, O., Kugler, S., and Ikezu, T. (2015). Depletion of microglia and inhibition of exosome synthesis halt tau propagation. Nature neuroscience *18*, 1584-1593.

Atagi, Y., Liu, C.C., Painter, M.M., Chen, X.F., Verbeeck, C., Zheng, H., Li, X., Rademakers, R., Kang, S.S., Xu, H.*, et al.* (2015). Apolipoprotein E Is a Ligand for Triggering Receptor Expressed on Myeloid Cells 2 (TREM2). The Journal of biological chemistry *290*, 26043-26050.

Babcock, A.A., Kuziel, W.A., Rivest, S., and Owens, T. (2003). Chemokine expression by glial cells directs leukocytes to sites of axonal injury in the CNS.

The Journal of neuroscience : the official journal of the Society for Neuroscience *23*, 7922-7930.

Baggiolini, M. (1998). Chemokines and leukocyte traffic. Nature *392*, 565-568.

Bailey, C.C., DeVaux, L.B., and Farzan, M. (2015). The Triggering Receptor Expressed on Myeloid Cells 2 Binds Apolipoprotein E. The Journal of biological chemistry *290*, 26033-26042.

Bamberger, M.E., Harris, M.E., McDonald, D.R., Husemann, J., and Landreth, G.E. (2003). A cell surface receptor complex for fibrillar beta-amyloid mediates microglial activation. The Journal of neuroscience : the official journal of the Society for Neuroscience *23*, 2665-2674.

Barrett, J.P., Minogue, A.M., Falvey, A., and Lynch, M.A. (2015). Involvement of IGF-1 and Akt in M1/M2 activation state in bone marrow-derived macrophages. Exp Cell Res *335*, 258-268.

Basu, A., Krady, J.K., Enterline, J.R., and Levison, S.W. (2002). Transforming growth factor beta1 prevents IL-1beta-induced microglial activation, whereas TNFalpha- and IL-6-stimulated activation are not antagonized. Glia *40*, 109-120.

Benilova, I., Karran, E., and De Strooper, B. (2012). The toxic Abeta oligomer and Alzheimer's disease: an emperor in need of clothes. Nature neuroscience *15*, 349-357.

Benitez, B.A., Cooper, B., Pastor, P., Jin, S.C., Lorenzo, E., Cervantes, S., and Cruchaga, C. (2013). TREM2 is associated with the risk of Alzheimer's disease in Spanish population. Neurobiology of aging *34*, 1711 e1715-1717.

Bhattacharjee, S., Zhao, Y., Dua, P., Rogaev, E.I., and Lukiw, W.J. (2016). microRNA-34a-Mediated Down-Regulation of the Microglial-Enriched Triggering Receptor and Phagocytosis-Sensor TREM2 in Age-Related Macular Degeneration. PloS one *11*, e0150211.

Birch, A.M., Katsouri, L., and Sastre, M. (2014). Modulation of inflammation in transgenic models of Alzheimer's disease. Journal of neuroinflammation *11*, 25.

Boche, D., Perry, V.H., and Nicoll, J.A. (2013). Review: activation patterns of microglia and their identification in the human brain. Neuropathology and applied neurobiology *39*, 3-18.

Bolos, M., Llorens-Martin, M., Jurado-Arjona, J., Hernandez, F., Rabano, A., and Avila, J. (2016). Direct Evidence of Internalization of Tau by Microglia In Vitro and In Vivo. J Alzheimers Dis *50*, 77-87.

Bose, S., and Cho, J. (2013). Role of chemokine CCL2 and its receptor CCR2 in neurodegenerative diseases. Arch Pharm Res *36*, 1039-1050.

Bouchon, A., Dietrich, J., and Colonna, M. (2000). Cutting edge: inflammatory responses can be triggered by TREM-1, a novel receptor expressed on neutrophils and monocytes. Journal of immunology *164*, 4991-4995.

Bouchon, A., Hernandez-Munain, C., Cella, M., and Colonna, M. (2001). A DAP12-mediated pathway regulates expression of CC chemokine receptor 7 and maturation of human dendritic cells. The Journal of experimental medicine *194*, 1111-1122.

Braak, H., and Braak, E. (1991). Neuropathological stageing of Alzheimer-related changes. Acta neuropathologica *82*, 239-259.

Braak, H., and Braak, E. (1997). Frequency of stages of Alzheimer-related lesions in different age categories. Neurobiology of aging *18*, 351-357.

Braak, H., Thal, D.R., Ghebremedhin, E., and Del Tredici, K. (2011). Stages of the pathologic process in Alzheimer disease: age categories from 1 to 100 years. Journal of neuropathology and experimental neurology *70*, 960-969.

Butovsky, O., Jedrychowski, M.P., Moore, C.S., Cialic, R., Lanser, A.J., Gabriely, G., Koeglsperger, T., Dake, B., Wu, P.M., Doykan, C.E.*, et al.* (2014). Identification of a unique TGF-beta-dependent molecular and functional signature in microglia. Nature neuroscience *17*, 131-143.

Cady, J., Koval, E.D., Benitez, B.A., Zaidman, C., Jockel-Balsarotti, J., Allred, P., Baloh, R.H., Ravits, J., Simpson, E., Appel, S.H.*, et al.* (2014). TREM2 variant p.R47H as a risk factor for sporadic amyotrophic lateral sclerosis. JAMA Neurol *71*, 449-453.

Caglayan, S., Bauerfeind, A., Schmidt, V., Carlo, A.S., Prabakaran, T., Hubner, N., and Willnow, T.E. (2012). Identification of Alzheimer disease risk genotype that predicts efficiency of SORL1 expression in the brain. Arch Neurol *69*, 373-379.

Cannon, J.P., O'Driscoll, M., and Litman, G.W. (2012). Specific lipid recognition is a general feature of CD300 and TREM molecules. Immunogenetics *64*, 39-47.

Castellano, J.M., Kim, J., Stewart, F.R., Jiang, H., DeMattos, R.B., Patterson, B.W., Fagan, A.M., Morris, J.C., Mawuenyega, K.G., Cruchaga, C.*, et al.* (2011). Human apoE isoforms differentially regulate brain amyloid-beta peptide clearance. Science translational medicine *3*, 89ra57.

Chan, S.L., Kim, W.S., Kwok, J.B., Hill, A.F., Cappai, R., Rye, K.A., and Garner, B. (2008). ATP-binding cassette transporter A7 regulates processing of amyloid precursor protein in vitro. Journal of neurochemistry *106*, 793-804.

Chandra, G., Rangasamy, S.B., Roy, A., Kordower, J.H., and Pahan, K. (2016). Neutralization of RANTES and Eotaxin Prevents the Loss of Dopaminergic Neurons in a Mouse Model of Parkinson Disease. The Journal of biological chemistry *291*, 15267-15281.

Chavez-Gutierrez, L., Bammens, L., Benilova, I., Vandersteen, A., Benurwar, M., Borgers, M., Lismont, S., Zhou, L., Van Cleynenbreugel, S., Esselmann, H.*, et al.* (2012). The mechanism of gamma-Secretase dysfunction in familial Alzheimer disease. EMBO J *31*, 2261-2274.

Cho, H., Hashimoto, T., Wong, E., Hori, Y., Wood, L.B., Zhao, L., Haigis, K.M., Hyman, B.T., and Irimia, D. (2013). Microfluidic chemotaxis platform for differentiating the roles of soluble and bound amyloid-beta on microglial accumulation. Sci Rep *3*, 1823.

Condello, C., Yuan, P., Schain, A., and Grutzendler, J. (2015). Microglia constitute a barrier that prevents neurotoxic protofibrillar Abeta42 hotspots around plaques. Nat Commun *6*, 6176.

Corder, E.H., Saunders, A.M., Strittmatter, W.J., Schmechel, D.E., Gaskell, P.C., Small, G.W., Roses, A.D., Haines, J.L., and Pericak-Vance, M.A. (1993). Gene dose of apolipoprotein E type 4 allele and the risk of Alzheimer's disease in late onset families. Science *261*, 921-923.

Crimins, J.L., Rocher, A.B., and Luebke, J.I. (2012). Electrophysiological changes precede morphological changes to frontal cortical pyramidal neurons in the rTg4510 mouse model of progressive tauopathy. Acta neuropathologica *124*, 777-795.

Cummings, D.M., Liu, W., Portelius, E., Bayram, S., Yasvoina, M., Ho, S.H., Smits, H., Ali, S.S., Steinberg, R., Pegasiou, C.M.*, et al.* (2015). First effects of rising amyloid-

beta in transgenic mouse brain: synaptic transmission and gene expression. Brain : a journal of neurology *138*, 1992-2004.

Cunningham, C., Campion, S., Lunnon, K., Murray, C.L., Woods, J.F., Deacon, R.M., Rawlins, J.N., and Perry, V.H. (2009). Systemic inflammation induces acute behavioral and cognitive changes and accelerates neurodegenerative disease. Biol Psychiatry *65*, 304-312.

Cuyvers, E., De Roeck, A., Van den Bossche, T., Van Cauwenberghe, C., Bettens, K., Vermeulen, S., Mattheijssens, M., Peeters, K., Engelborghs, S., Vandenbulcke, M.*, et al.* (2015). Mutations in ABCA7 in a Belgian cohort of Alzheimer's disease patients: a targeted resequencing study. Lancet Neurol *14*, 814-822.

Dardiotis, E., Siokas, V., Pantazi, E., Dardioti, M., Rikos, D., Xiromerisiou, G., Markou, A., Papadimitriou, D., Speletas, M., and Hadjigeorgiou, G.M. (2017). A novel mutation in TREM2 gene causing Nasu-Hakola disease and review of the literature. Neurobiology of aging *53*, 194 e113-194 e122.

Davalos, D., Grutzendler, J., Yang, G., Kim, J.V., Zuo, Y., Jung, S., Littman, D.R., Dustin, M.L., and Gan, W.B. (2005). ATP mediates rapid microglial response to local brain injury in vivo. Nature neuroscience *8*, 752-758.

Daws, M.R., Lanier, L.L., Seaman, W.E., and Ryan, J.C. (2001). Cloning and characterization of a novel mouse myeloid DAP12-associated receptor family. European journal of immunology *31*, 783-791.

Daws, M.R., Sullam, P.M., Niemi, E.C., Chen, T.T., Tchao, N.K., and Seaman, W.E. (2003). Pattern recognition by TREM-2: binding of anionic ligands. Journal of immunology *171*, 594-599.

de Calignon, A., Polydoro, M., Suarez-Calvet, M., William, C., Adamowicz, D.H., Kopeikina, K.J., Pitstick, R., Sahara, N., Ashe, K.H., Carlson, G.A.*, et al.* (2012). Propagation of tau pathology in a model of early Alzheimer's disease. Neuron *73*, 685-697.

Elmore, M.R., Najafi, A.R., Koike, M.A., Dagher, N.N., Spangenberg, E.E., Rice, R.A., Kitazawa, M., Matusow, B., Nguyen, H., West, B.L.*, et al.* (2014). Colony-stimulating factor 1 receptor signaling is necessary for microglia viability, unmasking a microglia progenitor cell in the adult brain. Neuron *82*, 380-397.

Eyo, U.B., Gu, N., De, S., Dong, H., Richardson, J.R., and Wu, L.J. (2015). Modulation of microglial process convergence toward neuronal dendrites by extracellular

calcium. The Journal of neuroscience : the official journal of the Society for Neuroscience *35*, 2417-2422.

Fernandez, A.M., and Torres-Aleman, I. (2012). The many faces of insulin-like peptide signalling in the brain. Nature reviews Neuroscience *13*, 225-239.

Frank, S., Burbach, G.J., Bonin, M., Walter, M., Streit, W., Bechmann, I., and Deller, T. (2008). TREM2 is upregulated in amyloid plaque-associated microglia in aged APP23 transgenic mice. Glia *56*, 1438-1447.

Gao, X., Dong, Y., Liu, Z., and Niu, B. (2013). Silencing of triggering receptor expressed on myeloid cells-2 enhances the inflammatory responses of alveolar macrophages to lipopolysaccharide. Mol Med Rep *7*, 921-926.

Giannakopoulos, P., Herrmann, F.R., Bussiere, T., Bouras, C., Kovari, E., Perl, D.P., Morrison, J.H., Gold, G., and Hof, P.R. (2003). Tangle and neuron numbers, but not amyloid load, predict cognitive status in Alzheimer's disease. Neurology *60*, 1495-1500.

Ginhoux, F., Greter, M., Leboeuf, M., Nandi, S., See, P., Gokhan, S., Mehler, M.F., Conway, S.J., Ng, L.G., Stanley, E.R.*, et al.* (2010). Fate mapping analysis reveals that adult microglia derive from primitive macrophages. Science *330*, 841-845.

Goate, A., Chartier-Harlin, M.C., Mullan, M., Brown, J., Crawford, F., Fidani, L., Giuffra, L., Haynes, A., Irving, N., James, L.*, et al.* (1991). Segregation of a missense mutation in the amyloid precursor protein gene with familial Alzheimer's disease. Nature *349*, 704-706.

Gomez-Isla, T., Hollister, R., West, H., Mui, S., Growdon, J.H., Petersen, R.C., Parisi, J.E., and Hyman, B.T. (1997). Neuronal loss correlates with but exceeds neurofibrillary tangles in Alzheimer's disease. Annals of neurology *41*, 17-24.

Gomez-Isla, T., Price, J.L., McKeel, D.W., Jr., Morris, J.C., Growdon, J.H., and Hyman, B.T. (1996). Profound loss of layer II entorhinal cortex neurons occurs in very mild Alzheimer's disease. The Journal of neuroscience : the official journal of the Society for Neuroscience *16*, 4491-4500.

Gordon, M.N., Holcomb, L.A., Jantzen, P.T., DiCarlo, G., Wilcock, D., Boyett, K.W., Connor, K., Melachrino, J., O'Callaghan, J.P., and Morgan, D. (2002). Time course of the development of Alzheimer-like pathology in the doubly transgenic PS1+APP mouse. Experimental neurology *173*, 183-195.

Gordon, S., and Martinez, F.O. (2010). Alternative activation of macrophages: mechanism and functions. Immunity *32*, 593-604.

Gotz, J., Streffer, J.R., David, D., Schild, A., Hoerndli, F., Pennanen, L., Kurosinski, P., and Chen, F. (2004). Transgenic animal models of Alzheimer's disease and related disorders: histopathology, behavior and therapy. Molecular psychiatry *9*, 664-683.

Griciuc, A., Serrano-Pozo, A., Parrado, A.R., Lesinski, A.N., Asselin, C.N., Mullin, K., Hooli, B., Choi, S.H., Hyman, B.T., and Tanzi, R.E. (2013). Alzheimer's disease risk gene CD33 inhibits microglial uptake of amyloid beta. Neuron *78*, 631-643.

Guerreiro, R., Bilgic, B., Guven, G., Bras, J., Rohrer, J., Lohmann, E., Hanagasi, H., Gurvit, H., and Emre, M. (2013a). Novel compound heterozygous mutation in TREM2 found in a Turkish frontotemporal dementia-like family. Neurobiology of aging *34*, 2890 e2891-2895.

Guerreiro, R., Wojtas, A., Bras, J., Carrasquillo, M., Rogaeva, E., Majounie, E., Cruchaga, C., Sassi, C., Kauwe, J.S., Younkin, S.*, et al.* (2013b). TREM2 variants in Alzheimer's disease. The New England journal of medicine *368*, 117-127.

Guerreiro, R.J., Lohmann, E., Bras, J.M., Gibbs, J.R., Rohrer, J.D., Gurunlian, N., Dursun, B., Bilgic, B., Hanagasi, H., Gurvit, H.*, et al.* (2013c). Using exome sequencing to reveal mutations in TREM2 presenting as a frontotemporal dementia-like syndrome without bone involvement. JAMA Neurol *70*, 78-84.

Hamelin, L., Lagarde, J., Dorothee, G., Leroy, C., Labit, M., Comley, R.A., de Souza, L.C., Corne, H., Dauphinot, L., Bertoux, M.*, et al.* (2016). Early and protective microglial activation in Alzheimer's disease: a prospective study using 18F-DPA-714 PET imaging. Brain : a journal of neurology *139*, 1252-1264.

Hanisch, U.K., and Kettenmann, H. (2007). Microglia: active sensor and versatile effector cells in the normal and pathologic brain. Nature neuroscience *10*, 1387-1394.

Hardy, J., and Allsop, D. (1991). Amyloid deposition as the central event in the aetiology of Alzheimer's disease. Trends Pharmacol Sci *12*, 383-388.

Hardy, J.A., and Higgins, G.A. (1992). Alzheimer's disease: the amyloid cascade hypothesis. Science *256*, 184-185.

Harris, J.A., Koyama, A., Maeda, S., Ho, K., Devidze, N., Dubal, D.B., Yu, G.Q., Masliah, E., and Mucke, L. (2012). Human P301L-mutant tau expression in mouse

entorhinal-hippocampal network causes tau aggregation and presynaptic pathology but no cognitive deficits. PloS one *7*, e45881.

Haskill, S., Peace, A., Morris, J., Sporn, S.A., Anisowicz, A., Lee, S.W., Smith, T., Martin, G., Ralph, P., and Sager, R. (1990). Identification of three related human GRO genes encoding cytokine functions. Proceedings of the National Academy of Sciences of the United States of America *87*, 7732-7736.

Henjum, K., Almdahl, I.S., Arskog, V., Minthon, L., Hansson, O., Fladby, T., and Nilsson, L.N. (2016). Cerebrospinal fluid soluble TREM2 in aging and Alzheimer's disease. Alzheimers Res Ther *8*, 17.

Herrera-Molina, R., and von Bernhardi, R. (2005). Transforming growth factor-beta 1 produced by hippocampal cells modulates microglial reactivity in culture. Neurobiol Dis *19*, 229-236.

Heslegrave, A., Heywood, W., Paterson, R., Magdalinou, N., Svensson, J., Johansson, P., Ohrfelt, A., Blennow, K., Hardy, J., Schott, J.*, et al.* (2016). Increased cerebrospinal fluid soluble TREM2 concentration in Alzheimer's disease. Molecular neurodegeneration *11*, 3.

Hollingworth, P., Harold, D., Sims, R., Gerrish, A., Lambert, J.C., Carrasquillo, M.M., Abraham, R., Hamshere, M.L., Pahwa, J.S., Moskvina, V.*, et al.* (2011). Common variants at ABCA7, MS4A6A/MS4A4E, EPHA1, CD33 and CD2AP are associated with Alzheimer's disease. Nature genetics *43*, 429-435.

Holness, C.L., and Simmons, D.L. (1993). Molecular cloning of CD68, a human macrophage marker related to lysosomal glycoproteins. Blood *81*, 1607-1613.

Holtman, I.R., Raj, D.D., Miller, J.A., Schaafsma, W., Yin, Z., Brouwer, N., Wes, P.D., Moller, T., Orre, M., Kamphuis, W.*, et al.* (2015). Induction of a common microglia gene expression signature by aging and neurodegenerative conditions: a co-expression meta-analysis. Acta Neuropathol Commun *3*, 31.

Holtzman, D.M., Bales, K.R., Tenkova, T., Fagan, A.M., Parsadanian, M., Sartorius, L.J., Mackey, B., Olney, J., McKeel, D., Wozniak, D.*, et al.* (2000). Apolipoprotein E isoform-dependent amyloid deposition and neuritic degeneration in a mouse model of Alzheimer's disease. Proceedings of the National Academy of Sciences of the United States of America *97*, 2892-2897.

Hong, S., Beja-Glasser, V.F., Nfonoyim, B.M., Frouin, A., Li, S., Ramakrishnan, S., Merry, K.M., Shi, Q., Rosenthal, A., Barres, B.A.*, et al.* (2016). Complement and

microglia mediate early synapse loss in Alzheimer mouse models. Science *352*, 712-716.

Horuk, R., Martin, A.W., Wang, Z., Schweitzer, L., Gerassimides, A., Guo, H., Lu, Z., Hesselgesser, J., Perez, H.D., Kim, J.*, et al.* (1997). Expression of chemokine receptors by subsets of neurons in the central nervous system. Journal of immunology *158*, 2882-2890.

Howlett, D.R., Bowler, K., Soden, P.E., Riddell, D., Davis, J.B., Richardson, J.C., Burbidge, S.A., Gonzalez, M.I., Irving, E.A., Lawman, A.*, et al.* (2008). Abeta deposition and related pathology in an APP x PS1 transgenic mouse model of Alzheimer's disease. Histol Histopathol *23*, 67-76.

Howlett, D.R., and Richardson, J.C. (2009). The pathology of APP transgenic mice: a model of Alzheimer's disease or simply overexpression of APP? Histol Histopathol *24*, 83-100.

Howlett, D.R., Richardson, J.C., Austin, A., Parsons, A.A., Bate, S.T., Davies, D.C., and Gonzalez, M.I. (2004). Cognitive correlates of Abeta deposition in male and female mice bearing amyloid precursor protein and presenilin-1 mutant transgenes. Brain Res *1017*, 130-136.

Hu, S., Chao, C.C., Ehrlich, L.C., Sheng, W.S., Sutton, R.L., Rockswold, G.L., and Peterson, P.K. (1999). Inhibition of microglial cell RANTES production by IL-10 and TGF-beta. J Leukoc Biol *65*, 815-821.

Huang, D.R., Wang, J., Kivisakk, P., Rollins, B.J., and Ransohoff, R.M. (2001). Absence of monocyte chemoattractant protein 1 in mice leads to decreased local macrophage recruitment and antigen-specific T helper cell type 1 immune response in experimental autoimmune encephalomyelitis. The Journal of experimental medicine *193*, 713-726.

Huang, K.L., Marcora, E., Pimenova, A.A., Di Narzo, A.F., Kapoor, M., Jin, S.C., Harari, O., Bertelsen, S., Fairfax, B.P., Czajkowski, J.*, et al.* (2017). A common haplotype lowers PU.1 expression in myeloid cells and delays onset of Alzheimer's disease. Nature neuroscience *20*, 1052-1061.

Humphrey, M.B., Daws, M.R., Spusta, S.C., Niemi, E.C., Torchia, J.A., Lanier, L.L., Seaman, W.E., and Nakamura, M.C. (2006). TREM2, a DAP12-associated receptor, regulates osteoclast differentiation and function. J Bone Miner Res *21*, 237-245.

Imai, Y., Ibata, I., Ito, D., Ohsawa, K., and Kohsaka, S. (1996). A novel gene iba1 in the major histocompatibility complex class III region encoding an EF hand protein expressed in a monocytic lineage. Biochemical and biophysical research communications *224*, 855-862.

Itagaki, S., McGeer, P.L., Akiyama, H., Zhu, S., and Selkoe, D. (1989). Relationship of microglia and astrocytes to amyloid deposits of Alzheimer disease. Journal of neuroimmunology *24*, 173-182.

Ito, D., Imai, Y., Ohsawa, K., Nakajima, K., Fukuuchi, Y., and Kohsaka, S. (1998). Microglia-specific localisation of a novel calcium binding protein, Iba1. Brain research Molecular brain research *57*, 1-9.

Jaworski, T., Lechat, B., Demedts, D., Gielis, L., Devijver, H., Borghgraef, P., Duimel, H., Verheyen, F., Kugler, S., and Van Leuven, F. (2011). Dendritic degeneration, neurovascular defects, and inflammation precede neuronal loss in a mouse model for tau-mediated neurodegeneration. The American journal of pathology *179*, 2001-2015.

Jay, T.R., Hirsch, A.M., Broihier, M.L., Miller, C.M., Neilson, L.E., Ransohoff, R.M., Lamb, B.T., and Landreth, G.E. (2017). Disease Progression-Dependent Effects of TREM2 Deficiency in a Mouse Model of Alzheimer's Disease. The Journal of neuroscience : the official journal of the Society for Neuroscience *37*, 637-647.

Jay, T.R., Miller, C.M., Cheng, P.J., Graham, L.C., Bemiller, S., Broihier, M.L., Xu, G., Margevicius, D., Karlo, J.C., Sousa, G.L., *et al.* (2015). TREM2 deficiency eliminates TREM2+ inflammatory macrophages and ameliorates pathology in Alzheimer's disease mouse models. The Journal of experimental medicine *212*, 287-295.

Jiang, T., Tan, L., Chen, Q., Tan, M.S., Zhou, J.S., Zhu, X.C., Lu, H., Wang, H.F., Zhang, Y.D., and Yu, J.T. (2016a). A rare coding variant in TREM2 increases risk for Alzheimer's disease in Han Chinese. Neurobiology of aging *42*, 217 e211-213.

Jiang, T., Tan, L., Zhu, X.C., Zhang, Q.Q., Cao, L., Tan, M.S., Gu, L.Z., Wang, H.F., Ding, Z.Z., Zhang, Y.D., *et al.* (2014). Upregulation of TREM2 Ameliorates Neuropathology and Rescues Spatial Cognitive Impairment in a Transgenic Mouse Model of Alzheimer's Disease. Neuropsychopharmacology : official publication of the American College of Neuropsychopharmacology *39*, 2949-2962.

Jiang, T., Wan, Y., Zhang, Y.D., Zhou, J.S., Gao, Q., Zhu, X.C., Shi, J.Q., Lu, H., Tan, L., and Yu, J.T. (2016b). TREM2 Overexpression has No Improvement on Neuropathology and Cognitive Impairment in Aging APPswe/PS1dE9 Mice. Mol Neurobiol.

Jimenez-Garcia, L., Herranz, S., Luque, A., and Hortelano, S. (2015). Critical role of p38 MAPK in IL-4-induced alternative activation of peritoneal macrophages. European journal of immunology *45*, 273-286.

Jin, M., Shepardson, N., Yang, T., Chen, G., Walsh, D., and Selkoe, D.J. (2011). Soluble amyloid beta-protein dimers isolated from Alzheimer cortex directly induce Tau hyperphosphorylation and neuritic degeneration. Proceedings of the National Academy of Sciences of the United States of America *108*, 5819-5824.

Jin, S.C., Benitez, B.A., Karch, C.M., Cooper, B., Skorupa, T., Carrell, D., Norton, J.B., Hsu, S., Harari, O., Cai, Y.*, et al.* (2014). Coding variants in TREM2 increase risk for Alzheimer's disease. Hum Mol Genet *23*, 5838-5846.

Jonsson, T., Stefansson, H., Steinberg, S., Jonsdottir, I., Jonsson, P.V., Snaedal, J., Bjornsson, S., Huttenlocher, J., Levey, A.I., Lah, J.J.*, et al.* (2013). Variant of TREM2 associated with the risk of Alzheimer's disease. The New England journal of medicine *368*, 107-116.

Katzman, R., Terry, R., DeTeresa, R., Brown, T., Davies, P., Fuld, P., Renbing, X., and Peck, A. (1988). Clinical, pathological, and neurochemical changes in dementia: a subgroup with preserved mental status and numerous neocortical plaques. Annals of neurology *23*, 138-144.

Kawabori, M., Kacimi, R., Kauppinen, T., Calosing, C., Kim, J.Y., Hsieh, C.L., Nakamura, M.C., and Yenari, M.A. (2015). Triggering Receptor Expressed on Myeloid Cells 2 (TREM2) Deficiency Attenuates Phagocytic Activities of Microglia and Exacerbates Ischemic Damage in Experimental Stroke. The Journal of neuroscience : the official journal of the Society for Neuroscience *35*, 3384-3396.

Keren-Shaul, H., Spinrad, A., Weiner, A., Matcovitch-Natan, O., Dvir-Szternfeld, R., Ulland, T.K., David, E., Baruch, K., Lara-Astaiso, D., Toth, B.*, et al.* (2017). A Unique Microglia Type Associated with Restricting Development of Alzheimer's Disease. Cell *169*, 1276-1290 e1217.

Kettenmann, H., Hanisch, U.K., Noda, M., and Verkhratsky, A. (2011). Physiology of microglia. Physiological reviews *91*, 461-553.

Kierdorf, K., Erny, D., Goldmann, T., Sander, V., Schulz, C., Perdiguero, E.G., Wieghofer, P., Heinrich, A., Riemke, P., Holscher, C., *et al.* (2013). Microglia emerge from erythromyeloid precursors via Pu.1- and Irf8-dependent pathways. Nature neuroscience *16*, 273-280.

Kim, C.C., Nakamura, M.C., and Hsieh, C.L. (2016). Brain trauma elicits non-canonical macrophage activation states. Journal of neuroinflammation *13*, 117.

Kim, W.S., Li, H., Ruberu, K., Chan, S., Elliott, D.A., Low, J.K., Cheng, D., Karl, T., and Garner, B. (2013). Deletion of Abca7 increases cerebral amyloid-beta accumulation in the J20 mouse model of Alzheimer's disease. The Journal of neuroscience : the official journal of the Society for Neuroscience *33*, 4387-4394.

Kleinberger, G., Yamanishi, Y., Suarez-Calvet, M., Czirr, E., Lohmann, E., Cuyvers, E., Struyfs, H., Pettkus, N., Wenninger-Weinzierl, A., Mazaheri, F., *et al.* (2014). TREM2 mutations implicated in neurodegeneration impair cell surface transport and phagocytosis. Science translational medicine *6*, 243ra286.

Kohman, R.A., DeYoung, E.K., Bhattacharya, T.K., Peterson, L.N., and Rhodes, J.S. (2012). Wheel running attenuates microglia proliferation and increases expression of a proneurogenic phenotype in the hippocampus of aged mice. Brain, behavior, and immunity *26*, 803-810.

Kondo, T., Takahashi, K., Kohara, N., Takahashi, Y., Hayashi, S., Takahashi, H., Matsuo, H., Yamazaki, M., Inoue, K., Miyamoto, K., *et al.* (2002). Heterogeneity of presenile dementia with bone cysts (Nasu-Hakola disease): three genetic forms. Neurology *59*, 1105-1107.

Kretner, B., Trambauer, J., Fukumori, A., Mielke, J., Kuhn, P.H., Kremmer, E., Giese, A., Lichtenthaler, S.F., Haass, C., Arzberger, T., *et al.* (2016). Generation and deposition of Abeta43 by the virtually inactive presenilin-1 L435F mutant contradicts the presenilin loss-of-function hypothesis of Alzheimer's disease. EMBO Mol Med *8*, 458-465.

Lambert, J.C., Ibrahim-Verbaas, C.A., Harold, D., Naj, A.C., Sims, R., Bellenguez, C., DeStafano, A.L., Bis, J.C., Beecham, G.W., Grenier-Boley, B., *et al.* (2013). Meta-analysis of 74,046 individuals identifies 11 new susceptibility loci for Alzheimer's disease. Nature genetics *45*, 1452-1458.

Levy-Lahad, E., Wasco, W., Poorkaj, P., Romano, D.M., Oshima, J., Pettingell, W.H., Yu, C.E., Jondro, P.D., Schmidt, S.D., Wang, K.*, et al.* (1995). Candidate gene for the chromosome 1 familial Alzheimer's disease locus. Science *269*, 973-977.

Li, Y., Du, X.F., Liu, C.S., Wen, Z.L., and Du, J.L. (2012). Reciprocal regulation between resting microglial dynamics and neuronal activity in vivo. Dev Cell *23*, 1189-1202.

Liebmann, T., Renier, N., Bettayeb, K., Greengard, P., Tessier-Lavigne, M., and Flajolet, M. (2016). Three-Dimensional Study of Alzheimer's Disease Hallmarks Using the iDISCO Clearing Method. Cell Rep *16*, 1138-1152.

Liu, L., Drouet, V., Wu, J.W., Witter, M.P., Small, S.A., Clelland, C., and Duff, K. (2012). Trans-synaptic spread of tau pathology in vivo. PloS one *7*, e31302.

Lue, L.F., Brachova, L., Civin, W.H., and Rogers, J. (1996). Inflammation, A beta deposition, and neurofibrillary tangle formation as correlates of Alzheimer's disease neurodegeneration. Journal of neuropathology and experimental neurology *55*, 1083-1088.

Luo, Y., Fischer, F.R., Hancock, W.W., and Dorf, M.E. (2000). Macrophage inflammatory protein-2 and KC induce chemokine production by mouse astrocytes. Journal of immunology *165*, 4015-4023.

Luzina, I.G., Keegan, A.D., Heller, N.M., Rook, G.A., Shea-Donohue, T., and Atamas, S.P. (2012). Regulation of inflammation by interleukin-4: a review of "alternatives". J Leukoc Biol *92*, 753-764.

Maezawa, I., Zimin, P.I., Wulff, H., and Jin, L.W. (2011). Amyloid-beta protein oligomer at low nanomolar concentrations activates microglia and induces microglial neurotoxicity. The Journal of biological chemistry *286*, 3693-3706.

Malik, M., Simpson, J.F., Parikh, I., Wilfred, B.R., Fardo, D.W., Nelson, P.T., and Estus, S. (2013). CD33 Alzheimer's risk-altering polymorphism, CD33 expression, and exon 2 splicing. The Journal of neuroscience : the official journal of the Society for Neuroscience *33*, 13320-13325.

Maphis, N., Xu, G., Kokiko-Cochran, O.N., Jiang, S., Cardona, A., Ransohoff, R.M., Lamb, B.T., and Bhaskar, K. (2015). Reactive microglia drive tau pathology and contribute to the spreading of pathological tau in the brain. Brain : a journal of neurology *138*, 1738-1755.

Matarin, M., Salih, D.A., Yasvoina, M., Cummings, D.M., Guelfi, S., Liu, W., Nahaboo Solim, M.A., Moens, T.G., Paublete, R.M., Ali, S.S*., et al.* (2015). A genome-wide gene-expression analysis and database in transgenic mice during development of amyloid or tau pathology. Cell Rep *10*, 633-644.

Matcovitch-Natan, O., Winter, D.R., Giladi, A., Vargas Aguilar, S., Spinrad, A., Sarrazin, S., Ben-Yehuda, H., David, E., Zelada Gonzalez, F., Perrin, P*., et al.* (2016). Microglia development follows a stepwise program to regulate brain homeostasis. Science *353*, aad8670.

Mazaheri, F., Snaidero, N., Kleinberger, G., Madore, C., Daria, A., Werner, G., Krasemann, S., Capell, A., Trumbach, D., Wurst, W*., et al.* (2017). TREM2 deficiency impairs chemotaxis and microglial responses to neuronal injury. EMBO Rep *18*, 1186-1198.

McGeer, P.L., Itagaki, S., Tago, H., and McGeer, E.G. (1987). Reactive microglia in patients with senile dementia of the Alzheimer type are positive for the histocompatibility glycoprotein HLA-DR. Neuroscience letters *79*, 195-200.

McKercher, S.R., Torbett, B.E., Anderson, K.L., Henkel, G.W., Vestal, D.J., Baribault, H., Klemsz, M., Feeney, A.J., Wu, G.E., Paige, C.J*., et al.* (1996). Targeted disruption of the PU.1 gene results in multiple hematopoietic abnormalities. EMBO J *15*, 5647-5658.

Melchior, B., Garcia, A.E., Hsiung, B.K., Lo, K.M., Doose, J.M., Thrash, J.C., Stalder, A.K., Staufenbiel, M., Neumann, H., and Carson, M.J. (2010). Dual induction of TREM2 and tolerance-related transcript, Tmem176b, in amyloid transgenic mice: implications for vaccine-based therapies for Alzheimer's disease. ASN neuro *2*, e00037.

Meurs, I., Calpe-Berdiel, L., Habets, K.L., Zhao, Y., Korporaal, S.J., Mommaas, A.M., Josselin, E., Hildebrand, R.B., Ye, D., Out, R*., et al.* (2012). Effects of deletion of macrophage ABCA7 on lipid metabolism and the development of atherosclerosis in the presence and absence of ABCA1. PloS one *7*, e30984.

Minett, T., Classey, J., Matthews, F.E., Fahrenhold, M., Taga, M., Brayne, C., Ince, P.G., Nicoll, J.A., Boche, D., and Mrc, C. (2016). Microglial immunophenotype in dementia with Alzheimer's pathology. Journal of neuroinflammation *13*, 135.

Morales, I., Jimenez, J.M., Mancilla, M., and Maccioni, R.B. (2013). Tau oligomers and fibrils induce activation of microglial cells. J Alzheimers Dis *37*, 849-856.

Morganti, J.M., Riparip, L.K., and Rosi, S. (2016). Call Off the Dog(ma): M1/M2 Polarization Is Concurrent following Traumatic Brain Injury. PloS one *11*, e0148001.

Mullan, M., Crawford, F., Axelman, K., Houlden, H., Lilius, L., Winblad, B., and Lannfelt, L. (1992). A pathogenic mutation for probable Alzheimer's disease in the APP gene at the N-terminus of beta-amyloid. Nature genetics *1*, 345-347.

Naj, A.C., Jun, G., Beecham, G.W., Wang, L.S., Vardarajan, B.N., Buros, J., Gallins, P.J., Buxbaum, J.D., Jarvik, G.P., Crane, P.K.*, et al.* (2011). Common variants at MS4A4/MS4A6E, CD2AP, CD33 and EPHA1 are associated with late-onset Alzheimer's disease. Nature genetics *43*, 436-441.

Nelms, K., Keegan, A.D., Zamorano, J., Ryan, J.J., and Paul, W.E. (1999). The IL-4 receptor: signaling mechanisms and biologic functions. Annual review of immunology *17*, 701-738.

Nimmerjahn, A., Kirchhoff, F., and Helmchen, F. (2005). Resting microglial cells are highly dynamic surveillants of brain parenchyma in vivo. Science *308*, 1314-1318.

Ohmori, Y., and Hamilton, T.A. (2000). Interleukin-4/STAT6 represses STAT1 and NF-kappa B-dependent transcription through distinct mechanisms. The Journal of biological chemistry *275*, 38095-38103.

Otero, K., Shinohara, M., Zhao, H., Cella, M., Gilfillan, S., Colucci, A., Faccio, R., Ross, F.P., Teitelbaum, S.L., Takayanagi, H.*, et al.* (2012). TREM2 and beta-catenin regulate bone homeostasis by controlling the rate of osteoclastogenesis. Journal of immunology *188*, 2612-2621.

Otero, K., Turnbull, I.R., Poliani, P.L., Vermi, W., Cerutti, E., Aoshi, T., Tassi, I., Takai, T., Stanley, S.L., Miller, M.*, et al.* (2009). Macrophage colony-stimulating factor induces the proliferation and survival of macrophages via a pathway involving DAP12 and beta-catenin. Nature immunology *10*, 734-743.

Owen, D.R., and Matthews, P.M. (2011). Imaging brain microglial activation using positron emission tomography and translocator protein-specific radioligands. Int Rev Neurobiol *101*, 19-39.

Owens, R., Grabert, K., Davies, C.L., Alfieri, A., Antel, J.P., Healy, L.M., and McColl, B.W. (2017). Divergent Neuroinflammatory Regulation of Microglial TREM

Expression and Involvement of NF-kappaB. Frontiers in cellular neuroscience *11*, 56.

Paloneva, J., Kestila, M., Wu, J., Salminen, A., Bohling, T., Ruotsalainen, V., Hakola, P., Bakker, A.B., Phillips, J.H., Pekkarinen, P.*, et al.* (2000). Loss-of-function mutations in TYROBP (DAP12) result in a presenile dementia with bone cysts. Nature genetics *25*, 357-361.

Paloneva, J., Mandelin, J., Kiialainen, A., Bohling, T., Prudlo, J., Hakola, P., Haltia, M., Konttinen, Y.T., and Peltonen, L. (2003). DAP12/TREM2 deficiency results in impaired osteoclast differentiation and osteoporotic features. The Journal of experimental medicine *198*, 669-675.

Paloneva, J., Manninen, T., Christman, G., Hovanes, K., Mandelin, J., Adolfsson, R., Bianchin, M., Bird, T., Miranda, R., Salmaggi, A.*, et al.* (2002). Mutations in two genes encoding different subunits of a receptor signaling complex result in an identical disease phenotype. American journal of human genetics *71*, 656-662.

Paolicelli, R.C., Bolasco, G., Pagani, F., Maggi, L., Scianni, M., Panzanelli, P., Giustetto, M., Ferreira, T.A., Guiducci, E., Dumas, L.*, et al.* (2011). Synaptic pruning by microglia is necessary for normal brain development. Science *333*, 1456-1458.

Paradowska-Gorycka, A., and Jurkowska, M. (2013). Structure, expression pattern and biological activity of molecular complex TREM-2/DAP12. Hum Immunol *74*, 730-737.

Parkhurst, C.N., Yang, G., Ninan, I., Savas, J.N., Yates, J.R., 3rd, Lafaille, J.J., Hempstead, B.L., Littman, D.R., and Gan, W.B. (2013). Microglia promote learning-dependent synapse formation through brain-derived neurotrophic factor. Cell *155*, 1596-1609.

Perlmutter, L.S., Scott, S.A., Barron, E., and Chui, H.C. (1992). MHC class II-positive microglia in human brain: association with Alzheimer lesions. J Neurosci Res *33*, 549-558.

Perry, V.H., Cunningham, C., and Holmes, C. (2007). Systemic infections and inflammation affect chronic neurodegeneration. Nature reviews Immunology *7*, 161-167.

Perry, V.H., and Holmes, C. (2014). Microglial priming in neurodegenerative disease. Nature reviews Neurology *10*, 217-224.

Pfeiffer, T., Avignone, E., and Nagerl, U.V. (2016). Induction of hippocampal long-term potentiation increases the morphological dynamics of microglial processes and prolongs their contacts with dendritic spines. Sci Rep *6*, 32422.

Piccio, L., Buonsanti, C., Cella, M., Tassi, I., Schmidt, R.E., Fenoglio, C., Rinker, J., 2nd, Naismith, R.T., Panina-Bordignon, P., Passini, N.*, et al.* (2008). Identification of soluble TREM-2 in the cerebrospinal fluid and its association with multiple sclerosis and CNS inflammation. Brain : a journal of neurology *131*, 3081-3091.

Piccio, L., Deming, Y., Del-Aguila, J.L., Ghezzi, L., Holtzman, D.M., Fagan, A.M., Fenoglio, C., Galimberti, D., Borroni, B., and Cruchaga, C. (2016). Cerebrospinal fluid soluble TREM2 is higher in Alzheimer disease and associated with mutation status. Acta neuropathologica *131*, 925-933.

Poliani, P.L., Wang, Y., Fontana, E., Robinette, M.L., Yamanishi, Y., Gilfillan, S., and Colonna, M. (2015). TREM2 sustains microglial expansion during aging and response to demyelination. J Clin Invest *125*, 2161-2170.

Pooler, A.M., Phillips, E.C., Lau, D.H., Noble, W., and Hanger, D.P. (2013). Physiological release of endogenous tau is stimulated by neuronal activity. EMBO Rep *14*, 389-394.

Pottier, C., Hannequin, D., Coutant, S., Rovelet-Lecrux, A., Wallon, D., Rousseau, S., Legallic, S., Paquet, C., Bombois, S., Pariente, J.*, et al.* (2012). High frequency of potentially pathogenic SORL1 mutations in autosomal dominant early-onset Alzheimer disease. Molecular psychiatry *17*, 875-879.

Pottier, C., Wallon, D., Rousseau, S., Rovelet-Lecrux, A., Richard, A.C., Rollin-Sillaire, A., Frebourg, T., Campion, D., and Hannequin, D. (2013). TREM2 R47H variant as a risk factor for early-onset Alzheimer's disease. J Alzheimers Dis *35*, 45-49.

Prokop, S., Miller, K.R., and Heppner, F.L. (2013). Microglia actions in Alzheimer's disease. Acta neuropathologica *126*, 461-477.

Ransohoff, R.M. (2016). A polarizing question: do M1 and M2 microglia exist? Nature neuroscience *19*, 987-991.

Rauh, M.J., Ho, V., Pereira, C., Sham, A., Sly, L.M., Lam, V., Huxham, L., Minchinton, A.I., Mui, A., and Krystal, G. (2005). SHIP represses the generation of alternatively activated macrophages. Immunity *23*, 361-374.

Rayaprolu, S., Mullen, B., Baker, M., Lynch, T., Finger, E., Seeley, W.W., Hatanpaa, K.J., Lomen-Hoerth, C., Kertesz, A., Bigio, E.H., *et al.* (2013). TREM2 in neurodegeneration: evidence for association of the p.R47H variant with frontotemporal dementia and Parkinson's disease. Molecular neurodegeneration *8*, 19.

Reed-Geaghan, E.G., Savage, J.C., Hise, A.G., and Landreth, G.E. (2009). CD14 and toll-like receptors 2 and 4 are required for fibrillar A{beta}-stimulated microglial activation. The Journal of neuroscience : the official journal of the Society for Neuroscience *29*, 11982-11992.

Rogaev, E.I., Sherrington, R., Rogaeva, E.A., Levesque, G., Ikeda, M., Liang, Y., Chi, H., Lin, C., Holman, K., Tsuda, T., *et al.* (1995). Familial Alzheimer's disease in kindreds with missense mutations in a gene on chromosome 1 related to the Alzheimer's disease type 3 gene. Nature *376*, 775-778.

Rogaeva, E., Meng, Y., Lee, J.H., Gu, Y., Kawarai, T., Zou, F., Katayama, T., Baldwin, C.T., Cheng, R., Hasegawa, H., *et al.* (2007). The neuronal sortilin-related receptor SORL1 is genetically associated with Alzheimer disease. Nature genetics *39*, 168-177.

Rogers, J., Luber-Narod, J., Styren, S.D., and Civin, W.H. (1988). Expression of immune system-associated antigens by cells of the human central nervous system: relationship to the pathology of Alzheimer's disease. Neurobiology of aging *9*, 339-349.

Ruiz, A., Dols-Icardo, O., Bullido, M.J., Pastor, P., Rodriguez-Rodriguez, E., Lopez de Munain, A., de Pancorbo, M.M., Perez-Tur, J., Alvarez, V., Antonell, A., *et al.* (2014). Assessing the role of the TREM2 p.R47H variant as a risk factor for Alzheimer's disease and frontotemporal dementia. Neurobiology of aging *35*, 444 e441-444.

Saito, N., Pulford, K.A., Breton-Gorius, J., Masse, J.M., Mason, D.Y., and Cramer, E.M. (1991). Ultrastructural localization of the CD68 macrophage-associated antigen in human blood neutrophils and monocytes. The American journal of pathology *139*, 1053-1059.

Saito, T., Matsuba, Y., Mihira, N., Takano, J., Nilsson, P., Itohara, S., Iwata, N., and Saido, T.C. (2014). Single App knock-in mouse models of Alzheimer's disease. Nature neuroscience *17*, 661-663.

Satoh, J., Asahina, N., Kitano, S., and Kino, Y. (2014). A Comprehensive Profile of ChIP-Seq-Based PU.1/Spi1 Target Genes in Microglia. Gene Regul Syst Bio *8*, 127-139.

Saura, J., Tusell, J.M., and Serratosa, J. (2003). High-yield isolation of murine microglia by mild trypsinization. Glia *44*, 183-189.

Savage, J.C., Jay, T., Goduni, E., Quigley, C., Mariani, M.M., Malm, T., Ransohoff, R.M., Lamb, B.T., and Landreth, G.E. (2015). Nuclear receptors license phagocytosis by trem2+ myeloid cells in mouse models of Alzheimer's disease. The Journal of neuroscience : the official journal of the Society for Neuroscience *35*, 6532-6543.

Schafer, D.P., Lehrman, E.K., Kautzman, A.G., Koyama, R., Mardinly, A.R., Yamasaki, R., Ransohoff, R.M., Greenberg, M.E., Barres, B.A., and Stevens, B. (2012). Microglia sculpt postnatal neural circuits in an activity and complement-dependent manner. Neuron *74*, 691-705.

Schildge, S., Bohrer, C., Beck, K., and Schachtrup, C. (2013). Isolation and culture of mouse cortical astrocytes. J Vis Exp.

Schlepckow, K., Kleinberger, G., Fukumori, A., Feederle, R., Lichtenthaler, S.F., Steiner, H., and Haass, C. (2017). An Alzheimer-associated TREM2 variant occurs at the ADAM cleavage site and affects shedding and phagocytic function. EMBO Mol Med.

Schmid, C.D., Sautkulis, L.N., Danielson, P.E., Cooper, J., Hasel, K.W., Hilbush, B.S., Sutcliffe, J.G., and Carson, M.J. (2002). Heterogeneous expression of the triggering receptor expressed on myeloid cells-2 on adult murine microglia. Journal of neurochemistry *83*, 1309-1320.

Schulz, C., Gomez Perdiguero, E., Chorro, L., Szabo-Rogers, H., Cagnard, N., Kierdorf, K., Prinz, M., Wu, B., Jacobsen, S.E., Pollard, J.W.*, et al.* (2012). A lineage of myeloid cells independent of Myb and hematopoietic stem cells. Science *336*, 86-90.

Selkoe, D.J. (1991). The molecular pathology of Alzheimer's disease. Neuron *6*, 487-498.

Selkoe, D.J. (2008). Soluble oligomers of the amyloid beta-protein impair synaptic plasticity and behavior. Behav Brain Res *192*, 106-113.

Sherrington, R., Rogaev, E.I., Liang, Y., Rogaeva, E.A., Levesque, G., Ikeda, M., Chi, H., Lin, C., Li, G., Holman, K.*, et al.* (1995). Cloning of a gene bearing missense mutations in early-onset familial Alzheimer's disease. Nature *375*, 754-760.

Shrestha, B.R., Vitolo, O.V., Joshi, P., Lordkipanidze, T., Shelanski, M., and Dunaevsky, A. (2006). Amyloid beta peptide adversely affects spine number and motility in hippocampal neurons. Molecular and cellular neurosciences *33*, 274-282.

Sims, R., van der Lee, S.J., Naj, A.C., Bellenguez, C., Badarinarayan, N., Jakobsdottir, J., Kunkle, B.W., Boland, A., Raybould, R., Bis, J.C.*, et al.* (2017). Rare coding variants in PLCG2, ABI3, and TREM2 implicate microglial-mediated innate immunity in Alzheimer's disease. Nature genetics.

Skuljec, J., Sun, H., Pul, R., Benardais, K., Ragancokova, D., Moharregh-Khiabani, D., Kotsiari, A., Trebst, C., and Stangel, M. (2011). CCL5 induces a pro-inflammatory profile in microglia in vitro. Cell Immunol *270*, 164-171.

Snyder, E.M., Nong, Y., Almeida, C.G., Paul, S., Moran, T., Choi, E.Y., Nairn, A.C., Salter, M.W., Lombroso, P.J., Gouras, G.K.*, et al.* (2005). Regulation of NMDA receptor trafficking by amyloid-beta. Nature neuroscience *8*, 1051-1058.

Song, W., Hooli, B., Mullin, K., Jin, S.C., Cella, M., Ulland, T.K., Wang, Y., Tanzi, R.E., and Colonna, M. (2017). Alzheimer's disease-associated TREM2 variants exhibit either decreased or increased ligand-dependent activation. Alzheimers Dement *13*, 381-387.

Spangenberg, E.E., Lee, R.J., Najafi, A.R., Rice, R.A., Elmore, M.R., Blurton-Jones, M., West, B.L., and Green, K.N. (2016). Eliminating microglia in Alzheimer's mice prevents neuronal loss without modulating amyloid-beta pathology. Brain : a journal of neurology *139*, 1265-1281.

Steinberg, S., Stefansson, H., Jonsson, T., Johannsdottir, H., Ingason, A., Helgason, H., Sulem, P., Magnusson, O.T., Gudjonsson, S.A., Unnsteinsdottir, U.*, et al.* (2015). Loss-of-function variants in ABCA7 confer risk of Alzheimer's disease. Nature genetics *47*, 445-447.

Stevens, B., Allen, N.J., Vazquez, L.E., Howell, G.R., Christopherson, K.S., Nouri, N., Micheva, K.D., Mehalow, A.K., Huberman, A.D., Stafford, B.*, et al.* (2007). The classical complement cascade mediates CNS synapse elimination. Cell *131*, 1164-1178.

Styren, S.D., Civin, W.H., and Rogers, J. (1990). Molecular, cellular, and pathologic characterization of HLA-DR immunoreactivity in normal elderly and Alzheimer's disease brain. Experimental neurology *110*, 93-104.

Suarez-Calvet, M., Araque Caballero, M.A., Kleinberger, G., Bateman, R.J., Fagan, A.M., Morris, J.C., Levin, J., Danek, A., Ewers, M., Haass, C.*, et al.* (2016a). Early changes in CSF sTREM2 in dominantly inherited Alzheimer's disease occur after amyloid deposition and neuronal injury. Science translational medicine *8*, 369ra178.

Suarez-Calvet, M., Kleinberger, G., Araque Caballero, M.A., Brendel, M., Rominger, A., Alcolea, D., Fortea, J., Lleo, A., Blesa, R., Gispert, J.D.*, et al.* (2016b). sTREM2 cerebrospinal fluid levels are a potential biomarker for microglia activity in early-stage Alzheimer's disease and associate with neuronal injury markers. EMBO Mol Med *8*, 466-476.

Suh, H.S., Zhao, M.L., Derico, L., Choi, N., and Lee, S.C. (2013). Insulin-like growth factor 1 and 2 (IGF1, IGF2) expression in human microglia: differential regulation by inflammatory mediators. Journal of neuroinflammation *10*, 37.

Suzumura, A., Sawada, M., Yamamoto, H., and Marunouchi, T. (1993). Transforming growth factor-beta suppresses activation and proliferation of microglia in vitro. Journal of immunology *151*, 2150-2158.

Takahashi, K., Rochford, C.D., and Neumann, H. (2005). Clearance of apoptotic neurons without inflammation by microglial triggering receptor expressed on myeloid cells-2. The Journal of experimental medicine *201*, 647-657.

Terry, R.D., Masliah, E., Salmon, D.P., Butters, N., DeTeresa, R., Hill, R., Hansen, L.A., and Katzman, R. (1991). Physical basis of cognitive alterations in Alzheimer's disease: synapse loss is the major correlate of cognitive impairment. Annals of neurology *30*, 572-580.

Thored, P., Heldmann, U., Gomes-Leal, W., Gisler, R., Darsalia, V., Taneera, J., Nygren, J.M., Jacobsen, S.E., Ekdahl, C.T., Kokaia, Z.*, et al.* (2009). Long-term accumulation of microglia with proneurogenic phenotype concomitant with persistent neurogenesis in adult subventricular zone after stroke. Glia *57*, 835-849.

Thornton, P., Sevalle, J., Deery, M.J., Fraser, G., Zhou, Y., Stahl, S., Franssen, E.H., Dodd, R.B., Qamar, S., Gomez Perez-Nievas, B.*, et al.* (2017). TREM2 shedding by

cleavage at the H157-S158 bond is accelerated for the Alzheimer's disease-associated H157Y variant. EMBO Mol Med.

Townsend, M., Shankar, G.M., Mehta, T., Walsh, D.M., and Selkoe, D.J. (2006). Effects of secreted oligomers of amyloid beta-protein on hippocampal synaptic plasticity: a potent role for trimers. The Journal of physiology *572*, 477-492.

Tremblay, M.E., Lowery, R.L., and Majewska, A.K. (2010). Microglial interactions with synapses are modulated by visual experience. PLoS biology *8*, e1000527.

Turnbull, I.R., Gilfillan, S., Cella, M., Aoshi, T., Miller, M., Piccio, L., Hernandez, M., and Colonna, M. (2006). Cutting edge: TREM-2 attenuates macrophage activation. Journal of immunology *177*, 3520-3524.

Ueno, M., Fujita, Y., Tanaka, T., Nakamura, Y., Kikuta, J., Ishii, M., and Yamashita, T. (2013). Layer V cortical neurons require microglial support for survival during postnatal development. Nature neuroscience *16*, 543-551.

Ulrich, J.D., Finn, M.B., Wang, Y., Shen, A., Mahan, T.E., Jiang, H., Stewart, F.R., Piccio, L., Colonna, M., and Holtzman, D.M. (2014). Altered microglial response to Abeta plaques in APPPS1-21 mice heterozygous for TREM2. Molecular neurodegeneration *9*, 20.

Wake, H., Moorhouse, A.J., Jinno, S., Kohsaka, S., and Nabekura, J. (2009). Resting microglia directly monitor the functional state of synapses in vivo and determine the fate of ischemic terminals. The Journal of neuroscience : the official journal of the Society for Neuroscience *29*, 3974-3980.

Walsh, D.M., Klyubin, I., Fadeeva, J.V., Cullen, W.K., Anwyl, R., Wolfe, M.S., Rowan, M.J., and Selkoe, D.J. (2002). Naturally secreted oligomers of amyloid beta protein potently inhibit hippocampal long-term potentiation in vivo. Nature *416*, 535-539.

Walsh, D.M., and Selkoe, D.J. (2007). A beta oligomers - a decade of discovery. Journal of neurochemistry *101*, 1172-1184.

Wang, Y., Balaji, V., Kaniyappan, S., Kruger, L., Irsen, S., Tepper, K., Chandupatla, R., Maetzler, W., Schneider, A., Mandelkow, E.*, et al.* (2017). The release and trans-synaptic transmission of Tau via exosomes. Molecular neurodegeneration *12*, 5.

Wang, Y., Cella, M., Mallinson, K., Ulrich, J.D., Young, K.L., Robinette, M.L., Gilfillan, S., Krishnan, G.M., Sudhakar, S., Zinselmeyer, B.H.*, et al.* (2015). TREM2 lipid

sensing sustains the microglial response in an Alzheimer's disease model. Cell *160*, 1061-1071.

Wang, Y., Ulland, T.K., Ulrich, J.D., Song, W., Tzaferis, J.A., Hole, J.T., Yuan, P., Mahan, T.E., Shi, Y., Gilfillan, S.*, et al.* (2016). TREM2-mediated early microglial response limits diffusion and toxicity of amyloid plaques. The Journal of experimental medicine *213*, 667-675.

Weisser, S.B., McLarren, K.W., Voglmaier, N., van Netten-Thomas, C.J., Antov, A., Flavell, R.A., and Sly, L.M. (2011). Alternative activation of macrophages by IL-4 requires SHIP degradation. European journal of immunology *41*, 1742-1753.

Wu, J.W., Hussaini, S.A., Bastille, I.M., Rodriguez, G.A., Mrejeru, A., Rilett, K., Sanders, D.W., Cook, C., Fu, H., Boonen, R.A.*, et al.* (2016). Neuronal activity enhances tau propagation and tau pathology in vivo. Nature neuroscience *19*, 1085-1092.

Wu, K., Byers, D.E., Jin, X., Agapov, E., Alexander-Brett, J., Patel, A.C., Cella, M., Gilfilan, S., Colonna, M., Kober, D.L.*, et al.* (2015). TREM-2 promotes macrophage survival and lung disease after respiratory viral infection. The Journal of experimental medicine *212*, 681-697.

Wunderlich, P., Glebov, K., Kemmerling, N., Tien, N.T., Neumann, H., and Walter, J. (2013). Sequential proteolytic processing of the triggering receptor expressed on myeloid cells-2 (TREM2) protein by ectodomain shedding and gamma-secretase-dependent intramembranous cleavage. The Journal of biological chemistry *288*, 33027-33036.

Wynes, M.W., and Riches, D.W. (2003). Induction of macrophage insulin-like growth factor-I expression by the Th2 cytokines IL-4 and IL-13. Journal of immunology *171*, 3550-3559.

Xia, M., and Hyman, B.T. (2002). GROalpha/KC, a chemokine receptor CXCR2 ligand, can be a potent trigger for neuronal ERK1/2 and PI-3 kinase pathways and for tau hyperphosphorylation-a role in Alzheimer's disease? Journal of neuroimmunology *122*, 55-64.

Xiang, X., Werner, G., Bohrmann, B., Liesz, A., Mazaheri, F., Capell, A., Feederle, R., Knuesel, I., Kleinberger, G., and Haass, C. (2016). TREM2 deficiency reduces the efficacy of immunotherapeutic amyloid clearance. EMBO Mol Med *8*, 992-1004.

Yamada, K., Holth, J.K., Liao, F., Stewart, F.R., Mahan, T.E., Jiang, H., Cirrito, J.R., Patel, T.K., Hochgrafe, K., Mandelkow, E.M.*, et al.* (2014). Neuronal activity regulates extracellular tau in vivo. The Journal of experimental medicine *211*, 387-393.

Yang, Z., and Ming, X.F. (2014). Functions of arginase isoforms in macrophage inflammatory responses: impact on cardiovascular diseases and metabolic disorders. Front Immunol *5*, 533.

Yeh, F.L., Wang, Y., Tom, I., Gonzalez, L.C., and Sheng, M. (2016). TREM2 Binds to Apolipoproteins, Including APOE and CLU/APOJ, and Thereby Facilitates Uptake of Amyloid-Beta by Microglia. Neuron *91*, 328-340.

Yoshiyama, Y., Higuchi, M., Zhang, B., Huang, S.M., Iwata, N., Saido, T.C., Maeda, J., Suhara, T., Trojanowski, J.Q., and Lee, V.M. (2007). Synapse loss and microglial activation precede tangles in a P301S tauopathy mouse model. Neuron *53*, 337-351.

Yu, J.T., Jiang, T., Wang, Y.L., Wang, H.F., Zhang, W., Hu, N., Tan, L., Sun, L., Tan, M.S., Zhu, X.C.*, et al.* (2014). Triggering receptor expressed on myeloid cells 2 variant is rare in late-onset Alzheimer's disease in Han Chinese individuals. Neurobiology of aging *35*, 937 e931-933.

Yuan, P., Condello, C., Keene, C.D., Wang, Y., Bird, T.D., Paul, S.M., Luo, W., Colonna, M., Baddeley, D., and Grutzendler, J. (2016). TREM2 Haplodeficiency in Mice and Humans Impairs the Microglia Barrier Function Leading to Decreased Amyloid Compaction and Severe Axonal Dystrophy. Neuron *90*, 724-739.

Zhang, Y., Chen, K., Sloan, S.A., Bennett, M.L., Scholze, A.R., O'Keeffe, S., Phatnani, H.P., Guarnieri, P., Caneda, C., Ruderisch, N.*, et al.* (2014). An RNA-sequencing transcriptome and splicing database of glia, neurons, and vascular cells of the cerebral cortex. The Journal of neuroscience : the official journal of the Society for Neuroscience *34*, 11929-11947.

Zhao, Y., Bhattacharjee, S., Jones, B.M., Dua, P., Alexandrov, P.N., Hill, J.M., and Lukiw, W.J. (2013). Regulation of TREM2 expression by an NF-small ka, CyrillicB-sensitive miRNA-34a. Neuroreport *24*, 318-323.

Zheng, H., Jia, L., Liu, C.C., Rong, Z., Zhong, L., Yang, L., Chen, X.F., Fryer, J.D., Wang, X., Zhang, Y.W.*, et al.* (2017). TREM2 Promotes Microglial Survival by Activating

Wnt/beta-Catenin Pathway. The Journal of neuroscience : the official journal of the Society for Neuroscience *37*, 1772-1784.

Zheng, H., Liu, C.C., Atagi, Y., Chen, X.F., Jia, L., Yang, L., He, W., Zhang, X., Kang, S.S., Rosenberry, T.L.*, et al.* (2016). Opposing roles of the triggering receptor expressed on myeloid cells 2 and triggering receptor expressed on myeloid cells-like transcript 2 in microglia activation. Neurobiology of aging *42*, 132-141.

Zhong, L., Chen, X.F., Wang, T., Wang, Z., Liao, C., Wang, Z., Huang, R., Wang, D., Li, X., Wu, L.*, et al.* (2017a). Soluble TREM2 induces inflammatory responses and enhances microglial survival. The Journal of experimental medicine *214*, 597-607.

Zhong, L., Chen, X.F., Zhang, Z.L., Wang, Z., Shi, X.Z., Xu, K., Zhang, Y.W., Xu, H., and Bu, G. (2015). DAP12 Stabilizes the C-terminal Fragment of the Triggering Receptor Expressed on Myeloid Cells-2 (TREM2) and Protects against LPS-induced Pro-inflammatory Response. The Journal of biological chemistry *290*, 15866-15877.

Zhong, L., Zhang, Z.L., Li, X., Liao, C., Mou, P., Wang, T., Wang, Z., Wang, Z., Wei, M., Xu, H.*, et al.* (2017b). TREM2/DAP12 Complex Regulates Inflammatory Responses in Microglia via the JNK Signaling Pathway. Front Aging Neurosci *9*, 204.

Zhou, L., Brouwers, N., Benilova, I., Vandersteen, A., Mercken, M., Van Laere, K., Van Damme, P., Demedts, D., Van Leuven, F., Sleegers, K.*, et al.* (2011). Amyloid precursor protein mutation E682K at the alternative beta-secretase cleavage beta'-site increases Abeta generation. EMBO Mol Med *3*, 291-302.

Zhou, X., Spittau, B., and Krieglstein, K. (2012). TGFbeta signalling plays an important role in IL4-induced alternative activation of microglia. Journal of neuroinflammation *9*, 210.

Zhu, C., Herrmann, U.S., Li, B., Abakumova, I., Moos, R., Schwarz, P., Rushing, E.J., Colonna, M., and Aguzzi, A. (2015). Triggering receptor expressed on myeloid cells-2 is involved in prion-induced microglial activation but does not contribute to prion pathogenesis in mouse brains. Neurobiology of aging *36*, 1994-2003.